Our Responses to Referees' and Colleagues' Comments

Dear Editors,

Please, find below our responses to all Referees' comments and related explanations for changes in the text, figures, and tables.

We thank very much the two Referees, the Editors, and all colleagues who provided constructive comments in the Discussion Forum.

Main changes in the submitted material are the following ones: following the Referee2 suggestions, we provided additional analyses on the sensitivity of the used cell size (Lines 16 onward p. 9, Figs. S1, S2, and S3) and on the null hypothesis analysis (Lines 9 onward p. 14, Fig. 14, Tables S1 and S2). Please, see below for explanations about these additional analyses.

Concerning the comments provided by Valensise et alii, we have already replied to all these comments in the Discussion Forum. Below, we report only those comments (with our responses and explanations) by Valensise et alii that involved changes in our submitted material.

We acknowledge also changes in the panel of authors. Dr. Fabio Chiaravalli stepped out as author for reasons connected with his Company (Sogin). Dr. Anna Maria Lombardi (annamaria.lombardi@ingv.it), who is a mathematician from INGV-Rome expert in statistical analysis of seismological data, joined this panel of author performing, in particular, some new statistical analyses requested by Referee2 (see Figure 14, and Tables S1 and S2).

Looking forward to hearing from you

Sincerely

Andrea Billi and co-authors

Rome, March 2019

Referee #1

Comment 1

Main comments

This manuscript describes an approach to evaluate the maximum possible earthquake

magnitude from the geometry of active faults in Italy. The topic has a broad interest, in

particular for fault-based seismic hazard modelling, because the correct evaluation of the

seismic potential of a seismogenic source is one of the main required parameters for seismic

hazard studies. The use of active faults in seismic hazard assessment has become extensive in

the last decades due to efforts of data compilation and analysis. Active faults provide the

information to extend the observational time of large magnitude earthquakes, which often is

not captured by the existing catalogues of observed seismicity.

The authors apply one empirical scaling relationship (not correctly defined by the authors as

scaling law!) between fault length and expected magnitude, to a clearly incomplete and

inhomogeneous fault database, to evaluate the maximum possible earthquake magnitude in

Italy. The manuscript is mostly well written and the figures are clear but, from my point of

view, the approach has several misconceptions and incompleteness and the conclusions are

not supported by the results.

For these reasons, the manuscript does not represent a substantial contribution to scientific

progress in seismic hazard assessment and seismic risk reduction, as required by a high-level

Journal as Solid Earth. The applied methods are valid but too simplistic and applied to

incomplete and inhomogeneous data with consequently a poor scientific significance of the

manuscript. Moreover, the references used for the fault database compilation is largely

incomplete.

Response 1

We acknowledge that the main goal of this paper is not the seismic hazard that is defined as:

"the probability that an earthquake will occur in a given geographic area, within a given window of time, and with ground motion intensity exceeding a given threshold. With a hazard thus estimated, risk can be assessed and included in such areas as building codes for standard buildings, designing larger buildings and infrastructure projects, land use planning and determining insurance rates.";

nor is the seismic risk that is defined as:

"the risk of damage from earthquake to a building, system, or other entity. It particular, it can be also defined, for most management purposes, as the potential economic, social and environmental consequences of hazardous events that may occur in a specified period of time."

Our main goal is different and is clearly stated (now improved in the new version) several times in the manuscript:

- In the title: "From mapped faults to Fault-Length Earthquake Magnitude (FLEM): A test on Italy with methodological implications"

- At Lines 1-4, p. 1: "Empirical scaling relationships between fault/slip dimensions and earthquake magnitudes are often used to assess the maximum possible earthquake magnitude of a territory. In this paper, upon the assumption of the reactivability of any fault, these seismic scaling relationships are benchmarked at the national scale in Italy against catalogued earthquake

magnitudes, considering all known faults regardless of their age, stress field orientation, strain rate, or else."

- At Lines 15-19, p. 1: "The main advantages of this method is its independence from temporal and (paleo)seismological information, whereas the main novelty is its use at the national scale also for faults considered inactive. Our work can provide a perspective time-independent seismic potential of faults; however, it cannot be a substitute for time-dependent (paleo)seismological methods for seismic hazard assessments."

- At Lines 13-22, p. 3: "We anticipate that, with this work, we do not intend to propose an alternative method for seismic hazard assessment or to better previous methods (e.g., Giardini et al., 1999; Jimenez et al., 2001; Michetti et al., 2005 Field et al., 2009, 2015; Reicherter et al., 2009). Our main aim is to test whether solely considering the known mapped faults (both active, inactive, and undetermined) and disregarding further information (e.g., historically- and instrumentally-recorded earthquakes as well as the regional stress field and strain rate) it is possible to provide, through existing seismic scaling relationships of faults and earthquakes, reasonable assessments of the maximum possible earthquake magnitude over an entire nation. The resulting (assessed) magnitudes (FLEMs) are compared (i.e., the mathematical difference) with catalogued earthquake magnitudes that are the only existing points of reference against which assessed magnitudes can be compared. Note that these results should be considered more in a theoretical and methodological perspective for comparison with future similar studies rather than in an applicative perspective for the case of Italy. In particular, our assessed earthquake magnitudes (FLEMs) for the Italian territory are proposed in this paper for scientific reasons and not for their use for civil protection and prevention purposes."

Therefore, our manuscript is not at all intended to be "a substantial contribution to scientific progress in seismic hazard assessment and seismic risk reduction" as stated by Referee 1. The possible perspective of this manuscript is now better stated at 13-22, p. 3.

Note also that we have modified the term FLEM (Potential Earthquake Maximum Magnitude) – that seemed a term for the seismic hazard assessment – into the term FLEM (Fault-Length Earthquake Magnitude) – that should merely represent what we have done in this work, i.e. computing the earthquake magnitude from the length of mapped faults through known empirical relationships.

We have now used the term scaling relationship rather than scaling law over the entire manuscript as suggested by Referee 1.

Following suggestions by Referee 2, the applied method has been significantly improved in the new version (e.g.,see the new Figures 14, S1, S2, and S3, and Tables S1 and S2), whereas the datasets and references are not incomplete as explained below.

Comment 2

Detailed comments

1. Fault database: the database is largely incomplete and inhomogeneous, with an

incompleteness variable in space. The suggestions to improve the database are:

a. Consider the abundant literature in the compilation of active fault database for

Italy, mostly more recent than the used one (in the following references a

partial and not yet complete list of papers not considered in the manuscript);

Response 2

As it is now specified in the manuscript (Lines 27-30, p. 8), our fault database is a big compilation of faults (total number of faults = 12467; specifically, 9169 A-type faults and 3298 B-type faults) from the main available datasets (from Line 5 onward, p. 6).

Obviously, any national fault database can be improved, but, in our case, considering 12467 faults in Italy as an incomplete database seems to be an underestimate. Note that, as stated in the Introduction, our focus is not on active faults (from Line 22 onward, p. 2).

Therefore, although our database can be improved with any single active fault discovered and published in the new literature, such literature-hunting is beyond the scope of our work, which becomes significant when done rather quickly with the available fault datasets; otherwise, other existing datasets (accurately compiled over long times) of active faults and/or seismogenic sources are already available for Italy (e.g., DISS, http://diss.rm.ingv.it/diss/).

Concerning the inhomogeneity, we specify what follows (from Lines 10 onward, p. 6): "The strength point of our approach is the assemblage of different fault datasets heterogeneously built for different purposes and based on different primary information and methods. In this approach, we consider all known faults (see above) to form a dataset as comprehensive as possible. Moreover, although different, the common point of all used datasets is that they have faults mapped and therefore measurable over the Earth's surface."

_____

Comment 3

b. Separate in the database the recognized active faults to the not clearly active

ones. In literature are available several definitions of fault activity, taking into

account the age of the involved deposits, the associated earthquakes, the

continuity and kinematics compatibility, and many others, and the authors need

to consider it. In this way the authors could define more classes of faults (more

than the two defined in the manuscript) based on the goodness of data and

recent activity and need to treat separately the classes in the approach to

evaluate the seismogenic potential;

Response 3

Please, see our previous response.

Our scope is not working only on (presumably-)active faults, but working on all faults and on their potential over future long terms (from Line 26 onward, p. 2, and from Line 12 onward, p. 3).

_____

Comment 4

c. Evaluate and handle with the spatial variable incompleteness of the database;

Response 4

Our dataset (12467 faults) cannot be considered incomplete (please, see Response 2). However, following the suggestions by Reviewer 2, we have now added a sensitivity analysis on the used cell size (Line 16 onward, p. 9 + Figures S1, S2, and S3). This analysis should help in better understanding the spatial relevance of our test and results as suggested by the Reviewers.

_____

Comment 5

Consider the fault segmentation variability in the correct evaluation of the seismogenic

potential, essential in fault-based seismic hazard approaches, as confirmed by recent

complex coseismic ruptures (e.g., 2010 M 7.1 Canterbury, 2012 Mw 8.6 Sumatra, 2016

Mw 7.8 Kaikōura, 2016 Mw 6.5 central Italy);

Response 5

On one hand, our input is simply the fault length in map view (Line 25 onward, p. 8: "Starting from the entire dataset of faults in Italy, as a first step, we measured the length of each fault as the real fault trace length in map view, i.e., the length of the vertical projection of the fault trace as observed on the Earth's surface over a horizontal plane (Fig. 2; supplement; Petricca et al., 2018)."). Therefore, fault segmentation is already properly considered when properly mapped in the original datasets used for this work.

On the other hand, the lack of a proper segmentation in the process of fault mapping is right one of the targets of our analysis. In other words, where the computed FLEM (largely) exceeds the corresponding catalogued earthquake magnitude, the most probable cause for such excess is the lack of high-resolution datasets that allow characterizing fault geometry and in particular segmentation. The most straightforward example in our study are the class B faults. Therefore our study is useful to detect areas where faults have not been properly characterized (i.e., segmented), these areas require further detailed studies for a better comprehension of the seismic potential.

To this end (fault segmentation), we have also added this relevant statement at Lines 2 onward, p. 14:

"To this end, it is also noteworthy that studies on the 2016 Amatrice-Norcia (central Italy) earthquakes (Mw 6.0 and 6.5) revealed that the length of the causative faults was only partially activated by the seismogenic slip (e.g., Cirella et al., 2018); however, as this co-seismic behaviour of faults seems rather frequent (Freymueller et al., 1994; Milliner et al., 2016; Chousianitis and Konca, 2018), it is most likely that this same behaviour is incorporated and implicitly expressed by the above-mentioned empirical scaling relationships between fault length and earthquake magnitude (e.g., Wells and Coppersmith, 1994; Leonard, 2010; Thingbaijan et al., 2017)."

_____

Comment 6

Organize a table with earthquake-fault associations, in order to avoid the double

counting or the source missing. There are several examples of 'problems' in the *kmz

of the authors, as the missing of the Paganica fault, responsible of the M6.3 2009

L'Aquila earthquake, the double counting of some faults in the Fucino area where the

M7 1915 earthquake occurred, and the not correct definition of the total length of the

fault responsible in the Irpinia region of the M6.8 1980 earthquake;

Response 6

As previously explained, we consider all faults (from a number of existing datasets) disregarding their age and/or their association with historical/instrumental earthquakes (Lines 2-5 p. 1, 14-16 p. 3, and 10-12 p. 6).

We do not double-count faults. Our only criterion to choose the fault from which the FLEM of the considered cell will be computed is the greatest fault length in map view. In such a way, only one fault (the longest one) will provide the FLEM in a given cell. Therefore, faults cannot be and are not double-counted (Line 30 onward p. 8).

_____

Comment 7

Consider also the seismogenic depth and the length of the faults along dip, to better

define the total potential rupture area, better linked to the seismogenic potential of the

sources;

Response 7

These parameters are available only for a limited number of (active) faults in Italy, whereas we consider all faults over the national territory (Lines 2-5 p. 1, 14-16 p. 3, and 10-12 p. 6). Moreover, the input of the used empirical relationship by Leonard (2010) is simply the fault length in map view (Line 5 onward p. 9).

_____

Comment 8

Deal with greater accuracy the empirical scaling relationships, by:

- *a. Compare the results of the approach using the different available relationships;*
- *b. Handle with the uncertainties, both inter- the different relationships and intrathe single relationships (sometimes the authors define very large standard deviation in the empirical relationship not treated in the manuscript);*

Response 8

This comparison is done in Fig. 6 and at Lines 16 onward p. 10. Moreover, the new analyses concerning the cell size sensitivity (Figs. S1-S3 and Lines 16 onward p. 9) and the null hypothesis (Fig. 14, Tables S1 and S2 and Lines 9 onward p. 14) provide new robustness and soundness to our results.

_____

Comment 9

Compare the results using different geometrical parameters, e.g. the surface

rupture length, the subsurface rupture length, the rupture area (and so

considering the seismogenic thickness) together with the different kinematics,

treated separately in the different scaling relationships;

Response 9

The one proposed by the Reviewer is a totally different approach. We only consider the length of all known faults. As stated in the Conclusions section, this approach has its pros and cons: "Our results are partly encouraging and suggest the testing and validation of this experiment elsewhere. This method cannot, however, be a substitute for time-dependent (paleo)seismological methods for seismic hazard assessments. Rather, it can provide an approximate perspective time-independent seismic potential of faults and highlight areas where further detailed studies are required."

For what concerns different kinematics, we refer the reader to Lines 11 onward p. 10.

Note also that, for the Italian territory, the influence of the seismogenic thickness on the potential earthquake magnitude has already been treated in recent articles by some of us (Petricca et al., 2015, Tectonophysics 656, 202-214; Chiarabba and De Gori, Terra Nova, 2016; Petricca et al., 2018, Physics of the Earth and Planetary Interiors 284, 72-81).

_____

Comment 10

Handle with the uncertainties in the results, comparing the differences between the

seismogenic potential of the faults estimated by the empirical relationships and the

earthquakes in the historical catalogue, in terms of seismic moment and not only

magnitude. Magnitude is a logarithmic quantity and so a simple comparison as done by

the authors in the conclusions has a clear bias;

Response 10

Although the suggestion is surely right from a theoretical point of view, practically, the problem of using seismic moments is that for many earthquakes (particularly in historical catalogs but also in old instrumental catalogs), independent assessments of the seismic moments do not exist. This makes impossible the use of seismic moments in our approach, which includes historical and instrumental earthquake catalogs for an entire nation. In other words, the only parameter available for the entire nation over the historical and instrumental periods is the earthquake magnitude and not the seismic moment.

_____

Comment 11

Treat the probability of occurrence in the conclusions. In seismic hazard models is

necessary to define the seismic rates for the different magnitude classes and so the

probability of occurrence of a defined magnitude depends on the average recurrence

time of that value in a specific area. The conclusions of the authors show the largest

expected magnitudes in areas with very low seismicity, like Sardinia, suggesting there

high seismic hazard values. Such conclusions have to be more strongly supported by

considerations in terms of probability of occurrence.

Response 11

As previously explained (Response 1), the seismic hazard and the probability of earthquake occurrence are not the scope of our work. Consider that, in a long term perspective (e.g. IAEA, www.iaea.org; Lines 29 onward p. 2), any fault could be reactivated. Our scope is stated at Lines 14 onward p. 3:

"Our main aim is to test whether solely considering the known mapped faults (both active, inactive, and undetermined) and disregarding further information (e.g., historically- and instrumentally-recorded earthquakes as well as the regional stress field and strain rate) it is possible to provide, through existing seismic scaling relationships of faults and earthquakes, reasonable assessments of the maximum possible earthquake magnitude over an entire nation."

Referee #2 (Nandan)

Comment 12

In general, I have found the work presented in the manuscript to be very clearly described.

I also like the style of writing of the authors as they have stated the caveats of

the study very clearly. However, I fail to appreciate the novelty of the work presented

in this paper. I am wondering if it is the compilation of the comprehensive fault catalog

using the existing databases or the estimation of the FLEMs. If it is the former, I would

suggest that the authors stress it more in the manuscript and show what were the hurdles

that they had to overcome when compiling the comprehensive fault database. If

it is the latter then, I feel that the authors have oversimplified the task of estimation of FLEMs.

Response 12

We thank Dr Nandan for its appreciation.

The scope and novelty of our work are not in the compilation of the fault database, rather they are in the estimation of FLEMs using all known faults over a national territory and in the comparison between FLEMs and catalogued earthquake magnitudes. These concepts are clearly stated and now better emphasized in the manuscript:

- In the title: "From mapped faults to Fault-Length Earthquake Magnitude (FLEM): A test on Italy with methodological implications"

- At Lines 1-4, p. 1: "Empirical scaling relationships between fault/slip dimensions and earthquake magnitudes are often used to assess the maximum possible earthquake magnitude of a territory. In this paper, upon the assumption of the reactivability of any fault, these seismic scaling relationships are benchmarked at the national scale in Italy against catalogued earthquake magnitudes, considering all known faults regardless of their age, stress field orientation, strain rate, or else."

- At Lines 15-19, p. 1: "The main advantages of this method is its independence from temporal and (paleo)seismological information, whereas the main novelty is its use at the national scale also for faults considered inactive. Our work can provide a perspective time-independent seismic potential of faults; however, it cannot be a substitute for time-dependent (paleo)seismological methods for seismic hazard assessments."

- At Lines 13-22, p. 3: "We anticipate that, with this work, we do not intend to propose an alternative method for seismic hazard assessment or to better previous methods (e.g., Giardini et al., 1999; Jimenez et al., 2001; Michetti et al., 2005 Field et al., 2009, 2015; Reicherter et al., 2009). Our main aim is to test whether solely considering the known mapped faults (both active, inactive, and undetermined) and disregarding further information (e.g., historically- and instrumentally-recorded earthquakes as well as the regional stress field and strain rate) it is possible to provide, through existing seismic scaling relationships of faults and earthquakes, reasonable assessments of the maximum possible earthquake magnitude over an entire nation. The resulting (assessed) magnitudes (FLEMs) are compared (i.e., the mathematical difference) with catalogued earthquake magnitudes that are the only existing points of reference against which

assessed magnitudes can be compared. Note that these results should be considered more in a theoretical and methodological perspective for comparison with future similar studies rather than in an applicative perspective for the case of Italy. In particular, our assessed earthquake magnitudes (FLEMs) for the Italian territory are proposed in this paper for scientific reasons and not for their use for civil protection and prevention purposes."

Since the focus of our work is the FLEM estimation and the comparison between FLEMs and catalogued earthquake magnitudes, to avoid an oversimplification of this task (as stated by Referee 2), we have followed the Referee's suggestions and provided additional analyses on the sensitivity of the used cell size (Lines 16 onward p. 9, Figs. S1, S2, and S3) and on the null hypothesis analysis (Lines 9 onward p. 14, Fig. 14, Tables S1 and S2). Please, see below for explanations about these additional analyses.

_____

Comment 13

1. What are the main challenges in

compiling the comprehensive fault database from existing fault databases? How is this

task difficult?

Response 13

As stated in our previous response (Response 12), our scope and novelty is not the fault database that is a compilation from existing databases as thoroughly explained at Lines 5 onward p. 6.

_____

Comment 14

2. How do the authors identify and remove the duplicate faults in the

regions where the two databases overlap?

Response 14

Please, see above our Response 6. We do not double-count faults. Our only criterion to choose the fault from which the FLEM of the considered cell will be computed is the greatest fault length in map view. In such a way, only one fault (the longest one) will provide the FLEM in a given cell. Therefore, faults cannot be and are not double-counted (Line 30 onward p. 8).

_____

Comment 15

3. How sensitive are the results of the

authors to the assumptions described in section 4.2? For instance, would the results

dramatically change if one considers a different grid resolution? Same applies for the

other assumptions. I think authors should do more effort than just outlining their assumptions.

A sensitivity analysis is a minimum they should strive for.

Response 15

Following the Referee's suggestion, we have performed a sensitivity analysis on the grid size (Lines 16 onward p. 9, Figs. S1, S2, and S3).

_____

Comment 16

4. The authors

claim that the calculated FLEMs are consistent with the largest observed earthquakes

at least for the geologically well-constrained fault. First of all, it is obvious that this

consistency is strongly dependent on the grid resolution that the authors will choose.

Secondly, what is the reference level for consistency? What I mean to say is any prediction

and observation can be deemed consistent if allow for enough uncertainty. To

account for this, one needs to come up with a reasonable null hypothesis and compare

the new predictions to the predictions of the null hypothesis. In this case, a reasonable

null hypothesis could be an untruncated Gutenberg Richter law, with a given b-value.

The authors could pose their model as the GR law with the same b-value but with the

truncation at the FLEMs estimated using their approach. They can then estimate the

likelihood of the largest earthquakes (M>M_threshold) and compare the two likelihoods

using standard statistical tests. In this manner, the authors would have reference level

that would allow them to objectively assess the quality of their prediction.

Response 16

Following the Referee's suggestion, we have performed a statistical test to check, as far as possible, the reliability of our estimated FLEM values (Lines 9 onward p. 14, Fig. 14, Tables S1 and S2).

It is known that, even for excellent data and weak hypotheses (as the untruncated Gutenberg Richter), from an earthquake catalog alone it is substantially impossible, through a statistical test, to discriminate, with sufficient confidence, among competitive maximum magnitude values (Holschneider et al., 2014). This is mainly due to the upper cutoff of the Gutenberg-Richter distribution, where only rare earthquakes with magnitudes close to the maximum possible value

occur. In light of these limitations, we are able to check the reliability of the estimated FLEM values, but we cannot compare different competitive FLEMs.

Therefore, our analysis consisted in the following steps. Firstly, we selected cells for which the doubly truncated Gutenberg-Richter law, with a b-value equal to 1, could not be rejected. In this way, we excluded that a possible rejection of the estimated FLEM was actually due to the unreliability of the Gutenberg-Richter law or to the uncertainty about the b-value. Then, in the reliable cells, we tested the FLEM values, assuming them as null hypothesis. We found that in all the analyzed cells they cannot be rejected, both in the case of the CSIv1.1 catalog and in the case of the ISIDe catalog. However, we cannot exclude that the used data may be inadequate to reveal failure of the FLEM values, nor, for the above-mentioned reasons, we can compare alternative reliable FLEM values. This new analysis is now fully reported and explained at Lines 9 onward p. 14, Fig. 14, Tables S1 and S2.

Valensise et alii

Introduction

Comments by Valensise et alii, as happens also for most comments by Referee 1, seem influenced by an initial and radical misunderstanding. Our manuscript IS NOT titled "A new map of expected earthquake magnitudes for seismic hazard and risk mitigation in Italy Simply, this is not the goal of the article. Our maps (Figs. 7 and 8) ARE NOT AT ALL predictive maps of seismic hazard.

Our manuscript is titled "From mapped faults to earthquake magnitude: A test on Italy with

methodological implications" and our aim is stated clearly from the introduction where we say:

"We anticipate that, with this work, we do not intend to propose an alternative method for seismic hazard assessment or to better previous methods (e.g., Giardini, 1999; Jiménez et al., 2001; Michetti et al., 2005; Field et al., 2009, 2015; Reicherter et al., 2009). Our main aim is to test whether solely considering the known mapped faults (both active, inactive, and undetermined) and disregarding further information (e.g., historically- and instrumentally-recorded earthquakes as well as the regional stress field and strain rate) it is possible to provide, through existing seismic scaling laws of faults and earthquakes, reasonable assessments of the maximum possible earthquake magnitude over an entire area. The resulting (assessed) magnitudes (FLEM) are compared (i.e., the mathematical difference) with catalogued earthquake magnitudes that are the only existing points of reference against which assessed magnitudes can be presently compared."

The empirical relationships (used by many geoscientists including Valensise et alii) between fault size and earthquake magnitude are notoriously problematic for issues such as fault segmentation, fault continuity, and seismic partial activation of long faults. These problems have been ascertained ex-post on most single faults after earthquakes. We work on these same problems at the national scale with a different approach (ex-ante). That is, given a set of "official" faults of a nation (from geological maps and other official datasets), is it possible to test, quantify, and ascertain the above-mentioned problems connected with the empirical relationships? One way to do this, is to apply the relationship to the fault dataset and then compare the results with a seismic catalogue. This is what we do in Figs. 10, 11, 12, and 13 + Table 1.

The results of this work cannot be used for Seismic Hazard Assessment but rather, they can highlight areas where further studies are required to better asses expected earthquake magnitudes

In the revision we will better emphasize the above-mentioned concepts, starting from the abstract that in the previous version of the manuscript could have left some space for misinterpretation. We will also add disclaimers in Figures 7 and 8 saying that these figures are not at all for use for Civil Protection, officials, and, in general, for seismic hazard. (Lines 15-18 p. 1, 12-23 p. 3, + captions to Figs. 7 and 8).

Comment 3:

For instance, a very general statement such as "Larger earthquakes characterize the Apennines southern portion (Calabria), with historical seismic events that reached magnitudes up to 6.9-7.5" is backed by a reference to Cello et al. (2003), a 15 years-old paper dealing with a specific earthquake in Val d'Agri, 50 km north of Calabria, and to Gasparini et al. (1985), a 33 years-old paper that belongs to a distant past of seismotectonics in Italy. A simple reference to the Catalogo Parametrico dei Terremoti Italiani (CPTI), the Italian reference parametric catalogue, would have been enough; it would also have prevented a mistake, since no M 7.5 earthquake is reported anywhere in Italy

Response 3:

This criticism refers to a sentence extracted from the seismotectonic setting and not from the method and results sections. We will accept with pleasure the suggestion by Valensise et alii and will enrich the Seismotectonic Setting with some recent references in the revised version of our manuscript (Line 18 p. 5). However, we have to point out that the core and science of our paper is not at all affected by a supposed lack of consideration of previous works, as argued by the comment.

More importantly, in section 3.2 earthquake data, we do mention CPTI together with the most comprehensive catalogues of instrumental and historical seismicity like CSI1.1 and ISIDe.

Comment 5:

It is unfortunate that the fault database that should support this bold statement is not accessible (see Petricca, P., et al., Revised dataset of known faults in Italy, GFZ Data Services, https://doi.org/10.5880/fidgeo.2018.003, http://pmd.gfz-potsdam.de/panmetaworks/, 2018; the first link leads to an error page, while the second leads to a generic page of the GFZ website).

Response 5:

The database is fully and publicly available at the indicated database under this link that we will be report also on the revised manuscript (Lines 5 onward p. 17):

http://pmd.gfz-potsdam.de/panmetaworks/review/924b171fd21c78f295d58a7e9e321e8ad07667ab6201634b23d3cb5a3f170d10/

Comment 8:

A basic consideration is that by assembling faults from such different and nonhomogeneous sources, Petricca et al. inevitably put together a) alternative views on the same faults, possibly stemming from widely alternative conceptual models; b) faults that are mutually exclusive due to their geometry (typically, faults crossing each other in the subsurface: if one fault ends against another, its seismic potential based solely on length is largely overestimated); c) faults that cannot

be simultaneously active, or reactivated, in the current stress regime; and d) blind faults whose actual length may be strongly biased by the availability and density of subsurface data.

Response 8:

We think that this is the strength of our work. For the reasons explained above (Response 4) we propose that most of the faults within the Italian territory can host an earthquake. Therefore a comprehensive fault dataset, as the one used in the present work, can help in: 1) reducing bias induced by the availability and density of subsurface data; 2) highlighting areas where detailed future studies are required to improve seismic hazard, that is not the target of this work.

All this is clearly stated in the Introduction and in the Conclusions sections. However, we will better stress the above-mentioned concepts in the Abstract, Introduction, and Conclusions of the revised manuscript (Lines 15-18 p. 1, 12-23 p. 3, + captions to Figs. 7 and 8). This is a product for scientific use only (i.e. testing the empirical relationships).

Comment 13:

The authors never admit that their results are pointless, even when they remark (Page 12) that "... the negative occurrences are very limited...", i.e. that the number of predicted magnitudes that are larger than those observed in the historical record outnumbers by far the opposite case, resulting in the very asymmetric pattern shown in Figure 12. In fact, they refer to a "...limited difference... between FLEMs and the catalogued earthquake magnitudes..." (!), neglecting the obvious consideration that magnitude is a logarithmic quantity, implying that a 0.2 increase in Mw, for example from 6.0 to 6.2, doubles the seismic moment. For a typical continental fault having an aspect ratio in the range 2-3 and standard scaling for coseismic slip, doubling the moment implies that fault length may increase by over 20%. For a magnitude increase of 0.5, for example from 6.0 to 6.5, the seismic moment becomes 5.6 times larger, which may require a fault that is 100% or more longer than that necessary to generate the smaller earthquake.

Response 13:

Thanks. We accept this comment. We will rephrase this statement (the negative occurrences are very limited...). We agree that it is useless commenting this result as very limited. We will susbstitute "very limited" with the exact numbers that we obtain from the experiment. The term limited is too vague and subjective. However, once again, it is worth to underline that we are not proposing a forecast method, we are testing very well-known scaling laws at the national scale (Line 11 p. 13).

Comment 16:

The conclusions of this paper are worrisome, in consideration of the large number of areas where the authors envision the possibility of M 7.5 and larger earthquakes, that is to say earthquakes bigger than the largest magnitude ever recorded in Italy, without any consideration as to how frequently this may occur. In a standard PSHA approach these large magnitudes would be

assigned a very low probability of occurrence, leading to a minimal statistical impact on the expected ground shaking for short average return periods. The information about the possible largest earthquakes may generate a great deal of confusion if not appropriately communicated. We cannot imagine how the residents of Bologna, Ancona, Pescara, but also Padua, Trento, Vicenza and even Venice, cities lying in areas that are currently considered mid- to low-hazard, would react to knowing that very large earthquakes may occur below their feet at any moment.

Response 16:

We completely agree with the sentence "The information about the possible largest earthquakes may generate a great deal of confusion if not appropriately communicated". In fact, we are NOT proposing a new seismic hazard map, and this is really clear by reading the paper (not only looking at the figures). We simply compute potential earthquake magnitude from fault size and compare these results with seismic catalogs (Figs. 10-13 and Table1) to reason upon the validity of the scaling relationships between fault attributes and earthquake magnitude at the national scale with available fault datasets. The comment by Valensise et alii is therefore inappropriate.

However, in the revised manuscript we will better stress the above-mentioned concepts (i.e., our aim is not a new and reliable map of expected earthquakes in Italy). We will also add disclaimers in Figures 7 and 8 saying that these figures are not at all for use for Civil Protection, officials, and, in general, for seismic hazard. They are a product for scientific use only (i.e. testing the empirical relationships) (Lines 15-18 p. 1, 12-23 p. 3, + captions to Figs. 7 and 8).

Comment 17:

Another major flaw in the approach taken by Trippetta and co-workers lies in their discretisation of seismogenic zones into 25x25 km sub-areas. Of course, some discretisation is inevitable, but one has to be aware that a 25x25 km cell may host a 35 km-long fault, at the most. According to the equation proposed by Leonard (2010), the empirical law adopted by Trippetta and co-workers, a 35 km fault length corresponds to a Mw 6.8 earthquake. Hence, any larger earthquake will necessarily encompass two or more cells. A close inspection of Figures 7 and 8 of the paper, however, reveals that several cells filled in red or dark red, which according to the adopted colour-coding should correspond to an expected Mw in the range 7.4 to 7.8, occur isolated, i.e., surrounded by cells for which the expected FLEM is much smaller. According to same equation by Leonard (2010), this magnitude range corresponds to a fault length in the range 78 to 135 km, which should involve a minimum of 2 to 4 adjacent cells, depending on fault strike. An isolated cell capable of a Mw 7.4 earthquake is hence a seismological paradox that has no physical meaning, as the earthquake causative fault will necessarily extend to adjacent cells.

Response 17:

At which cell are Valensise et alii referring to? As we can see from figure 7 and 8 there are no red (M.7.5) isolated cells. In each cell, we consider the longest fault that touches/crosses the cell. This means that the faults can be longer than 35 km as indicated by Valensise et alii. This is clearly stated in our method section at Lines 27-28 Page 8: "The length of the longest fault crossing each cell determined the parameter "fault length" (Lf) of the considered cell."

Our computation is selfsustained and the complete database is available at the following link for reproducibility of our results (see also the Data availability section) (Lines 5 onward p. 17):

http://pmd.gfz-potsdam.de/panmetaworks/review/924b171fd21c78f295d58a7e9e321e8ad07667ab6201634b23d3cb5a3f170d10/

Thanks a lot

Andrea Billi and co-authors

From mapped faults to Fault-Length Earthquake Magnitude (FLEM): A test on Italy with methodological implications

Fabio Trippetta[1], Patrizio Petricca[1], Andrea Billi[2], Cristiano Collettini[1,3], Marco Cuffaro[2], Anna Maria Lombardi[3], Davide Scrocca[2], Giancarlo Ventura[4], Andrea Morgante[4], and Carlo Doglioni[1,3]

[1]Dipartimento di Scienze della Terra, Sapienza Universitá di Roma, Rome, Italy
[2]Istituto di Geologia Ambientale e Geoingegneria, CNR, Rome, Italy
[3]Istituto Nazionale di Geofisica e Vulcanologia, Rome, Italy
[4]Sogin (Società Gestione Impianti Nucleari) S.p.a., Rome, Italy

Correspondence: Andrea Billi (andrea.billi@cnr.it)

Abstract. Empirical scaling laws between fault/slip dimensions and earthquake magnitudes are often used to assess the maximum possible earthquake magnitude of a territory. In this paper, upon the assumption of the reactivability of any fault, these seismic scaling relationships are benchmarked at the national scale in Italy against catalogued magnitudes, considering all known faults regardless of their age, stress field orientation, strain rate, or else. Italy is a suitable case for comparing the fault-size-derived seismic magnitudes with the existing accurate catalogues of historical-instrumental earthquakes. To do so, (1) a comprehensive catalogue of all known faults is compiled by merging the most complete databases available, (2) the earthquakes magnitude (FLEM) is simply derived from fault length, and (3) the resulting FLEMs are compared (i.e., the mathematical difference) with catalogued earthquake magnitudes. Results show that the largest FLEMs as well as the largest differences between FLEMs and catalogued magnitudes are observed for poorly constrained faults, mainly inferred from subsurface data. It is suggested that these areas have to be further characterized to better estimate fault dimension and segmentation and hence properly assess the FLEM. Where, in contrast, the knowledge of faults is geologically well constrained, the calculated FLEM is often consistent with the catalogued seismicity, with the 2σ value of the distribution of differences being 1.47 and reducing to 0.53 when considering only the $M \geq 6.5$ earthquakes. This overall consistency gives credibility to the used empirical scaling laws; however, some large differences between the two datasets suggest further validation of this experiment in Italy and elsewhere. The main advantages of this method is its independence from temporal and (paleo)seismological information, whereas the main novelty is its use at the national scale also for faults considered inactive. Our work can provide a perspective time-independent seismic potential of faults; however, it cannot be a substitute for time-dependent (paleo)seismological methods for seismic hazard assessments.

1 Introduction

In some seismically active regions like California, information derived from geodesy, the geology of active faults, and seismology (both historical and instrumental) have been combined to develop a comprehensive method that predicts 99% of the chances of having one or more $M \geq 6.7$ earthquakes in the following 30 years (USGS Fact Sheet, 2008). Along the North

Anatolian Fault (Turkey), fault geometry and slip accumulated during strong earthquakes have been used to infer the transfer of stress during seismic sequences and to estimate the increase of earthquake probability with M ≥ 6.7 (Stein, 1997; Parsons et al., 2000; Bohnhoff et al., 2016). These case studies involve areas characterized by high strain rates and affected by large plate boundary faults that can be easily recognized in geological and/or geophysical records.

5   In contrast, other areas in the world where strain rates are low-to-intermediate and faults show smaller dimensions and unclear surface expression of recent activity, the connection between faults and earthquakes is not straightforward, particularly between potentially seismogenic faults and the maximum possible earthquake magnitude. Moreover, where lands were largely uninhabited during historical times (but are now densely populated and, therefore, potentially exposed at the seismic threat), the recurrence time of strong earthquakes is significantly longer with respect to the age of the seismological network, or

10   information on historical and instrumental seismicity can be largely incomplete, the assessment of the maximum possible earthquake magnitude can be difficult (Camelbeeck et al., 2007; Kafka, 2007; Stein and Mazzotti, 2007; Swafford et al., 2007; Dawson et al., 2008; Braun et al., 2009; Boyd et al., 2013; Leonard et al., 2014; Talwani, 2014; Campbell et al., 2015; Calais et al., 2016; Christophersen et al., 2017; Wang et al., 2019).

Where frequent earthquakes are absent and seismic history is unknown, the seismic potential and the temporal knowledge

15   of seismic activity of faults can be determined using geological studies such as paleoseismological trenching or radiometric dating of slip indicators (Galli, 2000; Rockwell et al., 2000; Palumbo et al., 2004; Dixon et al., 2003; Galli et al., 2008; McCalpin, 2009; Sherlock et al., 2009; Nuriel et al., 2012; Viete et al., 2018), but these studies are usually time-consuming and expensive. Alternatively, the maximum potential magnitude of earthquakes can be assessed using empirical scaling laws of active faults, that is, using fault length and/or fault slip (Wells and Coppersmith, 1994; Pegler and Das, 1996; Mai and Beroza,

20   2000; Henry and Das, 2001; Liu-Zeng et al., 2005; Leonard, 2010; Thingbaijam et al., 2017). In this latter case, however, a lack of information on fault age and earthquake recurrence time may induce to neglect some faults as potential seismogenic sources. One method to overcome the problems connected with the lack of information on the age of (seismogenic) faulting may be to apply the existing seismic scaling relationships, which directly link fault/slip dimensions and earthquake magnitudes (e.g., Wells and Coppersmith, 1994; Leonard, 2010; Thingbaijam et al., 2017), to the whole set of known faults including the

25   (presumably-)inactive and undetermined faults. This method would rely on the long-held concept of fault reactivation (Sibson, 1985) due to the weakness of the fault surface compared with the host rock (Zoback et al., 1987; Collettini et al., 2009). This concept is particularly relevant when considering the future behaviour of faults over long terms. For nuclear plants, for instance, it is important to assess the occurrence of events, even if very unlikely, also in areas historically free of damage, where normally these plants are built. In these sites (nuclear plants) indeed only a very low level of risk can be accepted. In other cases such

30   as the geological disposals of radioactive wastes, the lifetimes to be considered are on the order of 105 years at least (up to 1 Ma according to prescriptions by the Nuclear Energy Agency and International Atomic Energy Agency, www.oecd-nea.org, www.iaea.com; NEA, 2004; IAEA, 2016). Accordingly, very long seismic return times must be considered, far exceeding the lifespan of historical seismic catalogues (and also paleoseismological records) normally used in standard seismic hazard assessment practices.

2

For the richness of data (both tectonic and catalogued historical/instrumental-seismology; Fig. 1), Italy is a suitable country for deriving and comparing the potential maximum magnitude from earthquake data and from scaling relationships. Italy has, indeed, a long tradition of geological-structural mapping over the entire territory (since at least Murchison, 1849; von Zittel, 1869; Viola, 1893; Pagani, 1907, to the recent national geological maps available online at http://sgi.isprambiente.it/geoportal/) as well as a dense seismological network operating since at least the 1980s (available online at http://cnt.rm.ingv.it/ Iside Working Group, 2016), and a rare, if not unique, historic record of earthquakes (Rovida et al., 2016).

This work includes: (1) the composition of a comprehensive catalogue of all mapped faults in Italy, merging materials from previous documents; (2) the calculations of earthquake magnitudes (FLEM, Fault-Length Earthquake Magnitude) from the fault length in map view; (3) a comparison (i.e., the difference) of these calculations (FLEM) with catalogued seismological data (historical and instrumental earthquake magnitudes); and (4) a discussion of the agreements and differences between the calculated (FLEM) and catalogued magnitudes to determine the strengths and weaknesses of the proposed method.

We anticipate that, with this work, we do not intend to propose an alternative method for seismic hazard assessment or to better previous methods (e.g., Giardini, 1999; Jiménez et al., 2001; Michetti et al., 2005; Field et al., 2009, 2015; Reicherter et al., 2009). Our main aim is to test whether solely considering the known mapped faults (both active, inactive, and undetermined) and disregarding further information (e.g., historically- and instrumentally-recorded earthquakes as well as the regional stress field and strain rate) it is possible to provide, through existing seismic scaling relationships of faults and earthquakes, reasonable assessments of the maximum possible earthquake magnitude over an entire nation. The resulting (assessed) magnitudes (FLEMs) are compared (i.e., the mathematical difference) with catalogued earthquake magnitudes that are the only existing points of reference against which assessed magnitudes can be compared. Note that these results should be considered more in a theoretical and methodological perspective for comparison with future similar studies rather than in an applicative perspective for the case of Italy. In particular, our assessed earthquake magnitudes (FLEMs) for the Italian territory are proposed in this paper for scientific reasons and not for their use for civil protection and prevention purposes.

2 Seismotectonic setting

The present setting of the Italian peninsula (Fig. 1) derives from the interaction (mostly convergence) of at least three main plates, namely, Eurasia to the north, Africa to the south, and Adria to the east and southeast. During Cenozoic-Quaternary times, this tectonic interaction has led to the formation of two major mountain chains - the Alps to the north and the Apennines along the peninsula - and to the opening of two major oceanic basins - the Ligurian-Provencal basin to the west of Sardinia and Corsica and the Tyrrhenian Sea basin between the Italian peninsula and the Sicily and Sardinia major islands (Dewey et al., 1989; Malinverno and Ryan, 1986; Doglioni, 1991; Doglioni et al., 1999; Faccenna et al., 2004; Rosenbaum and Lister, 2004; Carminati et al., 2010; Carminati and Doglioni, 2012).

The Alps and Apennines are characterized by very different tectonic styles. Whereas the Alps show double-verging growth (northward and southward), with the involvement of large volumes of crystalline basement and the exhumation of metamorphic rocks (Nicolas et al., 1990; Schmid et al., 1996), the Apennines form a single-verging chain characterized by a radial vergence

and a strong curvature from northwest to southeast. The Apennines are characterized by thin-skinned tectonics with rare exposures of the crystalline basement and metamorphic rocks (Barchi et al., 1998; Patacca et al., 2008; Scrocca et al., 2005). The development of the Apennines (contraction) occurred partly at the same time with the development of the Ligurian-Provencal and Tyrrhenian oceanic basins (extension). The different tectonic styles of Alps and Apennines are also well represented by the different settings of the related foreland monoclines and basins. The foreland basin is shallow in front of the Alps with a monocline dipping by 2-4° and deep in front of the Apennines with a monocline dipping by 6-15° (Mariotti and Doglioni, 2000).

The present seismotectonic setting of Italy is still mainly ruled by the interaction between the African and Eurasian plates, presently converging at a rate of c. 10 mm/yr along a NNW-SSE direction (DeMets et al., 1990; Serpelloni et al., 2005; Billi et al., 2011). This kinematic setting is complicated by the Adria plate (an independent microplate or a promontory of the African plate), which contributes to cause contractional deformations along the central-northern Adriatic margins (both toward the Apennines to the west and toward the Dinarides to the east) and in the Po Plain between the northern Apennines and the southern Alps. Contractional deformations are in contrast absent or poorly active in the southern Apennines where these deformations have been inactive or poorly active since about mid-Pleistocene times. In synthesis, for the aims of this work, it is important to know that most of the Italian territory has been subject to numerous deformation phases with related activations, re-activations, and/or inversions of faults. These phases are schematically amenable to one or two main complex tectonic mechanisms: the Alpine orogenesis (Paleozoic to present times) and the Hercinian orogenesis (Paleozoic times) (Vai, 2001). At present, within the Alpine orogenesis, back-arc extensional seismic mechanisms prevail in large areas of the Italian territory (e.g., the axial portion of the Apennines), whereas compressional seismic mechanisms are less frequent and prevail elsewhere (e.g., the eastern or Adriatic portion of the Apennines) (e.g., Basili and Meghraoui, 2001; Neri et al., 2002, 2005; Roberts and Michetti, 2004; Chiarabba et al., 2005, 2015; Palano et al., 2012; Presti et al., 2013; Ferranti et al., 2014; Cowie et al., 2017; Orecchio et al., 2017). Strike-slip tectonics is limited to a few major fault zones (e.g., Grasso and Reuther, 1988; Billi et al., 2003; Viganò et al., 2015; Polonia et al., 2016, 2017).

Italy has a widespread crustal seismicity (depth < 35 km) that concentrates along some portions of the Alps and mostly on the Apennines, including Calabria and Sicily (Fig. 1). Deep earthquakes are mainly located beneath the Calabrian Arc and, secondarily, beneath the northern Apennines and eastern Alps, where sparse seismicity is recorded (Chiarabba et al., 2005). The eastern and western Alps show a clustered crustal seismicity (Fig. 1), whereas in the central Alps the number of recorded events seems to be less densely distributed. This is probably related to the lack of an appropriately-dense seismic network in this area (Amato, 2004; Chiarabba et al., 2005).

The western Alps are particularly active in their southern portion, where active N-S-striking faults accommodate most of the extensional and wrench deformations that characterize the present-day tectonics of the area (Chiarabba et al., 2005; Sanchez et al., 2010; Sue et al., 1999; Sue and Tricart, 2002). Focal mechanisms of the sparse seismicity in the central Alps show extensional kinematics on N-S-striking fault planes (Chiarabba et al., 2005); however, stress field studies in this area suggest mainly active N-S compression (Montone and Mariucci, 2016). The clustered seismicity recorded in the eastern Alps is mainly located along E-W trending structures, showing an overall compressive tectonics generating large thrust earthquakes

in response to a N-S trending compression, like the 1976 Friuli, Mw = 6.4 earthquake (Bressan et al., 1998; Cheloni et al., 2012; Michetti et al., 2012).

The Apennines seismicity is densely distributed along the whole chain (Fig. 1). Focal mechanisms of the chain show a rotation of the fault strike from NW-trending alignments to NNE-trending ones moving from north to south, along the arc-like shape of the Apennines. In general, in the middle portion (axis) of the Apennines, earthquakes are characterized by extensional kinematics, whereas the Adriatic front is mainly affected by compressive kinematics, which is in agreement with the regional stress field (Montone and Mariucci, 2016). In particular, the north-western portion of the Apennines shows a NW-SE trending cluster of seismicity. Moving eastward, beneath the Po Plain, seismicity involves the northern Apennines outer front (Fig. 1), where focal mechanisms are mainly compressive, highlighting E-W-striking fault planes consistent with the attitude of the main structures of the area. Here, the largest instrumentally measured earthquakes (Mw = 6.1) occurred in 2012 during the Emilia (N-Apennines) sequence (Govoni et al., 2014). Moving southward, crustal seismicity (M 4-6.5) is densely distributed and follows the Apennine chain axis. In this zone (Umbria-Marche), the largest instrumental earthquakes with extensional focal mechanisms occurred in the 1997 Colfiorito, Mw = 6.0 (Amato et al., 1998); 2016 Norcia, Mw = 6.5 (Chiaraluce et al., 2017); 2016 Amatrice, Mw = 6.0 (Chiaraluce et al., 2017); 2009 L'Aquila (Abruzzi), Mw = 6.3 (Chiarabba et al., 2009); and 1980 Irpinia (Campania), Mw = 6.9 (Nostro et al., 1997) earthquakes. A cluster of moderate (M 4.0-5.0) seismicity is recognized close to the Tyrrhenian coast in relation to active geothermal and volcanic districts (Gasparini et al., 1985). Larger earthquakes characterize the Apennines southern portion (Calabria), with historical seismic events that reached magnitudes up to $\simeq$7.1 (Rovida et al., 2016; Guidoboni et al., 2018).

The Calabrian Arc (Fig. 1) is mostly characterized by deep instrumental seismicity related to the NW dipping Benioff plane (Polonia et al., 2016; Selvaggi and Chiarabba, 1995). Both the Etna area and the northern on-shore portion of Sicily show clustered seismicity, where the latter is mainly characterized by extensional and oblique-extensional earthquakes (Azzaro and Barbano, 2000; Billi et al., 2006a). The strongest earthquakes (some of them with associated destructive tsunamis; Billi et al., 2010) from historical catalogues in the area occurred predominantly on extensional faults and are: the 1908 (Mw 7.2) earthquake of Messina and Reggio Calabria (Messina Straits, Sicily), the 1638 and 1905 (Mw 7.0) earthquakes of Nicastro (Calabria), and the 1693 (Mw 7.4) earthquake of eastern Sicily (Rovida et al., 2016).

The Southern Tyrrhenian (Fig. 1) is characterized by intense seismicity, with magnitudes up to 7.1, which occurred in 1938 at 290 km depth (Selvaggi and Chiarabba, 1995). The seismicity of shallow levels (< 30 km) below the southern Tyrrhenian Sea indicates the presence of two adjacent domains characterized by different tectonic environments: (1) to the northwest of the Aeolian Islands, a N-S compressive tectonics is present, whereas (2) to the east and southeast of these same islands, a NW-SE extensional tectonics occurs (Fig. 2) (Goes et al., 2004; Pondrelli et al., 2004; Billi et al., 2006a; Cuffaro et al., 2010). Intermediate and deep seismicity concentrates along a roughly uninterrupted, narrow, and steep (70°) Benioff zone, which strikes SW-NE, dips toward NW, and reaches a depth of about 500 km; only one earthquake occurred inland at depth of 350 km (Pondrelli et al., 2004; Selvaggi and Chiarabba, 1995). Shallow compressive seismicity (< 30 km deep) is characterized by epicentres mainly aligned E-W (Pondrelli et al., 2004; Presti et al., 2013), off-shore northern Sicily, and it rotates roughly

NNW-SSE moving eastward (Fig. 1). Sparse compressive events have also been recorded off-shore north-eastern and southern Sardinia.

3 Input data

3.1 Fault data

5   To build a comprehensive dataset of faults in Italy (Figs. 1-3; supplement; Petricca et al., 2018), the following databases were merged: (1) the entire fault collection of the Italian Geological Maps at the 1:100,000 scale (i.e., Carta Geologica d'Italia available online at www.isprambiente.it); (2) the fault compilation from the Structural Model of Italy at the 1:500,000 scale (Bigi et al., 1989); (3) all faults provided in the ITHACA-Italian Catalogue of Capable Faults (Michetti et al., 2000); and (4) the inventory of active faults from the GNDT (Gruppo Nazionale per la Difesa dai Terremoti; Galadini et al., 2000) database.

10 The strength point of our approach is the assemblage of different fault datasets heterogeneously built for different purposes and based on different primary information and methods. In this approach, we consider all known faults (see above) to form a dataset as comprehensive as possible.

   Faults from the 1:100,000 Italian Geological Maps and 1:500,000 Structural Model of Italy (black and black dashed lines, respectively, in Fig. 2) are essentially based on field surveys integrated with subsurface geophysical data and, therefore, were

15 drawn and constrained by geological and geophysical observations.

   The ITHACA-Italian Catalogue of Capable Faults (Michetti et al., 2000) is a database developed by the ISPRA (Istituto Superiore per la Protezione e la Ricerca Ambientale) containing cartographic and parametric information of active faults - i.e., faults with evidence of repeated reactivation during the last 40,000 years - capable of rupturing the ground surface in Italy. The database is available as a layer in a web GIS (http://www.isprambiente.gov.it/it/progetti/suolo-e-territorio-1/ithaca-catalogo-

20 delle-faglie-capaci) and contains both the geographic location and a text description of each fault. The entire set of capable faults is included in this compilation (blue lines in Fig. 2).

   The inventory of active faults of the GNDT database (Galadini et al., 2000) represents a collection of the Italian active faults. The activity of these faults is mainly deduced through surface geological evidence and (paleo)seismological data including historical information (red lines in Fig. 2).

25   To improve and implement these fault databases, we selected published complementary studies for some specific areas considered to not be exhaustively covered by the aforementioned collection of faults including Sardinia, SW Alps, Tuscany, the Adriatic front, Puglia, and the Calabrian Arc. For these areas, we selected faults on the grounds of scientific contributions that documented faults presence based on field, seismic, and paleoseismological data (pink lines in Fig. 2). In particular, for the Campidano area (southern Sardinia), we used the fault pattern proposed by Casula et al. (2001), who reconstructed fault

30 geometry with recent tectonic activity based on field and seismic reflection profiles. For the SW Alps, we followed the works of Augliera et al. (1994), Courboulex et al. (1998), Larroque et al. (2001), Christophe et al. (2012), Sue et al. (2007), Capponi et al. (2009), Turino et al. (2009) and Sanchez et al. (2010). For the Tuscany area, we consulted Brogi et al. (2003), Brogi et al. (2005), Brogi (2006), Brogi (2008), Brogi (2011) and Brogi and Fabbrini (2009). For the buried northern Apennines and

Adriatic front, we used the fault datasets provided by Scrocca (2006), Cuffaro et al. (2010) and Fantoni and Franciosi (2010). For the Puglia region, we used data from Patacca and Scandone (2004) and Del Gaudio et al. (2007), whereas, for the Calabrian Arc, we used data from Polonia et al. (2016) and Polonia et al. (2017).

Furthermore, we are aware of the DISS compilation of seismogenic sources in Italy (Basili et al., 2008; DISS Working Group, 2018) as one of the most important integrated datasets of the Italian territory in this field. However, we did not use this dataset in this work since, as described in Basili et al. (2008), the dataset aims to identify the "seismogenic sources" rather than the actual faults. A composite seismogenic source (CSS in the DISS nomenclature) is a complex fault system showing homogeneous kinematic and geometric parameters and contains an unspecified number of aligned possible ruptures (i.e., faults) that cannot be isolated. Hence, a CSS, for its own nature, cannot be considered a real fault as declared in our scope.

The above-mentioned fault datasets form a comprehensive tectonic image of the Italian territory (Fig. 2). These fault data and the spatial grid are available for download as ASCII files in the supplement (see also Petricca et al., 2018). The major thrust faults occur along (1) the N-verging western and north-western external front of the northern Alps, (2) the S-verging frontal ramp of the southern Alps (Po Plain and Veneto-Friuli regions), (3) the E- to N-verging external front of the central-northern Apennines from the Po Plain down to the central Adriatic off-shore, (4) the SE-verging outer front of the Calabrian Arc, (5) the outer (southern) front of the Maghrebian-Apennines chain in Sicily, and (6) the E-W-trending contractional belt located in the southern Tyrrhenian Sea, close to the northern Sicily coast.

The major normal faults occur along the median zone of the Apennines fold-thrust belt (Fig. 2), namely: (1) in northern Tuscany, (2) in central Italy including the Tuscany, Umbria, Marche, and Abruzzi regions, (3) in the southern Apennines including the Molise, Campania, Basilicata, and Calabria regions, and (4) in eastern Sicily including the Messina Straits, part of the Ionian Sea areas, and the Hyblean foreland. In particular, SW-dipping, high-angle normal faults (NW-striking) host the strongest seismicity recorded along the northern-central Apennines belt (Figs. 1 and 3). This fault pattern rotates to a NE-trending direction toward the southern Calabria region consistently with the focal solutions of the area (Fig. 1). Moreover, extensional faults have also been mapped in the Sardinian region, specifically in the Campidano graben, mainly based on subsurface data (Casula et al., 2001).

Strike-slip faults are located in some areas of the Italian territory (e.g., Billi et al., 2003, 2007), in particular: (1) in the southern Alps (Veneto) with NNW-striking structures, (2) across the external front of the central-southern Apennines foreland-fold-thrust belt (e.g., south of the Montemurro area, Fig. 1), (3) along the central Adriatic-Gargano-Molise belt with E-W-striking structures, (4) across the Calabrian Arc with radial structures cutting through the accretionary wedge, (5) in eastern Sicily from the Aeolian Islands (Tyrrhenian Sea) and southward into the Ionian Sea, and (6) in south-western Sicily and in the Sicily Channel with structures striking between N-S and NNE-SSW (Figs. 1 and 2).

3.2 Earthquake data

To obtain a complete earthquake dataset for the Italian territory (Figs. 1 and 3; supplement; Petricca et al., 2018), we integrated the existing most comprehensive catalogues of instrumental and historical seismicity: (1) the CSI1.1 instrumental database (csi.rm.ingv.it; Castello et al., 2006) for the 1981–2002 period; (2) the ISIDe instrumental database (iside.rm.ingv.it; Iside

Working Group, 2016) for the 2003–2017 period; and (3) the CPTI15 historical-instrumental database (emidius.mi.ingv.it; Rovida et al., 2016) for the 1000-1981 period.

The CSI 1.1 database (Castello et al., 2006) is a catalogue of Italian relocated earthquakes for the 1997–2002 period. This collection derives from the work by Chiarabba et al. (2005), who relocated, using a homogeneous procedure, approximately 45,000 events provided by several seismological networks (both national, regional, and local) operating in the Italian territory. Most seismic events are lower than 4.0 in magnitude and are mostly located in the upper 12 km of the crust. A few earthquakes exceed magnitude 5.0, whereas the largest event is Mw 6.0. The time-span of this compilation is 1981–2002. From the CSI 1.1 database, we selected events with Mw > 4.0 (Fig. 3).

The ISIDe database (Iside Working Group, 2016) provides the parameters of earthquakes from real-time recordings and from the Italian Seismic Bulletin. The main aim of this database is to supply information on the seismicity as soon as it becomes available by integrating it with updated information on past seismicity. The time-span of this compilation begins in 1985 and lasts up to the present day. To avoid an overlap with the CSI database (1981–2002), from the ISIDe database, we considered events with Mw > 4.0 only from the 2003–2017 period (Fig. 3).

The CPTI15 historic database integrates the Italian macroseismic database version 2015 (DBMI15; Locati et al., 2016) and instrumental data from 26 different catalogues, databases, and regional studies (including the CSI and ISIDe databases) for the Italian territory, starting from 1000 A.D. until 2014. This catalogue provides moment magnitudes from macroseismic determination for more than 3200 earthquakes with values in the 4-7 range of Mw. To avoid any overlapping of data with the aforementioned instrumental datasets, we used data from the 1000-1981 period from the CPTI2015 catalogue.

We acknowledge that the earthquake magnitude used in this paper is the moment magnitude (Mw) and it should be noted that, for a few earthquakes from the aforementioned datasets, only the Ml (local magnitude) is available. However, according to Grünthal and Wahlström (2003), the difference between Mw an Ml can be ignored for magnitudes above 4, which represents the main focus of this study.

4 Method

4.1 FLEM computation

Starting from the entire dataset of faults in Italy, as a first step, we measured the length of each fault as the real fault trace length in map view, i.e., the length of the vertical projection of the fault trace as observed on the Earth's surface over a horizontal plane (Fig. 2; supplement; Petricca et al., 2018). Our complete dataset includes 12467 faults. Specifically, it includes 9169 A-class faults and 3298 B-class faults. Explanations for the classification into A- and B-class faults are given in the following sections. As most faults have a horizontal length that is less than 25 km regardless of the selected database (Fig. 4), we divided the Italian territory into a grid with square cells of 25x25 km (Fig. 5; i.e., see also the explanation below). The length of the longest fault crossing each cell determined the parameter "fault length" (Lf) of the considered cell. In the second step, we used these lengths (Lf) as input parameters to empirically derive the earthquake magnitude (i.e., FLEM) of each cell containing at least one fault (Supplement; Petricca et al., 2018). Our only criterion to choose the fault from which the FLEM of the considered cell

is computed is the greatest fault length in map view. In such a way, only one fault (the longest one) will provide the FLEM in a given cell. Therefore, faults cannot be and are not double-counted. Several studies investigated the scaling relationship between earthquake magnitudes and various geometric-kinematic parameters (i.e., fault dimensions and slip) of causative faults (e.g., Wells and Coppersmith, 1994; Leonard, 2010; Thingbaijam et al., 2017, and references therein), providing similar empirical
5   equations. We used the equation proposed by Leonard (2010) (hereafter named as L10) that is expressed as:

$$FLEM = M = a + b * log(Lf) \hspace{4cm} (1)$$

where a and b are constants related to fault kinematics and are equal to 4.24 and 1.67, respectively (see table 6 in Leonard, 2010), and Lf is the fault length as explained above. From Eq. 1, in our study, FLEM values range from 4.74 to 7.40, where the two end members are obviously imposed by the minimum and maximum fault length of the dataset, i.e., $\simeq 2$ and $\simeq 75$ km,
10   respectively (Supplement; Petricca et al., 2018). Reasons for the choice of L10 are explained below.

4.2 Limits and assumptions

The method used in this study is based on some approximations and assumptions regarding the following points: (1) the arbitrary dimension of the cells (25x25 km); (2) the choice of the Leonard's equation and parameters (L10; Leonard, 2010) instead of others (e.g., Wells and Coppersmith, 1994); (3) the reliability of fault lengths; and (4) the assumption that all
15   considered faults are active or can be potentially reactivated.

(1) Cell dimensions: as explained above, we choose a cell size of 25x25 km after considering the mean length (Figs. 4 and 5) of our fault dataset (Supplement; Petricca et al., 2018). Moreover, crustal earthquakes in Italy are mostly generated at a depth of 4-10 km. Within this depth range, the attitude of faults determines the distance between the fault trace and the epicentre over the Earth's surface. For instance, a hypocentral depth of 10 km along a causative fault dipping 45° implies a horizontal shift of
20   about 10 km between the fault trace on the Earth's surface and the earthquake epicentre. Since the hypocentral depth is usually less than 10 km, a cell dimension of 25 km favours the occurrence of causative faults and related earthquake epicentres in the same cell. Moreover, to test the suitability of the size (25 km) of our square cells, we tested the sensitivity of the FLEM and the difference between the FLEM and the catalogued earthquake magnitudes on the cell size. We performed this sensitivity test on central Italy that is one of the most seismic areas of Italy. In this area, we changed our grid (i.e., cell size 25x25 km) both
25   into a finer grid characterized by a cell size of 12.5x12.5 km and into a coarser grid characterized by a cell size of 50x50 km (Figs. S1 and S2). Each 50 km side square cell includes four 25 km side square cells and sixteen 12.5 km side square cells. For all cells, we computed the FLEM (Fig. S1) and the difference between the FLEM and the catalogued earthquake magnitudes (Fig. S2). Then, cell by cell, we compared results (i.e., the FLEM) obtained for the largest and smallest grids (i.e., with square cell size of 12.5 and 50 km) against the FLEM obtained in the same geographical position using the intermediate grid (i.e.,
30   with square cell size of 25 km) (Fig. S3). This analysis shows that a change of grid size between 12.5 and 50 km does not provoke dramatic changes in the spatial distribution of both the FLEM (Fig. S1) and the difference between the FLEM and the catalogued earthquake magnitudes (Fig. S2). In particular, using the largest grid (cell size = 50 km), the FLEM tends to

be smoothed toward an upper boundary between magnitude 6 and 7 (Fig. S3a). This is due to the fact that only the longest faults of the dataset are considered for the FLEM computation. On the contrary, using the smallest grid (cell size = 12.5 km), the FLEM tends to be rather scattered and depressed around a magnitude 6 (Fig. S3a). This is due to the fact that reducing the cell size, in many cases, minor (small) faults result as being the longest ones in small cells. These results are also synthetically
5   expressed by the arithmetic averages of non-null FLEMs in the three different grids that are: $FLEM_{average}$ = 6.04, 6.19, and 6.62 for the grids with 12.5, 25, and 50 km sized cells, respectively. This sensitivity analysis shows that a microzonation (12.5 km sized cells) tends to locally overvalue small faults that are clearly poorly relevant when compared with adjacent (10-20 km distant) longer faults. On the contrary, a macrozonation (50 km sized cells) could overvalue long faults whose effect may be strongly reduced in a large area such as that included in a 50x50 km cell. Our choice (cell size = 25 km) appears therefore a
10 good compromise between significant faults and their potential areal influence.

   (2) Adopted equation parameters: The most popular scaling equations that directly relate fault length and earthquake magnitude are provided by Wells and Coppersmith (1994), Leonard (2010), and Thingbaijam et al. (2017), among others. In this work, we used the equation (L10) by Leonard (2010) for dip-slip faults (both extensional and compressional). This equation is particularly suitable for Italy, where most earthquakes are generated by dip-slip faults (e.g., Chiarabba et al., 2005). The main
15 advantage of using Eq. 1 is that L10 is valid for both buried and outcropping fault as well as for normal and reverse (dip-slip) faults. To assess the difference (i.e., Fig. 6) between L10 and the equations provided by others, in Fig. 6a, we plotted the computed earthquake magnitude as a function of fault length for all scaling equations by Wells and Coppersmith (1994), Leonard (2010), and Thingbaijam et al. (2017). Fig. 6b shows the difference between L10 and all other equations. For large fault lengths (i.e., corresponding to large earthquake magnitudes), the difference is mostly less than 5%. This difference increases to about
20 15% for smaller faults (i.e., for fault length ≤ 2 km) corresponding to earthquake magnitudes less than about 4.8 (Fig. 6a). These fault lengths (≤ c. 2 km) and earthquake magnitudes (≤ 4.8) represent the lower boundary of this study. For this reason, we assessed the difference of results from L10 with results from other scaling equations (Fig. 6) as acceptable for the aims of our study. In particular, also considering the version of L10 given for strike-slip faults, the difference with the version of L10 that we used (i.e., for dip-slip faults) is less than 3% (Fig. 6b). Note also that, due to the lower boundaries of the magnitude
25 range for which the equations considered in Fig. 6 are valid (i.e., Mw ≥ 4.8-5.0 forWells and Coppersmith (1994) and Mw ≥ 5.8 for Thingbaijam et al. (2017)), Fig. 6 is relevant for Mw higher than these lower boundaries.

   (3) Fault length reliability: FLEM is calculated through Eq. 1 from the longest fault falling in each cell (Fig. 5). For faults located on-shore and well exposed at the surface, detailed studies allow for a well-constrained and reliable characterization of fault length (class A faults). On the contrary, for some specific regions like the south-western Alps, the eastern front of the Po
30 Plain, the eastern Alps, the off-shore Adriatic front and Calabrian Arc, where fault planes are not exposed at the surface (i.e., buried and/or off-shore faults), fault geometry has been mainly constrained from regional seismic reflection profiles or from earthquake sequences. Therefore, fault length and along strike continuity are not well constrained, hence, producing the longest faults of the whole dataset. We assess the dimension of these latter faults as poorly constrained and reliable (class B faults). Following this analysis on the accuracy on fault dimension, we decided to divide the dataset into two quality classes. Class A
35 (high quality) includes exposed faults where subsurface and surface data allow for a detailed and reliable characterization of

fault length (light purple cells in Fig. 5), whereas class B (low quality) contains buried and off-shore faults investigated mainly by seismic surveys, for which a precise characterization of fault length cannot be achieved (dark grey cells in Fig. 5). Moreover, we acknowledge that FLEM (fault length earthquake magnitude) is indeed the maximum magnitude expectable from the actual size of the causal faults based on Eq. 1. A co-seismic lengthening of the causal faults through, for instance, the rupture of a

5 bridge separating two adjacent faults to form one may produce earthquakes with a magnitude greater than that expected from the length of each of the two faults as measured before the fault co-seismic junction.

(4) Fault orientation and activity: although it is well known that each earthquake is usually associated with a precise slip on a fault plane and that the potential of a fault to undergo (seismic) slip depends on its orientation within the stress field (Morris et al., 1996; Collettini and Trippetta, 2007), it is also true that the seismic history of the Earth is characterized by many

10 examples of unexpected earthquakes occurring where plate boundaries are far away (i.e., intraplate earthquakes), and/or the stress field is apparently badly oriented to trigger earthquakes (Bouchon et al., 1998; Camelbeeck et al., 2007; Kafka, 2007; Stein and Mazzotti, 2007; Swafford et al., 2007; Braun et al., 2009; Boyd et al., 2013; Leonard et al., 2014; Talwani, 2014; Campbell et al., 2015; Walsh III and Zoback, 2016; Christophersen et al., 2017). Since our study aims to define the Fault-Length Earthquake Magnitude (FLEM) of each fault and cell, based on the aforementioned instances, we assumed that all faults are

15 potentially reactivable. This notion becomes increasingly relevant when considering the prospective behaviour of faults over long terms. As mentioned above, indeed, for some societal challenges such as the safety of nuclear waste repositories, the recommendations are to consider the behaviour of faults in the future up to even 1 Ma (see, for instance, prescriptions by the Nuclear Energy Agency and International Atomic Energy Agency, www.oecd-nea.org, www.iaea.com; NEA, 2004; IAEA, 2016).

20 **5   Results and discussion**

Bearing in mind the limits mentioned above, we firstly calculated the FLEM for the Italian territory using the faults of class A (Fig. 7; supplement; Petricca et al., 2018). Most of the Italian territory, including the entire Apennine belt, the north-eastern Alps, and the central part of the Po Plain, is characterized by $6.0 \leq FLEM \leq 7.0$. The largest FLEMs have been obtained for the north-eastern Alps (FLEMs ≤ 7.4) and are mainly related to the E-W-striking thrusts of the area responsible for the 1976 Friuli

25 earthquake (Mw = 6.4; Bressan et al., 1998; Cheloni et al., 2012). In this area, we recall also the Carinthian great earthquake of 1348 (Villach, Mw 7.0; Rohr, 2003). In the central Alps, long and continuous thrust faults are reported in the ITHACA dataset (e.g., Maurer et al., 1997; Keller et al., 2006) and result in FLEMs of about 6.5. These large thrust faults also characterize the western part of the Po Plain, producing FLEMs of about 7.0. FLEMs between 6.5 and 7.0 are also estimated toward the south along the Apennine chain and in the Tuscany region, where large normal faults are reported from the ITHACA dataset and

30 confirmed by detailed studies (Brogi et al., 2003; Brogi and Fabbrini, 2009). The largest FLEMs along the northern Apennines (Fig. 7) are due to the Alto Tiberina low angle normal fault, a large regional structure that seems to accommodate part of the deformation by aseismic creep and microseismicity (Chiaraluce et al., 2007; Collettini, 2011; Anderlini et al., 2016).

Large FLEMs occur also in the Vesuvius area (Campania region), where faults longer than 30 km have been reported in the ITHACA dataset (Fig. 5). Several studies (Finetti and Morelli, 1974; Scandone and Cortini, 1982; Vilardo et al., 1996; Brozzetti, 2011) confirm the presence of these long faults in the Vesuvius area. In the southern Apennines (Campania, Basilicata, and Calabria regions), FLEMs are in the range of 6.5-7.0, being related to the largest extensional faults of the area (Figs. 2 and 5). To the south, in the northern portion of Sicily, FLEMs > 7.0 are related to long off-shore faults. Some of these FLEMs are related to the transtensional-transpressional Tindari Fault System, located in NE Sicily. Other FLEMs are connected to the extensional system of the Messina Straits (Ghisetti, 1979; Locardi and Nappi, 1979; Lanzafame and Bousquet, 1997; Billi et al., 2006b, 2007; Palano et al., 2012; Cultrera et al., 2017).

The map of FLEMs derived using class B faults (Fig. 8) shows seismic events in the magnitude interval of 5.0-6.0 in the Tyrrhenian sector and in the southern portions of Puglia. Large FLEMs (up to $M \simeq 7.85$) occur along the north-eastern Alps, the thrust fronts beneath the Po Delta, the north Adriatic front, the Ionian off-shore of the Calabria-Peloritani Arc, and some areas of Sardinia (Fig. 8). FLEMs $\simeq 8.0$ derive from structures constrained only by subsurface data, for which the along-strike continuity cannot be properly assessed and, hence, the total length is likely to be largely overestimated. The largest FLEMs calculated for the Sardinian territory are related to structures inferred from large-scale (1:500,000) maps. These structures are longer (Fig. 5, red segments) than those derived, in the same areas, from detailed studies (Fig. 5, pink segments) and, therefore, the actual length is also likely to be overestimated in this case.

To compare the FLEMs estimated on the grounds of geological fault length (Figs. 7 and 8) with the maximum magnitudes obtained from the historical and instrumental seismicity databases (i.e., catalogued earthquake magnitudes), we used the same grid presented above (Fig. 5). In particular, for each cell of Fig. 5, we selected the maximum earthquake magnitude recorded in historical or instrumental earthquake databases, applying a lower cut-off at magnitude 4.0 (Fig. 9). Large earthquake magnitudes - i.e., $M > 6.0$ earthquakes - were recorded in the north-eastern Alps, in the Po Plain, and along the entire Apennine chain. The strongest events ($M \leq 7.4$) were recorded in the north-eastern Alps and in the southern portion of the Apennines, including the Messina Straits and southern Sicily (Fig. 9). Earthquakes with magnitudes $\simeq 4.0-4.5$ occurred almost everywhere in the Italian territory.

To spatially compare the earthquake magnitudes obtained through the FLEM computation (Figs. 7 and 8) and those recorded in the historical-instrumental catalogues (Fig. 9), we realized a map of the earthquake magnitude differences to show for each cell the difference between FLEMs obtained from the length of class A (Fig. 10) and class B (Fig. 11) faults and the magnitudes of historically/instrumentally-recorded earthquakes. In the case of class A faults, this comparison (Fig. 10) shows, in general, a difference of $M \leq 1.5$. By fitting the differences distribution with a Gaussian curve, we obtained a mean of 0.86 with a 2σ (double standard deviation) of 1.47 on FLEMs derived from class A faults (Fig. 12a). The 2σ value is amplified to 1.85 (Fig. 12b) when also considering FLEMs from poorly reliable fault lengths (i.e., difference for class A+B faults in Fig. 12b).

Finally we compared FLEMs with only the strongest earthquakes ($M \geq 6.5$) in the historical and instrumental catalogues since 1000 A.D. to 2017 (Fig. 13 and also Table 1). In this case, the difference with the spatially-corresponding FLEMs (i.e., same cell) is less than 1.0 and, in most instances, less than 0.4 (Fig. 13a). In particular, the mean difference is -0.09 with a 2σ value of 0.53 (Fig. 13c). Note also that, even when not equal to the spatially-corresponding catalogued earthquake magnitudes,

yet many FLEMs fall within the uncertainty interval (i.e., in Fig. 13b, see the red circles falling along the blue vertical bars) associated with these catalogued magnitudes.

In the histograms of Figs. 12 and 13(c), the values in the negative fields can be interpreted as FLEM's underestimation (i.e., where FLEM values do not reach the catalogued earthquake magnitudes, which are in turn affected by uncertainty; e.g., Fig. 13b). In contrast, values in the positive fields of Figs. 12 and 13(c) could be interpreted either as FLEM's overestimation (i.e., where FLEM values unsuitably exceed the catalogued earthquake magnitudes) or as a sort of catalogue incompleteness (i.e., where the catalogued earthquake magnitudes do not properly represent larger seismic potentials of faults). Occurrences in the positive fields (green portions in Figs. 12 and 13c) are significantly more frequent than occurrences in the negative fields (red portions in Figs. 12 and 13c), particularly in Fig. 12. These positive and negative occurrences are also mapped in Figs. 10 and 11 with green and red tones, respectively, whereas white cells are where FLEM's differences with respect to catalogued earthquake magnitudes are about null. Figs. 10 and 11 show that negative (red) occurrences are very limited.

It is also interesting to note that, in the period between our dataset of catalogued earthquakes (i.e., in times younger than December 2017) and the time of writing (September 2018), only one crustal M>5 earthquake occurred in Italy. Namely, the Montecilfone Mw 5.1 earthquake occurred on August 16th, 2018, in the central Apennines at latitude 41.87N and Longitude 14.86E and depth of 20 km. In the same locality, our FLEM is 5.9, corroborating the observations and considerations made above on the difference between FLEMs and catalogued earthquake magnitudes.

Summarizing, the difference between FLEMs and catalogued earthquakes can be either real, indicating that some large earthquakes, possibly due to extremely long recurrence intervals, are not contained in the seismological records, or a bias induced mainly by the following factors: (1) impossibility to resolve fault continuity and segmentation with the adopted method and (2) deformation partially accommodated through aseismic creep.

The limited difference, as discussed above, between FLEMs and the catalogued earthquake magnitudes (Figs. 12a and 13c) is due to the comprehensive knowledge of the exposed faults (particularly faults of class A, Fig. 12a). A large amount of data is indeed available from detailed field surveys and subsurface investigations realized over the years. However, some portions of the eastern Alps, northern Apennines, and southern Italy, including Sicily, show a difference in the magnitude of 2.0-2.5 (i.e., faults of class B, Fig. 12b). In these areas, more detailed studies should be developed in order to better characterize fault dimensions and properly assess seismic hazards. It is, however, very encouraging that when considering only the historical and instrumental earthquakes with $M \geq 6.5$, the difference between FLEM values and the catalogued earthquake magnitudes significantly reduces (Fig. 13).

Regarding the FLEMs evaluated using class B faults (Fig. 11), we observe a significant difference with catalogued earthquakes in several regions. Differences of up to 4.0 in magnitude (Fig. 12b) are estimated in correspondence of the north Adriatic thrust front, off-shore from the Calabria-Peloritani Arc, and the northeast part of the Alps (Fig. 11). Smaller, but still relevant, differences of $M \simeq 2.0$ are documented in correspondence of the Apennines front beneath the Po Plain. As mentioned above, class B fault lengths have been evaluated mostly using seismic reflection profiles. Due to the resolution of this technique and the quality of some datasets, fault segmentation cannot be properly evaluated. More evidence would be needed. In general, the significant differences between FLEMs (class B faults) and the catalogued magnitudes require that extensive 3D geological

and geophysical investigation of the structures of these areas should be performed in order to better characterize the geometry and continuity of faults. To this end, it is also noteworthy that studies on the 2016 Amatrice-Norcia (central Italy) earthquakes (Mw 6.0 and 6.5) revealed that the length of the causative faults was only partially activated by the seismogenic slip (e.g., Chiaraluce et al., 2017); however, as this fault-slip behaviour seems rather frequent (Freymueller et al., 1994; Milliner et al.,

5 2016; Chousianitis and Konca, 2018), it is most likely that this same behaviour is incorporated and implicitly expressed by the above-mentioned empirical scaling relationships between fault length and earthquake magnitude (e.g., Wells and Coppersmith, 1994; Leonard, 2010; Thingbaijam et al., 2017).

6 Statistical Test of FLEM Values

The reliability of estimated FLEM values may be quantitatively checked, in principle, using a formal statistical test on earth-

10 quake catalogues. Anyway, models of expected maximum magnitude (Mmax) are not readily testable. A statistical test helping to discriminate between competitive FLEM values is impossible in practice, even in the simplest case of discriminating between a double truncated Gutenberg-Richter (DTGR) law and an unbounded Gutenberg-Richter (UGR, Mmax=∞) law on excellent datasets (Holschneider et al., 2014). Suffice is to say that the DTGR's probability distribution differs from the UGR's one by a constant $c = 1 - 10^{-b(M_{max} - M_c)}$ (where M_c is the minimum magnitude). This value is very close to 1, if not when

15 M_c is close to Mmax. This means that the upper cut-off of the Gutenberg-Richter distribution can be explored using only large, very rare earthquakes, with magnitudes close to the maximum possible value, on which statistical inference is necessarily limited (Holschneider et al., 2014). Therefore, it is essentially impossible to statistically infer, with sufficient confidence, the maximum possible earthquake magnitude, in terms of alternative testing, from an earthquake catalogue alone (Holschneider et al., 2014). In light of the limitations of purely statistical inference, geological and tectonic information provides, therefore,

20 important and exclusive constraints on the expected maximum magnitude. If we look at statistical testing in detail, we can check the FLEM values on a catalogue, while controlling the probability of wrongly rejecting them, but without reducing the probability of a wrong non-rejection (Holschneider et al., 2014). This makes it, indeed, impossible to discriminate between two likely values of FLEM. In other words, if we do not reject a FLEM value, we cannot say if it is true or if the data are inadequate in terms of revealing its failure. Keeping all these considerations in mind, we test the estimated FLEM values on

25 the CSI1.1 and ISIDe databases (available online at https://csi.rm.ingv.it/ and http://iside.rm.ingv.it/, respectively). Since our analysis requests a database containing small magnitudes events, we consider ISIDe data of earthquakes occurred before April 16 2005, when the new INGV (Istituto Nazionale di Geofisica e Vulcanologia) National Seismic Network, completely reorganized and equipped with a new acquisition system, became operational (Amato and Mele, 2008). Without this separation, the hypothesis of temporal homogeneity for magnitude data would not be appropriate. Moreover, most events in the ISIDe and

30 CSI1.1 databases have a ML magnitude, while FLEM values are in moment magnitude scale. Therefore, we repeat the same testing procedure, described below, twice, without any difference in results: firstly, we consider original FLEM values and, secondly, we convert them in local magnitude scale through the relations proposed by (Gasperini et al., 2013). We adopt the following test procedure.

14

a) We select cells for which a test is helpful, i.e. having a FLEM value above the related historical/instrumental observed magnitude. In this way we exclude 41 of 1100 cells for which FLEM values are estimated. A further selection consists of keeping only cells for which the Gutenberg-Richter model, with a b-value equal to 1, is not rejected. In this way, we are sure that a possible rejection of FLEM values cannot be ascribed to the low reliability of a Gutenberg-Richter relation or to wrong b-values. To this end, we apply a goodness of fit test (GFT, Wiemer and Wyss, 2000), at a 95% confidence level, that also provides a completeness magnitude value, M_c, for each cell. The GFT is based on difference R of the observed (O_i) and expected (E_i) numbers of events in each magnitude bin. Values E_i are computed by assuming a UGR distribution, with a b-value equal to 1, above an ascending magnitude cutoff Mt. So that R is given by:

$$R(M_t) = 1 - \frac{\sum_i |E_i - O_i|}{\sum_i O_i} \tag{2}$$

where sums are done for magnitude bins above M_t. The completeness magnitude M_c is defined as the first value of M_t for which R(M_t)>0.95. The cells passing this test are 30 (Table S1) and 67 (Table S2) for the CSI1.1 and ISIDe databases, respectively. We stress that this first test does not require a Mmax value.

b) A first specific check of the DTGR distribution, having FLEM as maximum magnitude, is carried out by using a log-likelihood test. Specifically, for each cell passing the previous test, the log-likelihood value of the DTGR model is computed. By considering that a DTGR distribution has a probability density function given by:

$$f_{DTGR}(M) = \frac{\beta e^{\beta(M-M_c)}}{1 - e^{\beta(Mmax-M_c)}} \tag{3}$$

where $b = \beta ln(10)$; we compute for each cell the real log-likelihood LL$_R$ on N events magnitudes $M_i, i = 1, .., N$, by equation:

$$LL_R = \sum_{i=1}^{N} ln[f_{DTGR}(M_i)] \tag{4}$$

The DTGR model is rejected if LL$_R$ is significantly lower than expected values. The probability of having smaller log-likelihood values than LL$_R$ is estimated using 10^4 simulated datasets (having the same size of real datasets) by model DTGR. Specifically, for each cell, we compute this probability pLL as the proportion of simulated log-likelihoods smaller than LL$_R$. We select cells for which these probabilities are larger than 5%. In this way, the cells are reduced to 20 and 45 for the CSI1.1 and ISIDe databases, respectively (Figure 14 and Tables S1 and S2). We stress that we select the same cells by assuming a UGR model, suggesting that the problem of excluded cells lies in the whole Gutenberg-Richter relation and not in the FLEM values.

c) Finally, FLEM values are tested by applying the procedure proposed by (Holschneider et al., 2014), involving a comparison of the maximum observed magnitude with a suitable threshold magnitude, computed by the DTGR model. Specifically, we reject the FLEM values, if the observed magnitude (oMmax) is larger than a threshold value M_t, given by:

$$M_t = M_c - \frac{1}{\beta} ln\{1 - (1-\alpha)^{\frac{1}{n}} (1 - e^{-\beta(FLEM-M_c)})\} \tag{5}$$

where $\alpha = 0.05$ (see Holschneider et al., 2014, for details). The computed threshold values (M_t1) are listed in Tables S1 and S2, together with oMmax values. All previously selected cells pass this test, for both the CSI1.1 and ISIDe databases, suggesting that related FLEM values cannot be rejected (Figure 14 and Tables S1 and S2).

d) The last two steps are repeated by reducing the magnitude range covered by data. Specifically, we increase, where possible, the minimum magnitude to FLEM-2.0. The relative threshold values M_t2 are listed in Tables S1 and S2 for the CSIv1.1 and ISIDe databases, respectively. Also in this case, we cannot reject the FLEM values. As stated above, this analysis does not exclude alternative values of FLEM; as matter of fact, it is also the case that a UGR model cannot be rejected in all the selected cells.

7 Conclusions

In this study, (1) we first provided an updated compilation of all mapped faults in Italy, (2) then, using known scaling laws, calculated the related Fault-Length Earthquake Magnitude (FLEM), and, (3) finally, compared FLEM values with historically/instrumentally-catalogued earthquake magnitudes. Where faults are geologically well constrained (class A faults), either good agreements or some differences are observed between FLEMs and historically/instrumentally-catalogued earthquake magnitudes: the agreement is increased for M ≥ 6.5 earthquakes. In areas where fault geometries are poorly constrained (class B faults inferred solely by subsurface 2D investigations), large differences are observed: these areas have to be further characterized to better estimate fault dimensions and hence properly assess the FLEM. Our results are partly encouraging and suggest the testing and validation of this experiment elsewhere. This method cannot, however, be a substitute for time-dependent (paleo)seismological methods for seismic hazard assessments. Rather, it can provide an approximate perspective time-independent seismic potential of faults and highlight areas where further detailed studies are required.

References

Amato, A.: Crustal and deep seismicity in Italy: a Review, Special volume of the Italian Geological Society for the IGC, 32, 201–208, 2004.

Amato, A. and Mele, F.: Performance of the INGV National Seismic Network from 1997 to 2007, Annals of Geophysics, 51, 417–431, https://doi.org/10.4401/ag-4454, 2008.

5 Amato, A., Azzara, R., Basili, A., Chiarabba, C., Ciaccio, M., Cimini, G., Di Bona, M., Frepoli, A., Hunstad, I., Lucente, F., et al.: Geodynamic evolution of the Northern Apennines from recent seismological studies, Mem. Soc. Geol. It, 52, 337–343, 1998.

Anderlini, L., Serpelloni, E., and Belardinelli, M. E.: Creep and locking of a low-angle normal fault: Insights from the Altotiberina fault in the Northern Apennines (Italy), Geophysical Research Letters, 43, 4321–4329, https://doi.org/10.1002/2016GL068604, 2016.

Augliera, P., Béthoux, N., Déverchère, J., and Eva, C.: The Ligurian Sea: new seismotectonic evidence, Bollettino di Geofisica Teorica ed
10 Applicata, 36, 363–380, 1994.

Azzaro, R. and Barbano, M. S.: Analysis of the seismicity of Southeastern Sicily: a proposed tectonic interpretation, Annals of Geophysics, 43, 171–188, https://doi.org/10.4401/ag-3628, 2000.

Barchi, M., Minelli, G., and Pialli, G.: The CROP 03 profile: a synthesis of results on deep structures of the Northern Apennines, Mem. Soc. Geol. Ital, 52, 383–400, 1998.

15 Basili, R. and Meghraoui, M.: Coseismic and postseismic displacements related with the 1997 Earthquake Sequence in Umbria-Marche (Central Italy), Geophysical research letters, 28, 2695–2698, https://doi.org/10.1029/2000GL012102, 2001.

Basili, R., Valensise, G., Vannoli, P., Burrato, P., Fracassi, U., Mariano, S., Tiberti, M. M., and Boschi, E.: The Database of Individual Seismogenic Sources (DISS), version 3: summarizing 20 years of research on Italy's earthquake geology, Tectonophysics, 453, 20–43, https://doi.org//10.1016/j.tecto.2007.04.014, 2008.

20 Bigi, G., Bonardi, G., Catalano, R., Cosentino, D., Lentini, F., Parotto, M., Sartori, R., Scandone, P., Turco, E., and (Eds.): Structural Model of Italy 1:500,000, C.N.R., Progetto Finalizzato Geodinamica, 1989.

Billi, A., Salvini, F., and Storti, F.: The damage zone-fault core transition in carbonate rocks: implications for fault growth, structure and permeability, Journal of Structural geology, 25, 1779–1794, https://doi.org/10.1016/S0191-8141(03)00037-3, 2003.

Billi, A., Barberi, G., Faccenna, C., Neri, G., Pepe, F., and Sulli, A.: Tectonics and seismicity of the Tindari Fault System, southern Italy:
25 Crustal deformations at the transition between ongoing contractional and extensional domains located above the edge of a subducting slab, Tectonics, 25, https://doi.org/10.1029/2004TC001763, 2006a.

Billi, A., Barberi, G., Faccenna, C., Neri, G., Pepe, F., and Sulli, A.: Tectonics and seismicity of the Tindari Fault System, southern Italy: Crustal deformations at the transition between ongoing contractional and extensional domains located above the edge of a subducting slab, Tectonics, 25, https://doi.org/10.1029/2004TC001763, 2006b.

30 Billi, A., Presti, D., Faccenna, C., Neri, G., and Orecchio, B.: Seismotectonics of the Nubia plate compressive margin in the south Tyrrhenian region, Italy: Clues for subduction inception, Journal of Geophysical Research: Solid Earth, 112, https://doi.org/10.1029/2006JB004837, 2007.

Billi, A., Minelli, L., Orecchio, B., and Presti, D.: Constraints to the cause of three historical tsunamis (1908, 1783, and 1693) in the Messina Straits region, Sicily, southern Italy, Seismological Research Letters, 81, 907–915, https://doi.org/10.1785/gssrl.81.6.907, 2010.

35 Billi, A., Faccenna, C., Bellier, O., Minelli, L., Neri, G., Piromallo, C., Presti, D., Scrocca, D., and Serpelloni, E.: Recent tectonic reorganization of the Nubia-Eurasia convergent boundary heading for the closure of the western Mediterranean, Bulletin de la Société Géologique de France, 182, 279–303, https://doi.org/10.2113/gssgfbull.182.4.279, 2011.

Bohnhoff, M., Martínez-Garzón, P., Bulut, F., Stierle, E., and Ben-Zion, Y.: Maximum earthquake magnitudes along different sections of the North Anatolian fault zone, Tectonophysics, 674, 147–165, https://doi.org/10.1016/j.tecto.2016.02.028, 2016.

Bouchon, M., Campillo, M., and Cotton, F.: Stress field associated with the rupture of the 1992 Landers, California, earthquake and its implications concerning the fault strength at the onset of the earthquake, Journal of Geophysical Research: Solid Earth, 103, 21 091–21 097, https://doi.org/10.1029/98JB01982, 1998.

Boyd, O., Calais, E., Langbein, J., Magistrale, H., Stein, S., and Zoback, M.: Workshop on New Madrid geodesy and the challenges of understanding intraplate earthquakes, Tech. rep., US Geological Survey, 2013.

Braun, J., Burbidge, D., Gesto, F., Sandiford, M., Gleadow, A. J. W., Kohn, B., and Cummins, P.: Constraints on the current rate of deformation and surface uplift of the Australian continent from a new seismic database and low-T thermochronological data, Australian Journal of Earth Sciences, 56, 99–110, https://doi.org/10.1080/08120090802546977, 2009.

Bressan, G., Snidarcig, A., and Venturini, C.: Present state of tectonic stress of the Friuli area (eastern Southern Alps), Tectonophysics, 292, 211–227, https://doi.org/10.1016/S0040-1951(98)00065-1, 1998.

Brogi, A.: Neogene extension in the Northern Apennines (Italy): insights from the southern part of the Mt. Amiata geothermal area, Geodinamica Acta, 19, 33–50, https://doi.org/10.3166/ga.19.33-50, 2006.

Brogi, A.: Fault zone architecture and permeability features in siliceous sedimentary rocks: insights from the Rapolano geothermal area (Northern Apennines, Italy), Journal of Structural Geology, 30, 237–256, https://doi.org/10.1016/j.jsg.2007.10.004, 2008.

Brogi, A.: Bowl-shaped basin related to low-angle detachment during continental extension: the case of the controversial Neogene Siena Basin (central Italy, Northern Apennines), Tectonophysics, 499, 54–76, https://doi.org/10.1016/j.tecto.2010.12.005, 2011.

Brogi, A. and Fabbrini, L.: Extensional and strike-slip tectonics across the Monte Amiata–Monte Cetona transect (Northern Apennines, Italy) and seismotectonic implications, Tectonophysics, 476, 195–209, https://doi.org/10.1016/j.tecto.2009.02.020, 2009.

Brogi, A., Lazzarotto, A., Liotta, D., and Ranalli, G.: Extensional shear zones as imaged by reflection seismic lines: the Larderello geothermal field (central Italy), Tectonophysics, 363, 127–139, https://doi.org/10.1016/S0040-1951(02)00668-6, 2003.

Brogi, A., Lazzarotto, A., and Liotta, D.: Structural features of southern Tuscany and geological interpretation of the CROP 18 Seismic Reflection Survey (Italy), Bollettino della Società Geologica Italiana. Volume speciale, pp. 213–236, 2005.

Brozzetti, F.: The Campania-Lucania Extensional Fault System, southern Italy: A suggestion for a uniform model of active extension in the Italian Apennines, Tectonics, 30, https://doi.org/10.1029/2010TC002794, 2011.

Calais, E., Camelbeeck, T., Stein, S., Liu, M., and Craig, T.: A new paradigm for large earthquakes in stable continental plate interiors, Geophysical Research Letters, 43, 10–621, https://doi.org/10.1002/2016GL070815, 2016.

Camelbeeck, T., Vanneste, K., Alexandre, P., Verbeeck, K., Petermans, T., Rosset, P., Everaerts, M., Warnant, R., Van Camp, M., Stein, S., et al.: Relevance of active faulting and seismicity studies to assessments of long-term earthquake activity and maximum magnitude in intraplate northwest Europe, between the Lower Rhine Embayment and the North Sea, SPECIAL PAPERS-GEOLOGICAL SOCIETY OF AMERICA, 425, 193, https://doi.org/10.1130/2007.2425(14), 2007.

Campbell, G., Walker, R., Abdrakhmatov, K., Jackson, J., Elliott, J., Mackenzie, D., Middleton, T., and Schwenninger, J.-L.: Great earthquakes in low strain rate continental interiors: an example from SE Kazakhstan, Journal of Geophysical Research: Solid Earth, 120, 5507–5534, https://doi.org/10.1002/2015JB011925, 2015.

Capponi, G., Crispini, L., Federico, L., Piazza, M., and Fabbri, B.: Late Alpine tectonics in the Ligurian Alps: constraints from the Tertiary Piedmont Basin conglomerates, Geological Journal, 44, 211–224, https://doi.org/10.1002/gj.1140, 2009.

Carminati, E. and Doglioni, C.: Alps vs. Apennines: the paradigm of a tectonically asymmetric Earth, Earth-Science Reviews, 112, 67–96, https://doi.org/10.1016/j.earscirev.2012.02.004, 2012.

Carminati, E., Lustrino, M., Cuffaro, M., and Doglioni, C.: Tectonics, magmatism and geodynamics of Italy: what we know and what we imagine, Journal of the Virtual Explorer, 36, 8, https://doi.org/10.3809/jvirtex.2009.00226, 2010.

5 Castello, B., Selvaggi, G., Chiarabba, C., and Amato, A.: CSI Catalogo della sismicità italiana 1981-2002, versione 1.1., INGV-CNT, Roma, https://doi.org/http://csi.rm.ingv.it/., 2006.

Casula, G., Cherchi, A., Montadert, L., Murru, M., and Sarria, E.: The Cenozoic graben system of Sardinia (Italy): geodynamic evolution from new seismic and field data, Marine and Petroleum Geology, 18, 863–888, https://doi.org/10.1016/S0264-8172(01)00023-X, 2001.

Cheloni, D., D'Agostino, N., D'Anastasio, E., and Selvaggi, G.: Reassessment of the source of the 1976 Friuli, NE Italy, earthquake se-
10 quence from the joint inversion of high-precision levelling and triangulation data, Geophysical Journal International, 190, 1279–1294, https://doi.org/10.1111/j.1365-246X.2012.05561.x, 2012.

Chiarabba, C., Jovane, L., and DiStefano, R.: A new view of Italian seismicity using 20 years of instrumental recordings, Tectonophysics, 395, 251–268, https://doi.org/10.1016/j.tecto.2004.09.013, 2005.

Chiarabba, C., De Gori, P., and Boschi, E.: Pore-pressure migration along a normal-fault system resolved by time-repeated seismic tomogra-
15 phy, Geology, 37, 67–70, https://doi.org/10.1130/G25220A.1, 2009.

Chiarabba, C., De Gori, P., and Mele, F. M.: Recent seismicity of Italy: Active tectonics of the central Mediterranean region and seismicity rate changes after the Mw 6.3 L'Aquila earthquake, Tectonophysics, 638, 82–93, https://doi.org/10.1016/j.tecto.2014.10.016, 2015.

Chiaraluce, L., Chiarabba, C., Collettini, C., Piccinini, D., and Cocco, M.: Architecture and mechanics of an active low-angle normal fault: Alto Tiberina fault, northern Apennines, Italy, Journal of Geophysical Research: Solid Earth, 112, https://doi.org/10.1029/2007JB005015,
20 2007.

Chiaraluce, L., Di Stefano, R., Tinti, E., Scognamiglio, L., Michele, M., Casarotti, E., Cattaneo, M., De Gori, P., Chiarabba, C., Monachesi, G., et al.: The 2016 central Italy seismic sequence: A first look at the mainshocks, aftershocks, and source models, Seismological Research Letters, 88, 757–771, https://doi.org/10.1785/0220160221, 2017.

Chousianitis, K. and Konca, A. O.: Coseismic slip distribution of the 12 June 2017 Mw= 6.3 Lesvos earthquake and imparted static stress
25 changes to the neighboring crust, Journal of Geophysical Research: Solid Earth, 123, 8926–8936, https://doi.org/10.1029/2018JB015950, 2018.

Christophe, L., Scotti, O., and Ioualalen, M.: Reappraisal of the 1887 Ligurian earthquake (western Mediterranean) from macroseismicity, ac-
tive tectonics and tsunami modelling, Geophysical Journal International, 190, 87–104, https://doi.org/10.1111/j.1365-246X.2012.05498.x, 2012.

30 Christophersen, A., Rhoades, D. A., and Colella, H. V.: Precursory seismicity in regions of low strain rate: insights from a physics-based earthquake simulator, Geophysical Journal International, 209, 1513–1525, https://doi.org/10.1093/gji/ggx104, 2017.

Collettini, C.: The mechanical paradox of low-angle normal faults: Current understanding and open questions, Tectonophysics, 510, 253–268, https://doi.org/10.1016/j.tecto.2011.07.015, 2011.

Collettini, C. and Trippetta, F.: A slip tendency analysis to test mechanical and structural control on aftershock rupture planes, Earth and
35 Planetary Science Letters, 255, 402–413, https://doi.org/10.1016/j.epsl.2007.01.001, 2007.

Collettini, C., Niemeijer, A., Viti, C., and Marone, C.: Fault zone fabric and fault weakness, Nature, 462, 907, https://doi.org/10.1038/nature08585, 2009.

Courboulex, F., Deschamps, A., Cattaneo, M., Costi, F., Deverchere, J., Virieux, J., Augliera, P., Lanza, V., and Spallarossa, D.: Source study and tectonic implications of the 1995 Ventimiglia (border of Italy and France) earthquake (M L= 4.7), Tectonophysics, 290, 245–257, https://doi.org/10.1016/S0040-1951(98)00024-9, 1998.

Cowie, P., Phillips, R., Roberts, G. P., McCaffrey, K., Zijerveld, L., Gregory, L., Walker, J. F., Wedmore, L., Dunai, T., Binnie, S., et al.: Orogen-scale uplift in the central Italian Apennines drives episodic behaviour of earthquake faults, Scientific Reports, 7, 44 858, https://doi.org/10.1038/srep44858, 2017.

Cuffaro, M., Riguzzi, F., Scrocca, D., Antonioli, F., Carminati, E., Livani, M., and Doglioni, C.: On the geodynamics of the northern Adriatic plate, Rendiconti Lincei, 21, 253–279, https://doi.org/10.1007/s12210-010-0098-9, 2010.

Cultrera, F., Barreca, G., Burrato, P., Ferranti, L., Monaco, C., Passaro, S., Pepe, F., and Scarfì, L.: Active faulting and continental slope instability in the Gulf of Patti (Tyrrhenian side of NE Sicily, Italy): a field, marine and seismological joint analysis, Natural Hazards, 86, 253–272, https://doi.org/10.1007/s11069-016-2547-y, 2017.

Dawson, J., Cummins, P., Tregoning, P., and Leonard, M.: Shallow intraplate earthquakes in Western Australia observed by interferometric synthetic aperture radar, Journal of Geophysical Research: Solid Earth, 113, https://doi.org/10.1029/2008JB005807, 2008.

Del Gaudio, C., Aquino, I., Ricco, C., and Serio, C.: Movimenti verticali del suolo ai Campi Flegrei: risultati della livellazione geometrica di precisione eseguita nel periodo Dicembre 2006-Gennaio 2007, Open File Report, 2007.

DeMets, C., Gordon, R. G., Argus, D., and Stein, S.: Current plate motions, Geophysical journal international, 101, 425–478, https://doi.org/10.1111/j.1365-246X.1990.tb06579.x, 1990.

Dewey, J., Helman, M., Knott, S., Turco, E., and Hutton, D.: Kinematics of the western Mediterranean, Geological Society, London, Special Publications, 45, 265–283, https://doi.org/10.1144/GSL.SP.1989.045.01.15, 1989.

DISS Working Group: Database of Individual Seismogenic Sources (DISS), Version 3.2.1: A compilation of potential sources for earthquakes larger than M 5.5 in Italy and surrounding areas., Istituto Nazionale di Geofisica e Vulcanologia, p. http://diss.rm.ingv.it/diss/, https://doi.org/10.6092/INGV.IT-DISS3.2.1, 2018.

Dixon, T. H., Norabuena, E., and Hotaling, L.: Paleoseismology and Global Positioning System: Earthquake-cycle effects and geodetic versus geologic fault slip rates in the Eastern California shear zone, Geology, 31, 55–58, https://doi.org/10.1130/0091-7613(2003)031<0055:PAGPSE>2.0.CO;2, 2003.

Doglioni, C.: A proposal for the kinematic modelling of W-dipping subductions-possible applications to the Tyrrhenian-Apennines system, Terra Nova, 3, 423–434, https://doi.org/10.1111/j.1365-3121.1991.tb00172.x, 1991.

Doglioni, C., Gueguen, E., Harabaglia, P., and Mongelli, F.: On the origin of west-directed subduction zones and applications to the western Mediterranean, Geological Society, London, Special Publications, 156, 541–561, https://doi.org/10.1144/GSL.SP.1999.156.01.24, 1999.

Faccenna, C., Piromallo, C., Crespo-Blanc, A., Jolivet, L., and Rossetti, F.: Lateral slab deformation and the origin of the western Mediterranean arcs, Tectonics, 23, https://doi.org/10.1029/2002TC001488, 2004.

Fantoni, R. and Franciosi, R.: Tectono-sedimentary setting of the Po Plain and Adriatic foreland, Rendiconti Lincei, 21, 197–209, https://doi.org/10.1007/s12210-010-0102-4, 2010.

Ferranti, L., Palano, M., Cannavò, F., Mazzella, M. E., Oldow, J. S., Gueguen, E., Mattia, M., and Monaco, C.: Rates of geodetic deformation across active faults in southern Italy, Tectonophysics, 621, 101–122, https://doi.org/10.1016/j.tecto.2014.02.007, 2014.

Field, E. H., Dawson, T. E., Felzer, K. R., Frankel, A. D., Gupta, V., Jordan, T. H., Parsons, T., Petersen, M. D., Stein, R. S., Weldon, R., et al.: Uniform California earthquake rupture forecast, version 2 (UCERF 2), Bulletin of the Seismological Society of America, 99, 2053–2107, https://doi.org/10.1785/0120080049, 2009.

Field, E. H., Biasi, G. P., Bird, P., Dawson, T. E., Felzer, K. R., Jackson, D. D., Johnson, K. M., Jordan, T. H., Madden, C., Michael, A. J., et al.: Long-term time-dependent probabilities for the third Uniform California Earthquake Rupture Forecast (UCERF3), Bulletin of the Seismological Society of America, 105, 511–543, https://doi.org/10.1785/0120140093, 2015.

Finetti, I. and Morelli, C.: Esplorazione sismica a riflessione dei Golfi di Napoli e Pozzuoli, Boll. Geofis. Teor. Appl, 16, 175–222, 1974.

5   Freymueller, J., King, N., and Segall, P.: The co-seismic slip distribution of the Landers earthquake, Bulletin of the Seismological Society of America, 84, 646–659, 1994.

Galadini, F., Meletti, C., and Vittori, E.: Stato delle conoscenze sulle faglie attive in Italia: elementi geologici di superficie, Le ricerche del GNDT nel campo della pericolosità sismica (1996–1999), pp. 107–136, 2000.

Galli, P.: New empirical relationships between magnitude and distance for liquefaction, Tectonophysics, 324, 169–187,
10   https://doi.org/10.1016/S0040-1951(00)00118-9, 2000.

Galli, P., Galadini, F., and Pantosti, D.: Twenty years of paleoseismology in Italy, Earth-Science Reviews, 88, 89–117, https://doi.org/10.1016/j.earscirev.2008.01.001, 2008.

Gasparini, C., Iannaccone, G., and Scarpa, R.: Fault-plane solutions and seismicity of the Italian peninsula, Tectonophysics, 117, 59–78, https://doi.org/10.1016/0040-1951(85)90236-7, 1985.

15   Gasperini, P., Lolli, B., and Vannucci, G.: Empirical calibration of local magnitude data sets versus moment magnitude in Italy, Bulletin of the Seismological Society of America, 103, 2227–2246, https://doi.org/10.1785/0120120356, 2013.

Ghisetti, F.: Evoluzione neotettonica dei principali sistemi di faglie della Calabria centrale, Bollettino della Società Geologica Italiana, 98, 387–430, 1979.

Giardini, D.: The global seismic hazard assessment program (GSHAP)-1992/1999, Annals of Geophysics, 42, 1999.

20   Goes, S., Giardini, D., Jenny, S., Hollenstein, C., Kahle, H.-G., and Geiger, A.: A recent tectonic reorganization in the south-central Mediterranean, Earth and Planetary Science Letters, 226, 335–345, https://doi.org/10.1016/j.epsl.2004.07.038, 2004.

Govoni, A., Marchetti, A., De Gori, P., Di Bona, M., Lucente, F. P., Improta, L., Chiarabba, C., Nardi, A., Margheriti, L., Agostinetti, N. P., et al.: The 2012 Emilia seismic sequence (Northern Italy): Imaging the thrust fault system by accurate aftershock location, Tectonophysics, 622, 44–55, https://doi.org/10.1016/j.tecto.2014.02.013, 2014.

25   Grasso, M. and Reuther, C.: The western margin of the Hyblean Plateau: a neotectonic transform system on the SE Sicilian foreland, Annales Tectonicae, 2, 107–120, 1988.

Grünthal, G. and Wahlström, R.: An Mw based earthquake Catalogue for central, northern and northwestern Europe using a hierarchy of magnitude conversions, Journal of Seismology, 7, 507–531, https://doi.org/10.1023/B:JOSE.0000005715.87363.13, 2003.

Guidoboni, E., Ferrari, G., Mariotti, D., Comastri, A., Tarabusi, G., Sgattoni, G., and Valensise, G.: CFTI5Med, Catalogo dei Forti Terremoti
30   in Italia (461 aC-1997) e nell'area Mediterranea (760 aC-1500), https://doi.org/10.6092/ingv.it-cfti5, 2018.

Henry, C. and Das, S.: Aftershock zones of large shallow earthquakes: fault dimensions, aftershock area expansion and scaling relations, Geophysical Journal International, 147, 272–293, https://doi.org/10.1046/j.1365-246X.2001.00522.x, 2001.

Holschneider, M., Zöller, G., Clements, R., and Schorlemmer, D.: Can we test for the maximum possible earthquake magnitude?, Journal of Geophysical Research: Solid Earth, 119, 2019–2028, https://doi.org/10.1002/2013JB010319, 2014.

35   IAEA: Environmental Change in Post-closure Safety Assessment of Solid Radioactive Waste Repositories. International Atomic Energy Agency, Report IAEA-TECDOC-1799, Vienna, pp.147, 2016.

Iside Working Group: Italian Seismological Instrumental and parametric Data–basE version 1.0, https://doi.org/10.13127/ISIDe, http://iside.rm.ingv.it, 2016.

Jiménez, M., Giardini, D., Grünthal, G., Group, S. W., et al.: Unified seismic hazard modelling throughout the Mediterranean region, Applicata, 42, 3–18, 2001.

Kafka, A. L.: Does seismicity delineate zones where future large earthquakes are likely to occur in intraplate environments?, Special Papers Geological Society of America, 425, 35, https://doi.org/10.1130/2007.2425(03), 2007.

5 Keller, L. M., Fügenschuh, B., Hess, M., Schneider, B., and Schmid, S. M.: Simplon fault zone in the western and central Alps: Mechanism of Neogene faulting and folding revisited, Geology, 34, 317–320, https://doi.org/10.1130/G22256.1, 2006.

Lanzafame, G. and Bousquet, J.: The Maltese escarpment and its extension from Mt. Etna to Aeolian Islands (Sicily): importance and evolution of a lithosphere discontinuity, Acta Vulcanologica, 9, 113–120, 1997.

Larroque, C., Béthoux, N., Calais, E., Courboulex, F., Deschamps, A., Déverchère, J., Stéphan, J., Ritz, J., and Gilli, E.: Active and recent
10   deformation at the Southern Alps-Ligurian basin junction, Geologie en Mijnbouw, 80, 255–272, 2001.

Leonard, M.: Earthquake Fault Scaling: Self-Consistent Relating of Rupture Length, Width, Average Displacement, and Moment ReleaseEarthquake Fault Scaling: Self-Consistent Relating of Rupture Length, Width, Average Displacement, Bulletin of the Seismological Society of America, 100, 1971, https://doi.org/10.1785/0120090189, 2010.

Leonard, M., Burbidge, D., Allen, T., Robinson, D., McPherson, A., Clark, D., and Collins, C.: The challenges of probabilistic seismic-hazard
15   assessment in stable continental interiors: An Australian example, Bulletin of the Seismological Society of America, 104, 3008–3028, https://doi.org/10.1785/0120130248, 2014.

Liu-Zeng, J., Heaton, T., and DiCaprio, C.: The effect of slip variability on earthquake slip-length scaling, Geophysical Journal International, 162, 841–849, https://doi.org/10.1111/j.1365-246X.2005.02679.x, 2005.

Locardi, E. and Nappi, G.: Tettonica e vulcanismo recente nell9isola di Lipari, Bollettino della Societa Geologica Italiana, 98, 447–456,
20   1979.

Locati, M., CCamassi, R. D., Rovida, A. N., Ercolani, E., Bernardini, F. M. A., Castelli, V., Caracciolo, C. H., Tertulliani, A., Rossi, A., Azzaro, R., et al.: DBMI15, the 2015 version of the Italian Macroseismic Database. Istituto Nazionale di Geofisica e Vulcanologia, 2016.

Mai, P. M. and Beroza, G. C.: Source scaling properties from finite-fault-rupture models, Bulletin of the Seismological Society of America, 90, 604–615, https://doi.org/10.1785/0119990126, 2000.

25 Malinverno, A. and Ryan, W. B.: Extension in the Tyrrhenian Sea and shortening in the Apennines as result of arc migration driven by sinking of the lithosphere, Tectonics, 5, 227–245, https://doi.org/10.1029/TC005i002p00227, 1986.

Mariotti, G. and Doglioni, C.: The dip of the foreland monocline in the Alps and Apennines, Earth and Planetary Science Letters, 181, 191–202, https://doi.org/10.1016/S0012-821X(00)00192-8, 2000.

Maurer, H., Burkhard, M., Deichmann, N., and Green, A.: Active tectonism in the central Alps: contrasting stress regimes north and south of
30   the Rhone Valley, Terra Nova, 9, 91–94, https://doi.org/10.1111/j.1365-3121.1997.tb00010.x, 1997.

McCalpin, J. P.: Paleoseismology, vol. 95, Academic press, 2009.

Michetti, A., Giardina, F., Livio, F., Mueller, K., Serva, L., Sileo, G., Vittori, E., Devoti, R., Riguzzi, F., Carcano, C., et al.: Active compressional tectonics, Quaternary capable faults, and the seismic landscape of the Po Plain (N Italy), Annals of geophysics, https://doi.org/10.4401/ag-5462, 2012.

35 Michetti, A. M., Serva, L., and Vittori, E.: ITHACA Italy Hazard from Capable Faults: a database of active faults of the Italian onshore territory, CD-Rom Explan. notes, pp. 1–150, 2000.

Michetti, A. M., Marco, S., et al.: Future trends in paleoseismology: Integrated study of the seismic landscape as a vital tool in seismic hazard analyses, Tectonophysics, 408, 3–21, https://doi.org/10.1016/j.tecto.2005.05.035, 2005.

23

Milliner, C., Sammis, C., Allam, A., Dolan, J., Hollingsworth, J., Leprince, S., and Ayoub, F.: Resolving fine-scale heterogeneity of co-seismic slip and the relation to fault structure, Scientific reports, 6, 27 201, https://doi.org/10.1038/srep27201, 2016.

Montone, P. and Mariucci, M. T.: The new release of the Italian contemporary stress map, Geophysical Journal International, 205, 1525–1531, https://doi.org/10.1093/gji/ggw100, 2016.

5   Morris, A., Ferrill, D. A., and Henderson, D. B.: Slip-tendency analysis and fault reactivation, Geology, 24, 275–278, https://doi.org/10.1130/0091-7613(1996)024<0275:STAAFR>2.3.CO;2, 1996.

Murchison, R. I.: On the Geological Structure of the Alps, Apennines and Carpathians, more especially to prove a transition from Secondary to Tertiary rocks, and the development of Eocene deposits in Southern Europe, Quarterly Journal of the Geological Society, 5, 157–312, https://doi.org/10.1144/GSL.JGS.1849.005.01-02.27, 1849.

10   NEA: Post-Closure Safety Case For Geological Repositories. Nuclear Energy Agency, Organisation for Economic Co-operation and Development, Report No. 3679, Paris, pp. 56, 2004.

Neri, G., Barberi, G., Orecchio, B., and Aloisi, M.: Seismotomography of the crust in the transition zone between the southern Tyrrhenian and Sicilian tectonic domains, Geophysical Research Letters, 29, https://doi.org/10.1029/2002GL015562, 2002.

Neri, G., Barberi, G., Oliva, G., and Orecchio, B.: Spatial variations of seismogenic stress orientations in Sicily, south Italy, Physics of the
15   Earth and Planetary Interiors, 148, 175–191, https://doi.org/10.1016/j.pepi.2004.08.009, 2005.

Nicolas, A., Hirn, A., Nicolich, R., and Polino, R.: Lithospheric wedging in the western Alps inferred from the ECORS-CROP traverse, Geology, 18, 587–590, https://doi.org/10.1130/0091-7613(1990)018<0587:LWITWA>2.3.CO;2, 1990.

Nostro, C., Cocco, M., and Belardinelli, M. E.: Static stress changes in extensional regimes: an application to southern Apennines (Italy), Bulletin of the Seismological Society of America, 87, 234–248, 1997.

20   Nuriel, P., Weinberger, R., Rosenbaum, G., Golding, S. D., Zhao, J.-x., Uysal, I. T., Bar-Matthews, M., and Gross, M. R.: Timing and mechanism of late-Pleistocene calcite vein formation across the Dead Sea Fault Zone, northern Israel, Journal of Structural Geology, 36, 43–54, https://doi.org/10.1016/j.jsg.2011.12.010, 2012.

Orecchio, B., Aloisi, M., Cannavo, F., Palano, M., Presti, D., Pulvirenti, F., Totaro, C., Siligato, G., and Neri, G.: Present-day kinematics and deformation processes in the southern Tyrrhenian region: new insights on the northern Sicily extensional belt, Italian Journal of
25   Geosciences, 136, 418–433, https://doi.org/10.3301/IJG.2017.01, 2017.

Pagani, U.: Linea di Faglia e terremoti del pesarese, Bolletino Della Soc. Geologica Italiana, 26, 175–188, 1907.

Palano, M., Ferranti, L., Monaco, C., Mattia, M., Aloisi, M., Bruno, V., Cannavò, F., and Siligato, G.: GPS velocity and strain fields in Sicily and southern Calabria, Italy: updated geodetic constraints on tectonic block interaction in the central Mediterranean, Journal of Geophysical Research: Solid Earth, 117, https://doi.org/10.1029/2012JB009254, 2012.

30   Palumbo, L., Benedetti, L., Bourles, D., Cinque, A., and Finkel, R.: Slip history of the Magnola fault (Apennines, Central Italy) from 36 Cl surface exposure dating: evidence for strong earthquakes over the Holocene, Earth and Planetary Science Letters, 225, 163–176, https://doi.org/10.1016/j.epsl.2004.06.012, 2004.

Parsons, T., Toda, S., Stein, R. S., Barka, A., and Dieterich, J. H.: Heightened odds of large earthquakes near Istanbul: an interaction-based probability calculation, Science, 288, 661–665, https://doi.org/10.1126/science.288.5466.661, 2000.

35   Patacca, E. and Scandone, P.: The 1627 Gargano earthquake (Southern Italy): identification and characterization of the causative fault, Journal of Seismology, 8, 259–273, https://doi.org/10.1023/B:JOSE.0000021393.77543.1e, 2004.

Patacca, E., Scandone, P., Di Luzio, E., Cavinato, G. P., and Parotto, M.: Structural architecture of the central Apennines: Interpretation of the CROP 11 seismic profile from the Adriatic coast to the orographic divide, Tectonics, 27, https://doi.org/10.1029/2005TC001917, 2008.

Pegler, G. and Das, S.: Analysis of the relationship between seismic moment and fault length for large crustal strike-slip earthquakes between 1977–92, Geophysical Research Letters, 23, 905–908, https://doi.org/10.1029/96GL00963, 1996.

Petricca, P., Trippetta, F., Billi, A., Collettini, C., Cuffaro, M., Scrocca, D., Doglioni, C., Ventura, G., Morgante, A., and Chiaravalli, F.: Revised dataset of known faults in Italy., GFZ Data Services, https://doi.org/10.5880/fidgeo.2018.003, http://pmd.gfz-potsdam.de/panmetaworks/, 2018.

Polonia, A., Torelli, L., Artoni, A., Carlini, M., Faccenna, C., Ferranti, L., Gasperini, L., Govers, R., Klaeschen, D., Monaco, C., et al.: The Ionian and Alfeo–Etna fault zones: New segments of an evolving plate boundary in the central Mediterranean Sea?, Tectonophysics, 675, 69–90, https://doi.org/10.1016/j.tecto.2016.03.016, 2016.

Polonia, A., Torelli, L., Gasperini, L., Cocchi, L., Muccini, F., Bonatti, E., Hensen, C., Schmidt, M., Romano, S., Artoni, A., et al.: Lower plate serpentinite diapirism in the Calabrian Arc subduction complex, Nature communications, 8, 2172, https://doi.org/10.1038/s41467-017-02273-x, 2017.

Pondrelli, S., Piromallo, C., and Serpelloni, E.: Convergence vs. retreat in Southern Tyrrhenian Sea: insights from kinematics, Geophysical Research Letters, 31, https://doi.org/10.1029/2003GL019223, 2004.

Pondrelli, S., Salimbeni, S., Ekström, G., Morelli, A., Gasperini, P., and Vannucci, G.: The Italian CMT dataset from 1977 to the present, Physics of the Earth and Planetary Interiors, 159, 286–303, https://doi.org/10.1016/j.pepi.2006.07.008, 2006.

Presti, D., Billi, A., Orecchio, B., Totaro, C., Faccenna, C., and Neri, G.: Earthquake focal mechanisms, seismogenic stress, and seismotectonics of the Calabrian Arc, Italy, Tectonophysics, 602, 153–175, https://doi.org/10.1016/j.tecto.2013.01.030, 2013.

Reicherter, K., Michetti, A. M., and Barroso, P. S.: Palaeoseismology: historical and prehistorical records of earthquake ground effects for seismic hazard assessment, Geological Society, London, Special Publications, 316, 1–10, https://doi.org/10.1144/SP316.1, 2009.

Roberts, G. P. and Michetti, A. M.: Spatial and temporal variations in growth rates along active normal fault systems: an example from The Lazio–Abruzzo Apennines, central Italy, Journal of Structural Geology, 26, 339–376, https://doi.org/10.1016/S0191-8141(03)00103-2, 2004.

Rockwell, T., Lindvall, S., Herzberg, M., Murbach, D., Dawson, T., and Berger, G.: Paleoseismology of the Johnson Valley, Kickapoo, and Homestead Valley faults: Clustering of earthquakes in the eastern California shear zone, Bulletin of the Seismological Society of America, 90, 1200–1236, https://doi.org/10.1785/0119990023, 2000.

Rohr, C.: Man and natural disaster in the Late Middle Ages: The earthquake in Carinthia and northern Italy on 25 January 1348 and its perception, Environment and History, 9, 127–149, https://doi.org/10.3197/096734003129342791, 2003.

Rosenbaum, G. and Lister, G. S.: Neogene and Quaternary rollback evolution of the Tyrrhenian Sea, the Apennines, and the Sicilian Maghrebides, Tectonics, 23, https://doi.org/10.1029/2003TC001518, 2004.

Rovida, A. N., Locati, M., CAMASSI, R. D., Lolli, B., and Gasperini, P.: CPTI15, the 2015 version of the Parametric Catalogue of Italian Earthquakes. Istituto Nazionale di Geofisica e Vulcanologia, 2016.

Sanchez, G., Rolland, Y., Schreiber, D., Giannerini, G., Corsini, M., and Lardeaux, J.-M.: The active fault system of SW Alps, Journal of Geodynamics, 49, 296–302, https://doi.org/10.1016/j.jog.2009.11.009, 2010.

Scandone, R. and Cortini, M.: Il Vesuvio: un vulcano ad alto rischio, Le Scienze, 163, 92–105, 1982.

Schmid, S. M., Pfiffner, O.-A., Froitzheim, N., Schönborn, G., and Kissling, E.: Geophysical-geological transect and tectonic evolution of the Swiss-Italian Alps, Tectonics, 15, 1036–1064, https://doi.org/10.1029/96TC00433, 1996.

Scrocca, D.: Thrust front segmentation induced by differential slab retreat in the Apennines (Italy), Terra Nova, 18, 154–161, https://doi.org/10.1111/j.1365-3121.2006.00675.x, 2006.

Scrocca, D., Carminati, E., and Doglioni, C.: Deep structure of the southern Apennines, Italy: Thin-skinned or thick-skinned?, Tectonics, 24, https://doi.org/10.1029/2004TC001634, 2005.

Selvaggi, G. and Chiarabba, C.: Seismicity and P-wave velocity image of the Southern Tyrrhenian subduction zone, Geophysical Journal International, 121, 818–826, https://doi.org/10.1111/j.1365-246X.1995.tb06441.x, 1995.

Serpelloni, E., Anzidei, M., Baldi, P., Casula, G., and Galvani, A.: Crustal velocity and strain-rate fields in Italy and surrounding regions: new results from the analysis of permanent and non-permanent GPS networks, Geophysical Journal International, 161, 861–880, https://doi.org/10.1111/j.1365-246X.2005.02618.x, 2005.

Sherlock, S. C., Strachan, R. A., and Jones, K. A.: High spatial resolution 40Ar/39Ar dating of pseudotachylites: geochronological evidence for multiple phases of faulting within basement gneisses of the Outer Hebrides (UK), Journal of the Geological Society, 166, 1049–1059, https://doi.org/10.1144/0016-76492008-125, 2009.

Sibson, R. H.: A note on fault reactivation, Journal of Structural Geology, 7, 751–754, https://doi.org/10.1016/0191-8141(85)90150-6, 1985.

Stein, R.: Progressive failure on the northern Anatolian fault since 1939 by earthquake triggering, Geophys. J. Int., 128, 694–704, 1997.

Stein, S. and Mazzotti, S.: Continental intraplate earthquakes: science, hazard, and policy issues, vol. 425, Geological Society of America, 2007.

Sue, C. and Tricart, P.: Widespread post-nappe normal faulting in the Internal Western Alps: a new constraint on arc dynamics, Journal of the Geological Society, 159, 61–70, https://doi.org/10.1144/0016-764901-026, 2002.

Sue, C., Thouvenot, F., Fréchet, J., and Tricart, P.: Widespread extension in the core of the western Alps revealed by earthquake analysis, Journal of Geophysical Research: Solid Earth, 104, 25 611–25 622, https://doi.org/10.1029/1999JB900249, 1999.

Sue, C., Delacou, B., Champagnac, J.-D., Allanic, C., Tricart, P., and Burkhard, M.: Extensional neotectonics around the bend of the Western/Central Alps: an overview, International Journal of Earth Sciences, 96, 1101–1129, https://doi.org/10.1007/s00531-007-0181-3, 2007.

Swafford, L., Stein, S., and Mazzotti, S.: Limitations of the short earthquake record for seismicity and seismic hazard studies, Special Papers Geological Society of America, 425, 49, https://doi.org/10.1130/2007.2425(04), 2007.

Talwani, P.: Unified model for intraplate earthquakes, Intraplate Earthquakes. Cambridge University Press, Cambridge, pp. 275–327, 2014.

Thingbaijam, K. K. S., Martin Mai, P., and Goda, K.: New Empirical Earthquake Source-Scaling Laws, Bulletin of the Seismological Society of America, 107, 2225–2246, https://doi.org/10.1785/0120170017, 2017.

Turino, C., Scafidi, D., Eva, E., and Solarino, S.: Inferences on active faults at the Southern Alps–Liguria basin junction from accurate analysis of low energy seismicity, Tectonophysics, 475, 470–479, https://doi.org/10.1016/j.tecto.2009.06.007, 2009.

Vai, G. B.: Structure and stratigraphy: an overview, in: Anatomy of an orogen: the Apennines and adjacent Mediterranean basins, pp. 15–31, Springer, 2001.

Viete, D. R., Hacker, B. R., Allen, M. B., Seward, G. G., Tobin, M. J., Kelley, C. S., Cinque, G., and Duckworth, A. R.: Metamorphic records of multiple seismic cycles during subduction, Science advances, 4, eaaq0234, https://doi.org/10.1126/sciadv.aaq0234, 2018.

Viganò, A., Scafidi, D., Ranalli, G., Martin, S., Della Vedova, B., and Spallarossa, D.: Earthquake relocations, crustal rheology, and active deformation in the central–eastern Alps (N Italy), Tectonophysics, 661, 81–98, https://doi.org/10.1016/j.tecto.2015.08.017, 2015.

Vilardo, G., De Natale, G., Milano, G., and Coppa, U.: The seismicity of Mt. Vesuvius, Tectonophysics, 261, 127–138, https://doi.org/10.1016/0040-1951(96)00061-3, 1996.

Viola, C.: Appunti geologici ed idrologici sui dintorni di Teramo, Boll. del R. Com. Geol. d'Italia, 1, 221–228, 1893.

von Zittel, K. A.: Geologische Beobachtungen aus den Central-Apenninen, vol. 2, Oldenbourg, 1869.

Walsh III, F. R. and Zoback, M. D.: Probabilistic assessment of potential fault slip related to injection-induced earthquakes: Application to north-central Oklahoma, USA, Geology, 44, 991–994, https://doi.org/10.1130/G38275.1, 2016.

Wang, S., Xu, W., Xu, C., Yin, Z., Bürgmann, R., Liu, L., and Jiang, G.: Changes in groundwater level possibly encourage shallow earthquakes in central Australia: The 2016 Petermann Ranges earthquake, Geophysical Research Letters, https://doi.org/10.1029/2018GL080510, 2019.

Wells, D. L. and Coppersmith, K. J.: New empirical relationships among magnitude, rupture length, rupture width, rupture area, and surface displacement, Bulletin of the seismological Society of America, 84, 974–1002, 1994.

Wiemer, S. and Wyss, M.: Minimum magnitude of complete reporting in earthquake catalogs: examples from Alaska, the Western United States, and Japan, Bulletin of the Seismological Society of America, 90, 859–869, https://doi.org/10.1785/0119990114, 2000.

Zoback, M. D., Zoback, M. L., Mount, V. S., Suppe, J., Eaton, J. P., Healy, J. H., Oppenheimer, D., Reasenberg, P., Jones, L., Raleigh, C. B., Wong, I. G., Scotti, O., and Wentworth, C.: New Evidence on the State of Stress of the San Andreas Fault System, Science, 238, 1105–1111, https://doi.org/10.1126/science.238.4830.1105, 1987.
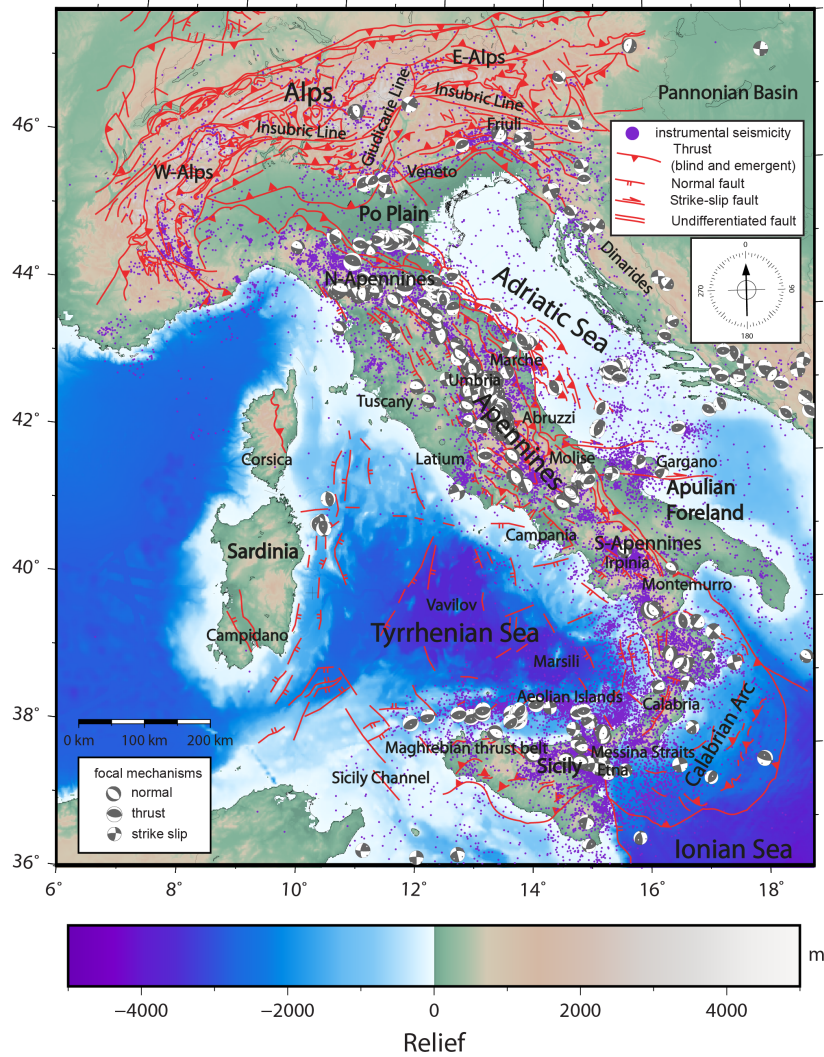
Figure 1. Tectonic map of Italy with instrumentally-recorded earthquakes (epicentres of M ≥ 2.0) in the 1981-2017 interval (ISIDe and CSI1.1 databases). Focal mechanisms are for M ≥ 4.0 events (Pondrelli et al., 2006), showing extensional tectonics along the Apennine chain and compressional tectonics in the NE portion of the Alps and in the N-NE portion of the Apennines.
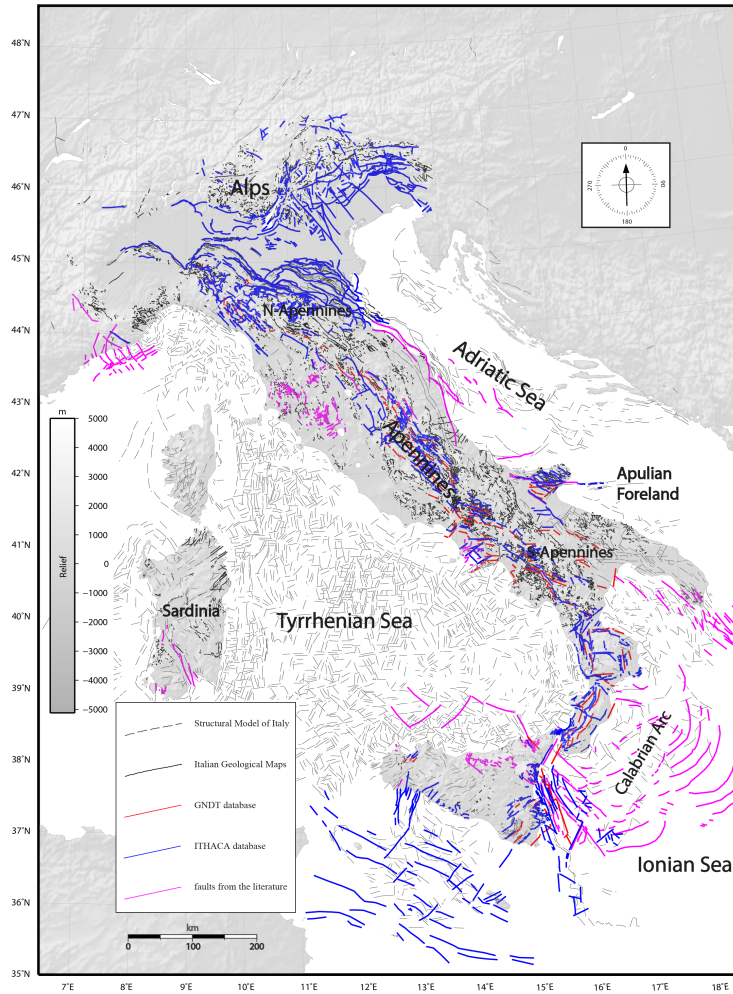
Figure 2. Map of faults from the five datasets used in this work: the Structural Model of Italy at the 1:500,000 scale (dashed black; Bigi et al., 1989); the Italian Geological Maps at the 1:100,000 scale (black; available online at www.isprambiente.it); the GNDT database of active faults (red; Galadini et al., 2000); the ITHACA database (blue; Michetti et al., 2000); and selected active faults from complementary studies published by different authors (pink; see text for explanations).
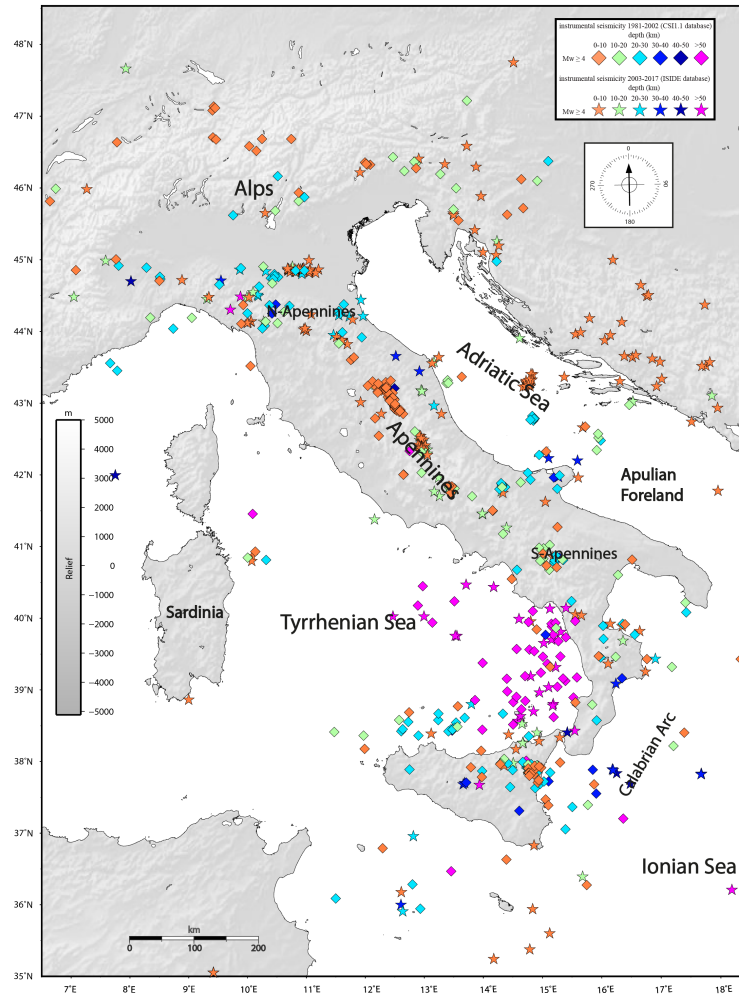
Figure 3. Instrumental seismicity (epicenters of M ≥ 4.0 earthquakes) distribution in Italy from ISIDe (stars) and CSI (diamonds) datasets. The CSI1.1 database (http://csi.rm.ingv.it; Castello et al., 2006) reports events in the 1981-2002 time interval, whereas the ISIDe database (http://iside.rm.ingv.it/iside/standard/index.jsp; Iside Working Group, 2016) reports events in the time interval 2003-2017. Events are differentiated by depth (change in color every 10 km).
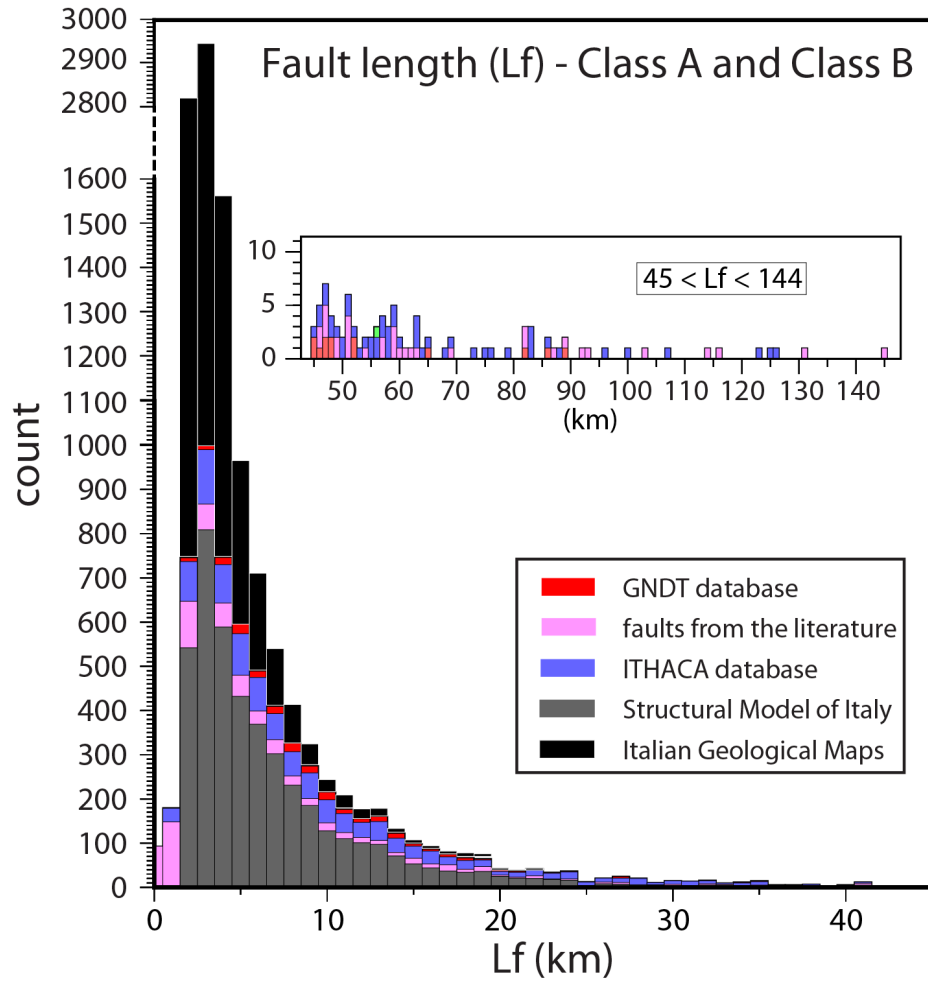
Figure 4. Histogram of fault lengths (Lf) derived from all analyzed datasets. Inset shows the same histogram for fault lengths ≥ 45 km.
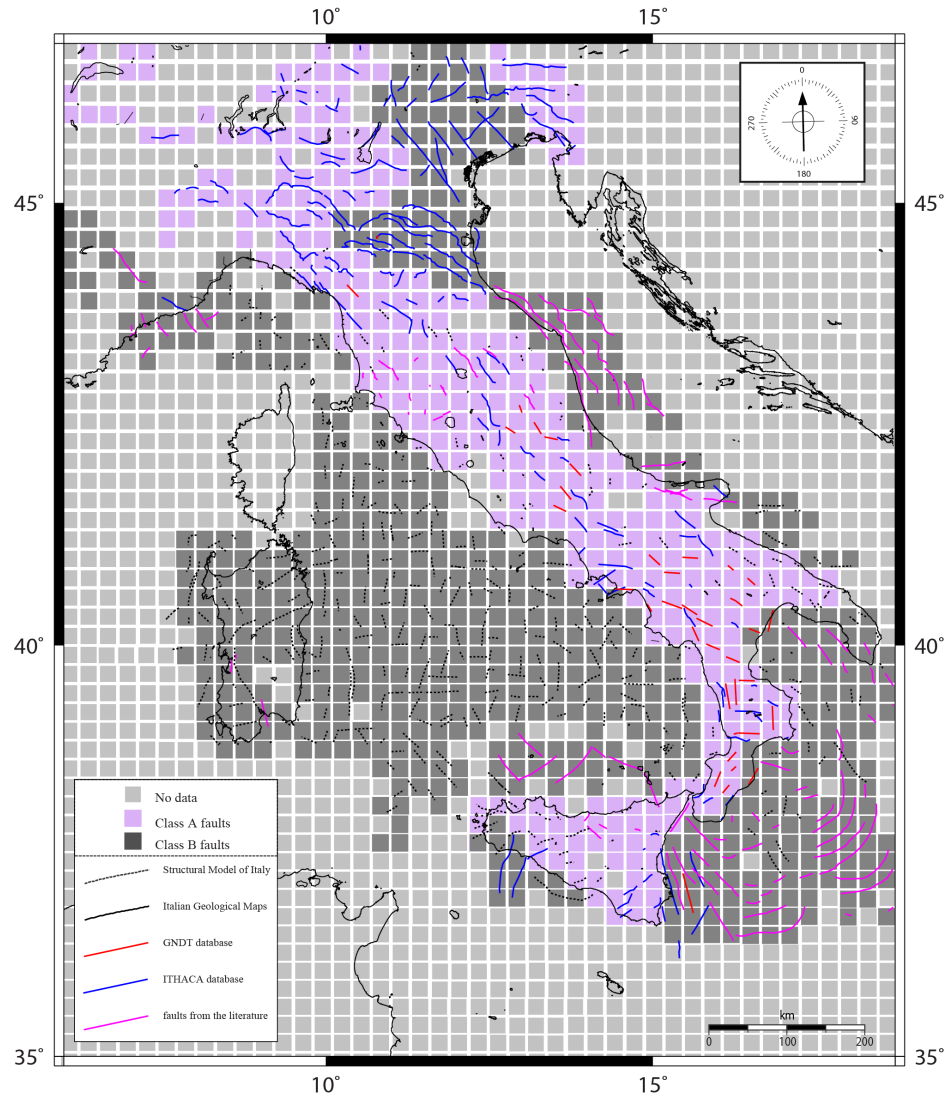
Figure 5. Map of the Italian territory divided into a grid with 25x25 km square cells. The map shows also the longest faults (from the analyzed datasets) falling into each cell. Light purple cells are for class A faults whereas dark grey cells are for class B faults.
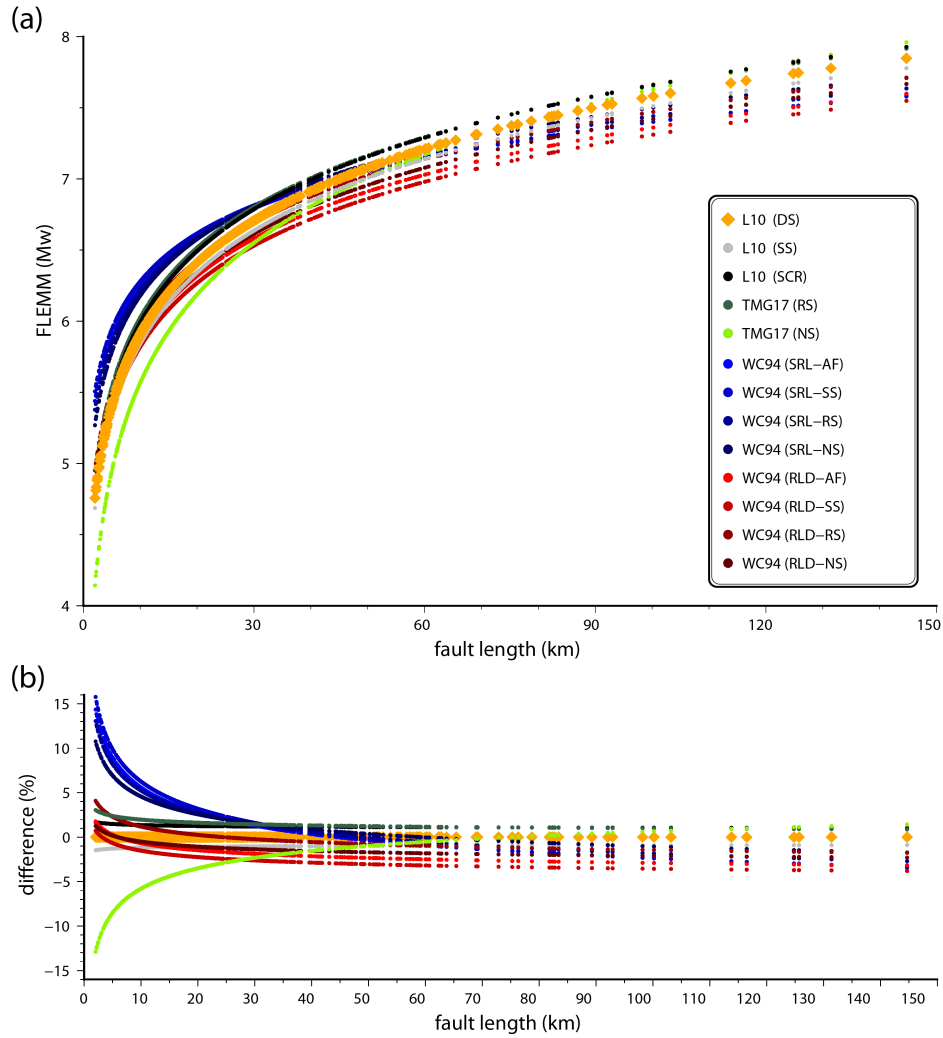
Figure 6. Earthquake magnitude vs. fault length, obtained using empirical scaling laws from: L10 = Leonard (2010); WC94 = Wells and Coppersmith (1994); and TMG17 = Thingbaijam et al. (2017). Keys: DS = dip slip faults; NS = normal slip faults; RS = reverse slip faults; SS = strike-slip faults; SCR = stable continental region faults; AF = all faults; SRL = surface rupture length; and RLD = sub-surface rupture length. (b) Difference vs. fault length. The difference is between earthquake magnitudes obtained from L10 vs. each of all other scaling laws (namely, WC94 and TMG17).
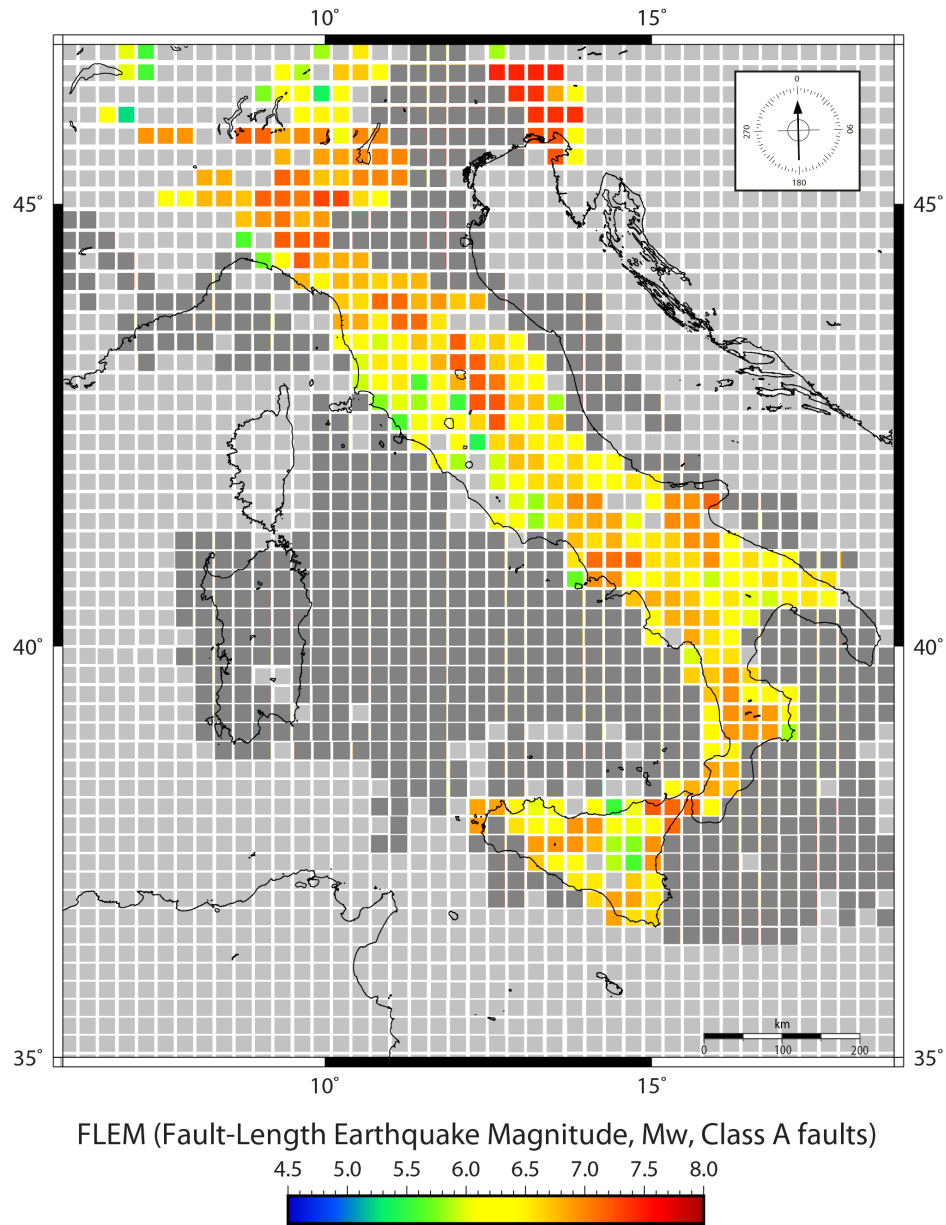
33

Figure 7. Map of the Fault-Length Earthquake Magnitude (FLEM) calculated, for each cell, from the length of class A faults. FLEM values are obtained using L10. Light grey is for cells with no data whereas dark grey is for cells where the longest faults belong to the class B set. Note that these results should be considered more in a theoretical and methodological perspective for comparison with future similar studies rather than in an applicative perspective for the case of Italy. In particular, our assessed earthquake magnitudes for the Italian territory are here proposed for scientific reasons and not for their use for civil protection and prevention purposes.
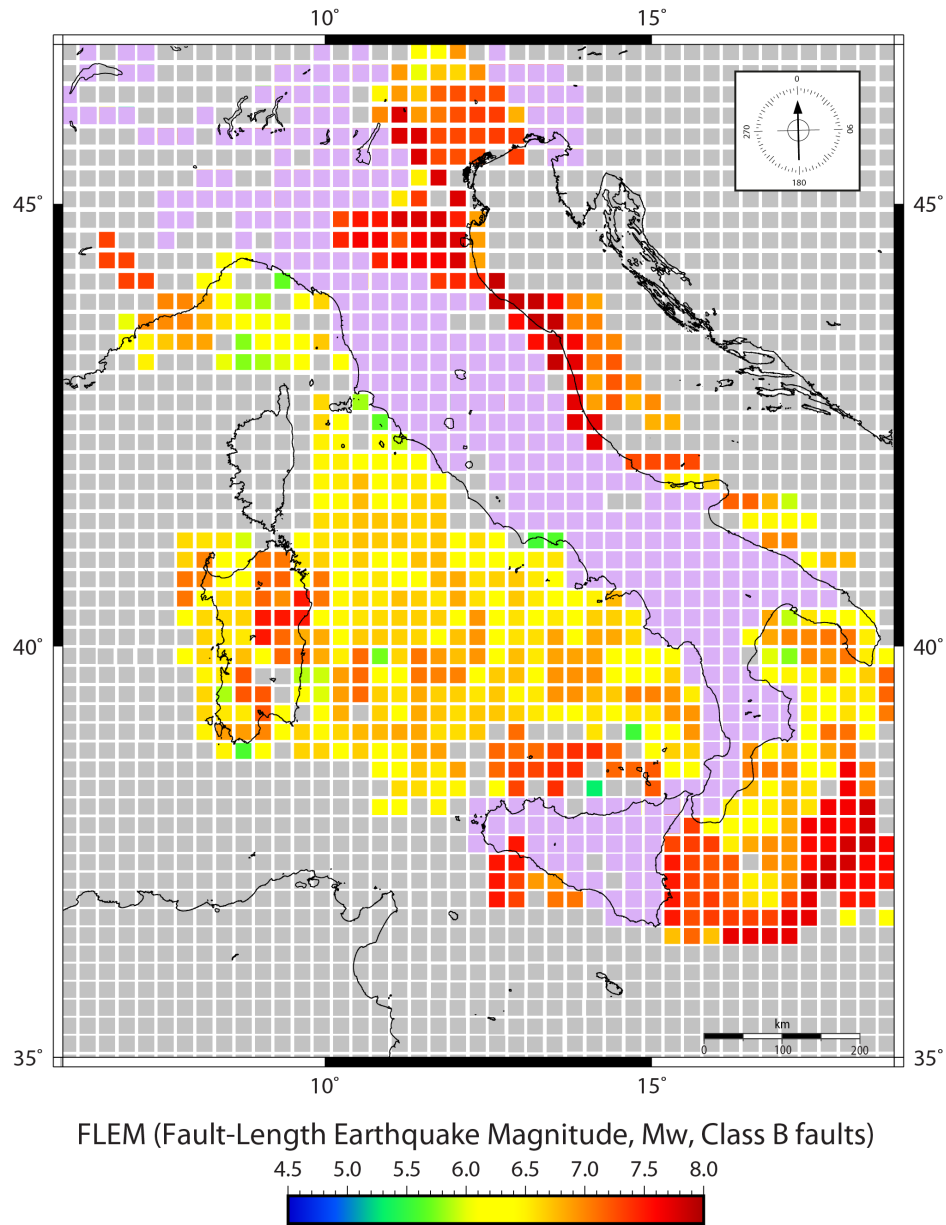
Figure 8. Map of the Fault-Length Earthquake Magnitude (FLEM) calculated, for each cell, from the length of class B faults. FLEM values are obtained using L10. Light grey is for cells with no data whereas light purple is for cells where the longest faults belong to the class A set. Note that these results should be considered more in a theoretical and methodological perspective for comparison with future similar studies rather than in an applicative perspective for the case of Italy. In particular, our assessed earthquake magnitudes for the Italian territory are here proposed for scientific reasons and not for their use for civil protection and prevention purposes.
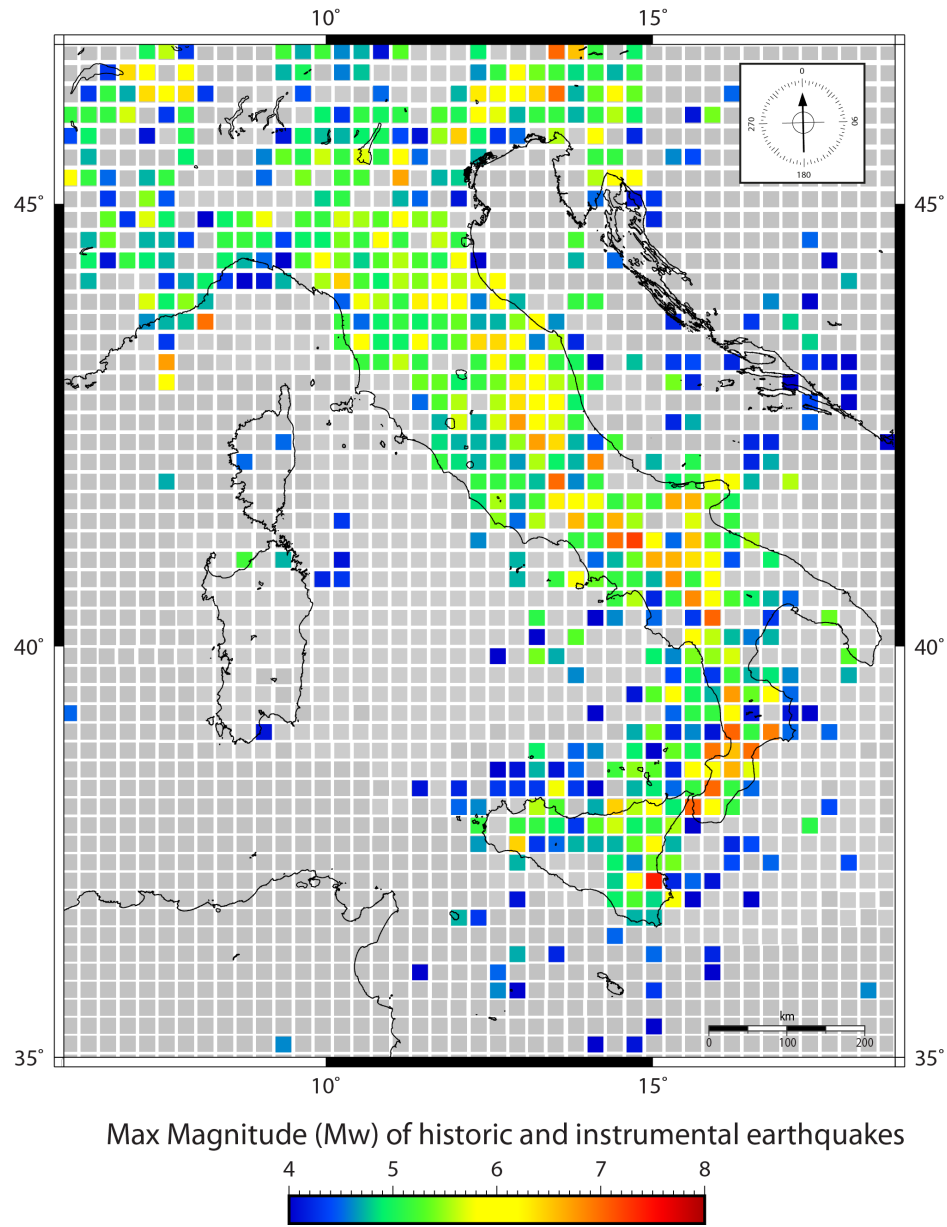
Figure 9. Map of maximum magnitude (for each cell) from historic or instrumental earthquakes as recorded in the CSI 1.1, ISIDe, and CPTI15 databases within the 1000-2017 period. Grey is for cells with no data.

Figure 10. Map of the difference between FLEM values (only from class A faults; Fig. 7) and maximum magnitudes from historic or instrumental earthquakes (Fig. 9). Light grey is for cells with no data whereas dark grey is for cells where the longest faults belong to the class B set. See Fig. 12 for the interpretation of red vs. green cells.
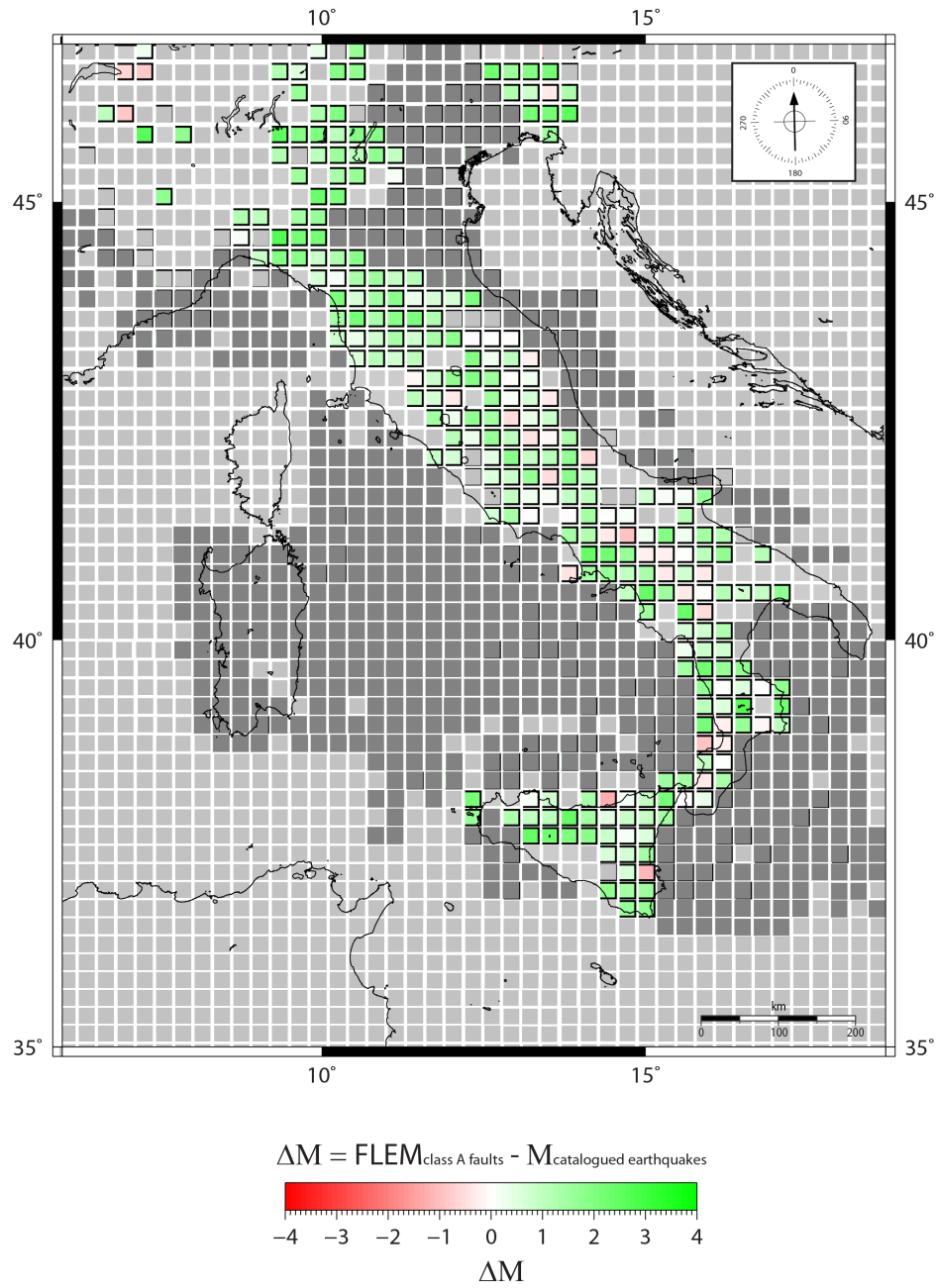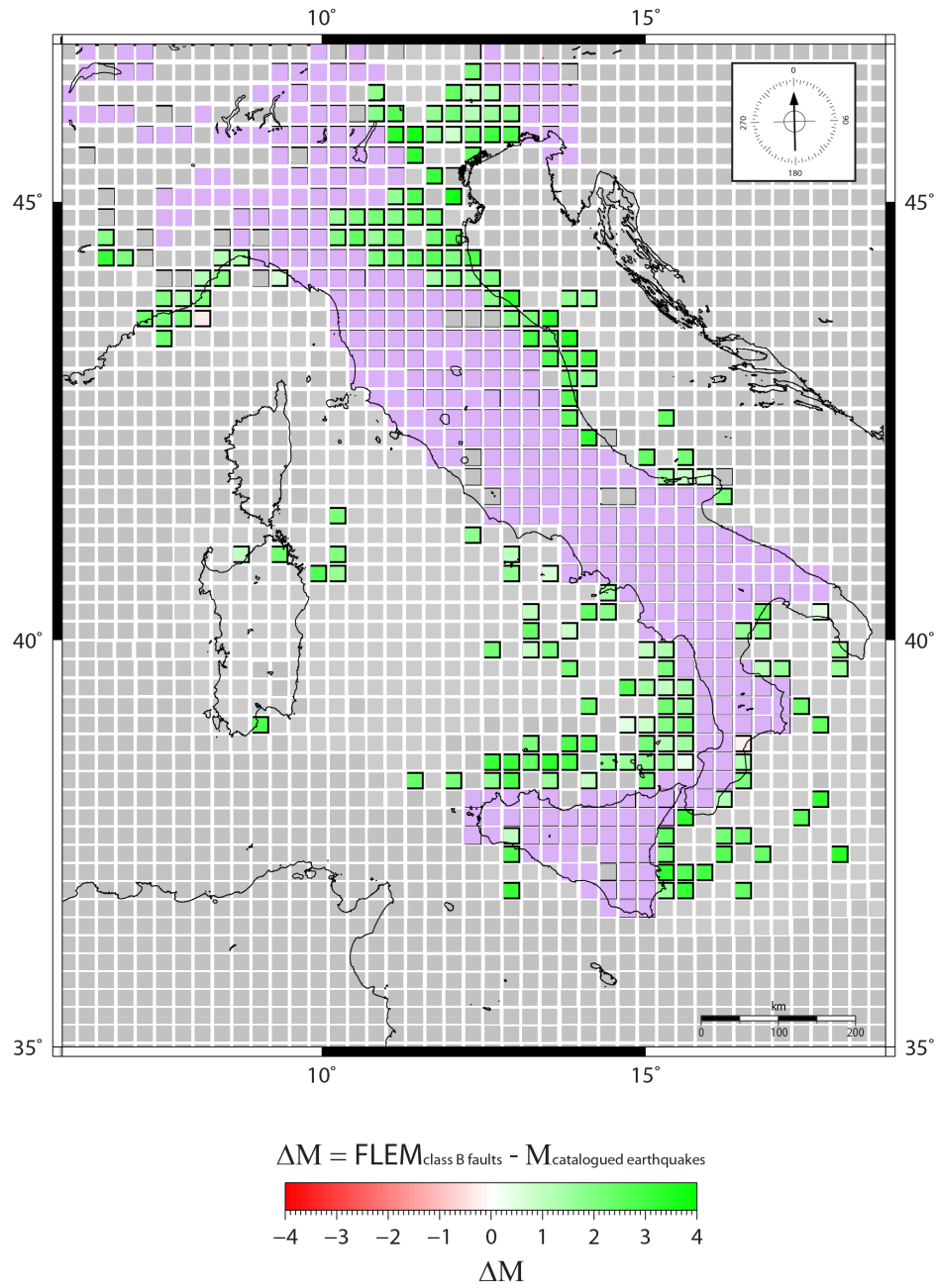
37

Figure 11. Map of the difference between FLEM values (only from class B faults; Fig. 8) and maximum magnitudes from historic or instrumental earthquakes (Fig. 9). Light grey is for cells with no data whereas light purple is for cells where the longest faults belong to the class A set. See Fig. 12 for the interpretation of red vs. green cells.
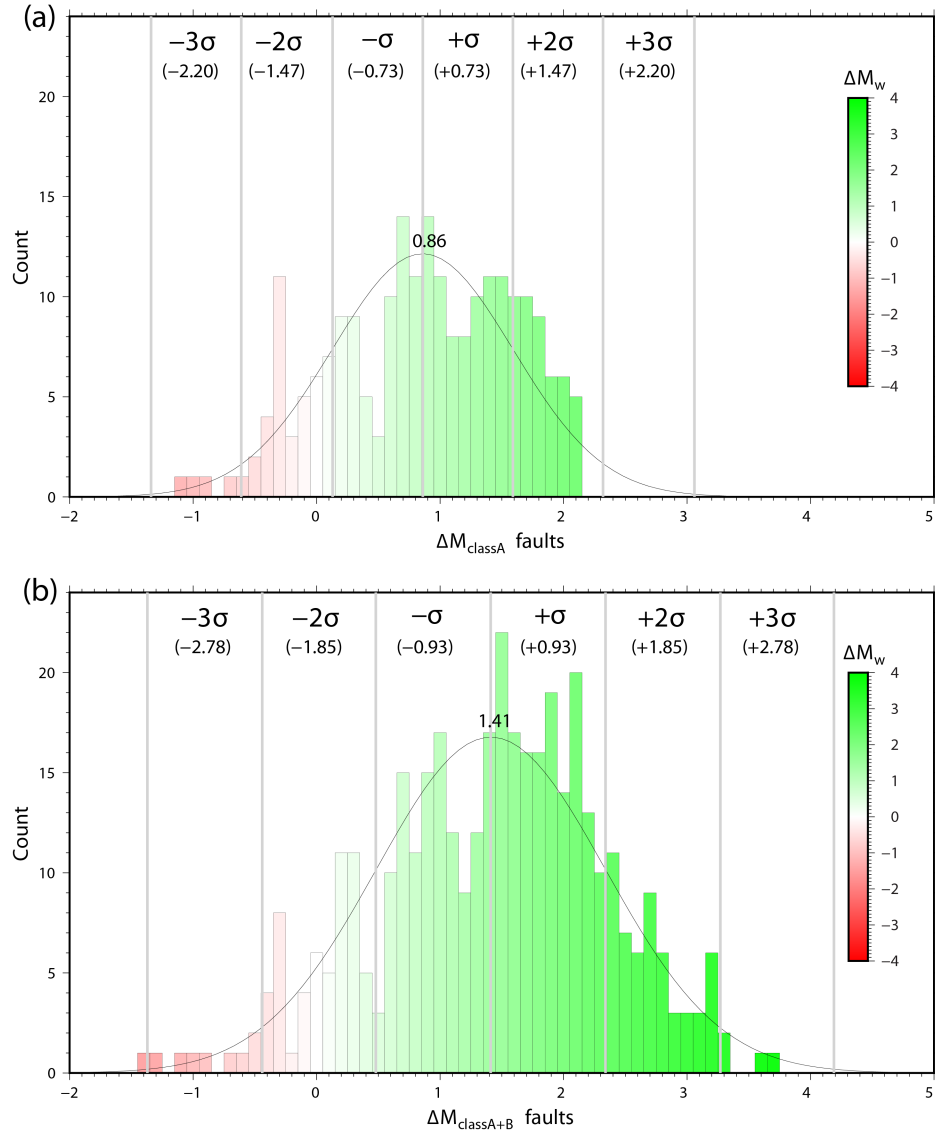
Figure 12. (a) Histogram of the difference between FLEMs (from class A faults) and spatially-coincident (same cell) historical/instrumental-catalogued magnitudes of earthquakes. Mean = 0.86; deviation standard $\sigma = 0.73$. (b) Histogram of the difference between FLEMs (from class A and B faults) and spatially-coincident (same cell) historical/instrumental-catalogued magnitudes of earthquakes. Mean = 1.41; deviation standard $\sigma = 0.93$. In both histograms, values in the negative fields can be interpreted as FLEM's underestimation with respect to catalogued earthquake magnitudes whereas values in the positive fields could be interpreted either as FLEM's overestimation with respect to catalogued magnitudes or as a sort of catalogue incompleteness. Occurrences in the positive fields (green portions) are significantly more frequent than occurrences in the negative fields (red portions). Green and red colors in Figs. 10, 11, and 13(c) have the same meaning as in this figure. See text for further information.

Figure 13. (a) Temporal series (since 1000 A.D.) of the difference between FLEMs (from class A faults) and spatially-coincident (same cell) historical/instrumental-catalogued magnitudes of earthquakes (only M ≥ 6.5). (b) In blue, temporal series of magnitudes from catalogued historical or instrumental earthquakes (M ≥ 6.5, 1000-2017 period). Blue vertical bars are for magnitude uncertainty. In red, FLEM values from the same cells hosting the catalogued historical or instrumental earthquakes drawn in blue. (c) Histogram of the difference between FLEMs (from class A faults) and spatially-coincident (same cell) historical/instrumental-catalogued magnitudes of earthquakes (M ≥ 6.5, 1000-2017 period). Mean = -0.09; standard deviation σ = 0.26. See Fig. 12 for the interpretation of red vs. green portions of the histogram.
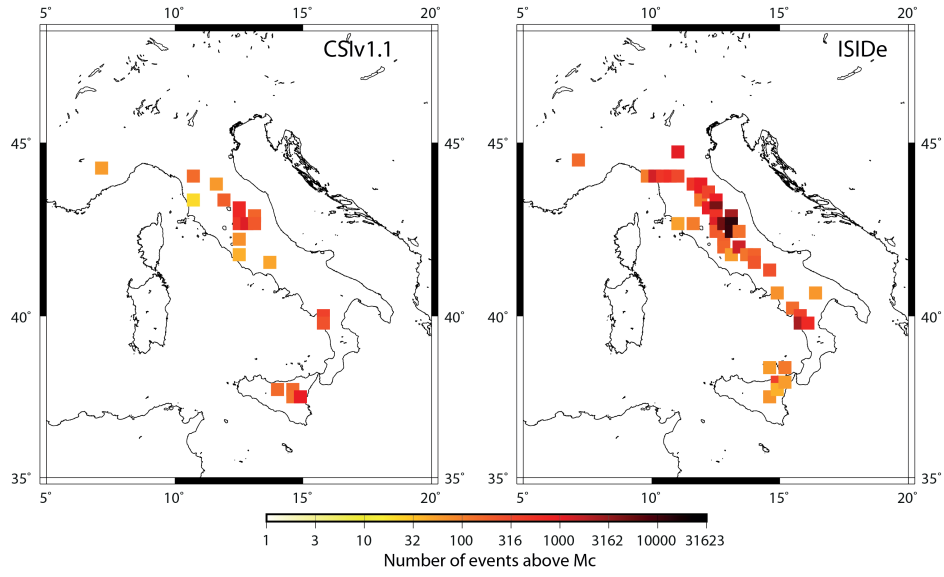
40

Figure 14. Maps of cells for which FLEM values are tested, on the CSiv1.1 (left panel, 20 cells) and ISIDe (right panel, 45 cells) databases (Tables S1 and S2). Colours are scaled with the number of events above the estimated completeness magnitude, M_c. In these cells the magnitude of events is distributed accordingly using a DTGR law, with a b-value equal to 1.

Table 1. Catalogued historical and instrumental earthquakes (M ≥ 6.5, 1000-2017 period) plotted in Fig. 13 with spatially-coincident (same 25x25 km cell) FLEM. Catalogued data are from Castello et al. (2006), Iside Working Group (2016), and Rovida et al. (2016).

Region	Year	Lat	Lon	Mw Data	Err Mw Data	FLEM	Min DIFF
Apennine (S)	1456	41.30	14.71	7.2	0.1	6.6	-0.5
Sicily (SE)	1693	37.14	15.01	7.3	0.1	6.8	-0.4
Calabria	1783	38.79	16.46	7.0	0.1	6.8	-0.1
Calabria	1783	38.30	15.97	7.1	0.1	6.7	-0.3
Apennine (S)	1857	40.35	15.84	7.1	0.1	6.5	-0.5
Calabria	1905	38.81	16.00	7.0	0.1	6.8	-0.1
Messina Straits	1908	38.15	15.69	7.1	0.2	7.0	0
Abruzzi	1915	42.01	13.53	7.1	0.1	6.5	-0.5
Apennine (S)	1688	41.28	14.56	7.1	0.1	6.6	-0.4
Calabria	1638	39.05	16.29	7.1	0.1	6.8	-0.2
Apennine (N)	1920	44.19	10.28	6.5	0.1	6.6	0
Apennine (S)	1930	41.07	15.32	6.7	0.1	6.4	-0.2
Alps (E)	1976	46.24	13.12	6.5	0.1	7.3	0.7
Irpinia	1980	40.84	15.28	6.8	0.1	6.4	-0.3
Umbria	2016	42.83	13.11	6.5	0.1	6.5	0
Po Plain	1117	45.27	11.02	6.5	0.1	6.9	0.3
Sicily	1169	37.22	14.95	6.5	0.5	6.3	0
Calabria	1184	39.40	16.19	6.8	0.3	6.8	0
Umbria	1328	42.86	13.02	6.5	0.3	6.5	0
Alps (E)	1348	46.50	13.58	6.6	0.1	7.4	0.7
Latium-Molise	1349	41.55	13.94	6.8	0.2	6.6	0
Abruzzi	1461	42.31	13.54	6.5	0.5	6.3	0
Sicily	1542	37.22	14.94	6.7	0.2	6.3	-0.1
Apennine (S)	1561	40.56	15.51	6.7	0.2	6.8	0
Gargano	1627	41.74	15.34	6.7	0.1	6.7	0
Calabria	1638	39.28	16.81	6.8	0.1	6.8	0
Gargano	1646	41.91	15.99	6.7	0.3	6.5	0
Calabria	1659	38.69	16.25	6.6	0.1	6.7	0
Irpinia	1694	40.86	15.41	6.7	0.1	6.4	-0.1
Irpinia	1702	41.12	14.99	6.6	0.1	6.4	-0.1
Abruzzi	1703	42.43	13.29	6.7	0.1	6.3	-0.3
Umbria	1703	42.71	13.07	6.9	0.1	6.5	-0.3
Abruzzi	1706	42.08	14.08	6.8	0.1	6.2	-0.5
Irpinia	1732	41.06	15.06	6.8	0.1	6.4	-0.2
Marche	1781	43.60	12.51	6.5	0.1	6.5	0
Calabria	1783	38.58	16.20	6.7	0.1	6.7	0
Molise	1805	41.50	14.47	6.7	0.1	6.7	0
Calabria	1832	39.08	16.92	6.7	0.1	6.8	0
Apennine (S)	1851	40.96	15.67	6.5	0.1	6.4	0

From mapped faults to ~~earthquake magnitude~~Fault-Length Earthquake Magnitude (FLEM): A test on Italy with methodological implications

Fabio Trippetta[1], Patrizio Petricca[1], Andrea Billi[2], Cristiano Collettini[1,3], Marco Cuffaro[2], Anna Maria Lombardi[3], Davide Scrocca[2], Giancarlo Ventura[4], Andrea Morgante[4], and Carlo Doglioni[1,3]

[1]Dipartimento di Scienze della Terra, Sapienza Universitá di Roma, Rome, Italy
[2]Istituto di Geologia Ambientale e Geoingegneria, CNR, Rome, Italy
[3]Istituto Nazionale di Geofisica e Vulcanologia, Rome, Italy
[4]Sogin (Societestione Impianti Nucleari) S.p.a., Rome, Italy

Correspondence: Andrea Billi (andrea.billi@cnr.it)

Abstract. ~~The maximum possible earthquake magnitude is one of the fundamental parameters to assess possible threats and effects on populations and infrastructures.~~ Empirical scaling laws between fault/slip dimensions and earthquake ~~magnitude can be~~ magnitudes are often used to assess ~~this fundamental parameter. Upon~~ the maximum possible earthquake magnitude of a territory. In this paper, upon the assumption of the reactivability of any fault, these seismic scaling ~~laws are used~~ relationships are benchmarked at the national scale in Italy against catalogued magnitudes, considering all known faults regardless of their age, stress field orientation, ~~or strain rate~~strain rate, or else. Italy is a suitable case for comparing the fault-size-derived seismic magnitudes with the existing accurate catalogues of historical-instrumental earthquakes. To do so, (1) a comprehensive catalogue of all known faults is compiled by merging the most complete databases available, (2) the ~~potential expected maximum magnitude of earthquakes (PEMM~~earthquakes magnitude (FLEM) is simply derived from fault ~~dimensions~~length, and (3) the resulting ~~PEMMs~~ FLEMs are compared (i.e., the mathematical difference) with catalogued earthquake magnitudes. Results show that the largest ~~PEMMs~~ FLEMs as well as the largest differences between ~~PEMMs~~ FLEMs and catalogued magnitudes are observed for poorly constrained faults~~(,~~ mainly inferred from subsurface data~~)~~. It is suggested that these areas have to be further characterized to better estimate fault dimension and segmentation and hence properly assess the FLEM. Where, in contrast, the knowledge of faults is geologically well constrained, the calculated ~~PEMM~~ FLEM is often consistent with the catalogued seismicity, with the 2σ value of the distribution of differences being 1.47 and reducing to 0.53 when considering only the M $\geq$ 6.5 earthquakes. This overall consistency gives credibility to the used empirical scaling laws; however, some large differences between the two datasets suggest ~~the~~ further validation of this experiment in Italy and elsewhere. The ~~largest differences are probably connected with the partial activation of presumed long continuous faults. The~~ main advantages of this method ~~are its rapidity, once the faults are mapped, and~~ is its independence from temporal and (paleo)seismological information~~. The novelty is not the method, but~~, whereas the main novelty is its use at the national scale also for faults considered inactive. ~~This method cannot, however,~~ Our work can provide a perspective time-independent seismic potential of faults;

however, it cannot be a substitute for time-dependent (paleo)seismological methods for seismic hazard assessments. ~~Rather, it can rapidly provide a perspective time-independent seismic potential of faults.~~

1 Introduction

~~The maximum expected earthquake magnitude is one of the fundamental parameters to assess and predict possible threats and~~
5 ~~effects on populations as well as damage to human infrastructures, that is, to mitigate the seismic risk (McGuire, 1995; Main, 1996; Bazzurr~~
~~This parameter can be determined through different methods depending on available data and local settings.~~

In some seismically active regions like California, information derived from geodesy, the geology of active faults, and seismology (both historical and instrumental) have been combined to develop a comprehensive method that predicts 99% of the chances of having one or more $M \geq 6.7$ earthquakes in the following 30 years (USGS Fact Sheet, 2008). Along the North
10 Anatolian Fault (Turkey), fault geometry and slip accumulated during strong earthquakes have been used to infer the transfer of stress during seismic sequences and to estimate the increase of earthquake probability with $M \geq 6.7$ (Stein, 1997; Parsons et al., 2000; Bohnhoff et al., 2016). These case studies involve areas characterized by high strain rates and affected by large plate boundary faults that can be easily recognized in geological and/or geophysical records.

In contrast, other areas in the world where strain rates are low-to-intermediate and faults show smaller dimensions and un-
15 clear surface expression of recent activity, the connection between faults and earthquakes is not straightforward, particularly between potentially seismogenic faults and the maximum possible earthquake magnitude. Moreover, where lands were largely uninhabited during historical times (but are now densely populated and, therefore, potentially exposed at the seismic threat), the recurrence time of strong earthquakes is significantly longer with respect to the age of the seismological network, or information on historical and instrumental seismicity can be largely incomplete, the assessment of the maximum possible earthquake magni-
20 tude can be difficult ~~(Camelbeeck et al., 2007; Kafka, 2007; Stein and Mazzotti, 2007; Swafford et al., 2007; Braun et al., 2009; Boyd et al~~

Where frequent earthquakes are absent and seismic history is unknown, the seismic potential and the temporal knowledge of seismic activity of faults can be determined using geological studies such as paleoseismological trenching or radiometric dating of slip indicators (Galli, 2000; Rockwell et al., 2000; Palumbo et al., 2004; Dixon et al., 2003; Galli et al., 2008; McCalpin, 2009; Sherlock et al., 2009; Nuriel et al., 2012; Viete et al., 2018), but these studies are usually time-consuming and expensive.
25 Alternatively, the maximum potential magnitude of earthquakes can be assessed using empirical scaling laws of active faults, that is, using fault length and/or fault slip ~~(Wells and Coppersmith, 1994; Pegler and Das, 1996; Mai and Beroza, 2000; Henry and Das, 200~~ In this latter case, however, a lack of information on fault age and earthquake recurrence time may induce to neglect some faults as potential seismogenic sources. One method to overcome the problems connected with the lack of information on the age of (seismogenic) faulting may be to apply the existing seismic scaling ~~laws~~relationships, which directly link fault/slip dimensions
30 and earthquake magnitudes ~~(e.g., Wells and Coppersmith, 1994; Leonard, 2010)~~(e.g., Wells and Coppersmith, 1994; Leonard, 2010; Thing to the whole set of known faults including the (presumably-)inactive and undetermined faults. This method would rely on the long-held concept of fault reactivation (Sibson, 1985) due to the weakness of the fault surface compared with the host rock ~~(Sibson, 1985; Walsh III and Zoback, 2016)~~(Zoback et al., 1987; Collettini et al., 2009). This concept is particularly relevant

when considering the future behaviour of faults over long terms. For nuclear plants, for instance, it is important to assess the occurrence of events, even if very unlikely, also in areas historically free of damage, where normally these plants are built. In these sites (nuclear plants) indeed only a very low level of risk can be accepted. In other cases such as the geological disposals of radioactive wastes, the lifetimes to be considered are on the order of 105 years at least (up to 1 Ma according to prescriptions by the Nuclear

5   Accordingly, very long seismic return times must be considered, far exceeding the lifespan of historical seismic catalogues (and also paleoseismological records) normally used in standard seismic hazard assessment practices.

For the richness of data (both tectonic and catalogued historical/instrumental-seismology; Fig. 1), Italy is a suitable country for deriving and comparing the potential maximum magnitude from earthquake data and from scaling ~~laws~~relationships. Italy has, indeed, a long tradition of geological-structural mapping over the entire territory (since at least Murchison, 1849; von Zit-

10 tel, 1869; Viola, 1893; Pagani, 1907, to the recent national geological maps available online at http://sgi.isprambiente.it/geoportal/) as well as a dense seismological network operating since at least the 1980s (available online at http://cnt.rm.ingv.it/ Iside Working Group, 2016), and a rare, if not unique, historic record of earthquakes (Rovida et al., 2016).

This work includes: (1) the composition of a comprehensive catalogue of all mapped faults in Italy, merging materials from previous documents; (2) the calculations of earthquake ~~potential expected maximum magnitudes (PEMM~~magnitudes

15 (FLEM, Fault-Length Earthquake Magnitude) from the fault length in map view; (3) a comparison (i.e., the difference) of these calculations (~~PEMM~~FLEM) with catalogued seismological data (historical and instrumental earthquake magnitudes); and (4) a discussion of the agreements and differences between the calculated (~~PEMM~~FLEM) and catalogued magnitudes to determine the strengths and weaknesses of the proposed method. ~~We also provide a comparison between our experiment and similar or dissimilar experiments performed both in Italy and elsewhere.~~

20 We anticipate that, with this work, we do not intend to propose an alternative method for seismic hazard assessment or to better previous methods (e.g., Giardini, 1999; Jiménez et al., 2001; Michetti et al., 2005; Field et al., 2009, 2015; Reicherter et al., 2009). Our main aim is to test whether solely considering the known mapped faults (both active, inactive, and undetermined) and disregarding further information (e.g., historically- and instrumentally-recorded earthquakes as well as the regional stress field and strain rate) it is possible to provide, through existing seismic scaling ~~laws~~ relationships of faults and earth-

25 quakes, reasonable assessments of the maximum possible earthquake magnitude over an entire nation. The resulting (assessed) magnitudes (~~PEMM~~FLEMs) are compared (i.e., the mathematical difference) with catalogued earthquake magnitudes that are the only existing points of reference against which assessed magnitudes can be compared. Note that these results should be considered more in a theoretical and methodological perspective for comparison with future similar studies rather than in an applicative perspective for the case of Italy. In particular, our assessed earthquake magnitudes (FLEMs) for the Italian territory

30 are proposed in this paper for scientific reasons and not for their use for civil protection and prevention purposes.

2   Seismotectonic setting

The present setting of the Italian peninsula (Fig. 1) derives from the interaction (mostly convergence) of at least three main plates, namely, Eurasia to the north, Africa to the south, and Adria to the east and southeast. During Cenozoic-Quaternary

times, this tectonic interaction has led to the formation of two major mountain chains - the Alps to the north and the Apennines along the peninsula - and to the opening of two major oceanic basins - the Ligurian-Provencal basin to the west of Sardinia and Corsica and the Tyrrhenian Sea basin between the Italian peninsula and the Sicily and Sardinia major islands (Dewey et al., 1989; Malinverno and Ryan, 1986; Doglioni, 1991; Doglioni et al., 1999; Faccenna et al., 2004; Rosenbaum and Lister, 2004; Carminati et al., 2010; Carminati and Doglioni, 2012).

The Alps and Apennines are characterized by very different tectonic styles. Whereas the Alps show double-verging growth (northward and southward), with the involvement of large volumes of crystalline basement and the exhumation of metamorphic rocks (Nicolas et al., 1990; Schmid et al., 1996), the Apennines form a single-verging chain characterized by a radial vergence and a strong curvature from northwest to southeast. The Apennines are characterized by thin-skinned tectonics with rare expo-sures of the crystalline basement and metamorphic rocks (Barchi et al., 1998; Patacca et al., 2008; Scrocca et al., 2005). The development of the Apennines (contraction) occurred partly at the same time with the development of the Ligurian-Provencal and Tyrrhenian oceanic basins (extension). The different tectonic styles of Alps and Apennines are also well represented by the different settings of the related foreland monoclines and basins. The foreland basin is shallow in front of the Alps with a monocline dipping by 2-4° and deep in front of the Apennines with a monocline dipping by 6-15° (Mariotti and Doglioni, 2000).

The present seismotectonic setting of Italy is still mainly ruled by the interaction between the African and Eurasian plates, presently converging at a rate of c. 10 mm/yr along a NNW-SSE direction (DeMets et al., 1990; Serpelloni et al., 2005; Billi et al., 2011). This kinematic setting is complicated by the Adria plate (an independent microplate or a promontory of the African plate), which contributes to cause contractional deformations along the central-northern Adriatic margins (both toward the Apennines to the west and toward the Dinarides to the east) and in the Po Plain between the northern Apennines and the southern Alps. Contractional deformations are in contrast absent or poorly active in the southern Apennines where these deformations have been inactive or poorly active since about mid-Pleistocene times. In synthesis, for the aims of this work, it is important to know that most of the Italian territory has been subject to numerous deformation phases with related activations, re-activations, and/or inversions of faults. These phases are schematically amenable to one or two main complex tectonic mechanisms: the Alpine orogenesis (Paleozoic to present times) and the Hercinian orogenesis (Paleozoic times) (Vai, 2001). At present, within the Alpine orogenesis, back-arc extensional seismic mechanisms prevail in large areas of the Italian territory (e.g., the axial portion of the Apennines), whereas compressional seismic mechanisms are less frequent and prevail elsewhere (e.g., the eastern or Adriatic portion of the Apennines) (e.g., Basili and Meghraoui, 2001; Neri et al., 2002, 2005; Roberts and Michetti, 2004; Chiarabba et al., 2005, 2015; Palano et al., 2012; Presti et al., 2013; Ferranti et al., 2014; Cowie et al., 2017; Orecchio et al., 2017). Strike-slip tectonics is limited to a few major fault zones (e.g., Grasso and Reuther, 1988; Billi et al., 2003; Viganò et al., 2015; Polonia et al., 2016, 2017).

Italy has a widespread crustal seismicity (depth < 35 km) that concentrates along some portions of the Alps and mostly on the Apennines, including Calabria and Sicily (Fig. 1). Deep earthquakes are mainly located beneath the Calabrian Arc and, secondarily, beneath the northern Apennines and eastern Alps, where sparse seismicity is recorded (Chiarabba et al., 2005). The eastern and western Alps show a clustered crustal seismicity (Fig. 1), whereas in the central Alps the number of recorded

events seems to be less densely distributed. This is probably related to the lack of an appropriately-dense seismic network in this area (Amato, 2004; Chiarabba et al., 2005).

The western Alps are particularly active in their southern portion, where active N-S-striking faults accommodate most of the extensional and wrench deformations that characterize the present-day tectonics of the area (Chiarabba et al., 2005; Sanchez et al., 2010; Sue et al., 1999; Sue and Tricart, 2002). Focal mechanisms of the sparse seismicity in the central Alps show extensional kinematics on N-S-striking fault planes (Chiarabba et al., 2005); however, stress field studies in this area suggest mainly active N-S compression (Montone and Mariucci, 2016). The clustered seismicity recorded in the eastern Alps is mainly located along E-W trending structures, showing an overall compressive tectonics generating large thrust earthquakes in response to a N-S trending compression, like the 1976 Friuli, Mw = 6.4 earthquake (Bressan et al., 1998; Cheloni et al., 2012; Michetti et al., 2012).

The Apennines seismicity is densely distributed along the whole chain (Fig. 1). Focal mechanisms of the chain show a rotation of the fault strike from NW-trending alignments to NNE-trending ones moving from north to south, along the arc-like shape of the Apennines. In general, in the middle portion (axis) of the Apennines, earthquakes are characterized by extensional kinematics, whereas the Adriatic front is mainly affected by compressive kinematics, which is in agreement with the regional stress field (Montone and Mariucci, 2016). In particular, the north-western portion of the Apennines shows a NW-SE trending cluster of seismicity. Moving eastward, beneath the Po Plain, seismicity involves the northern Apennines outer front (Fig. 1), where focal mechanisms are mainly compressive, highlighting E-W-striking fault planes consistent with the attitude of the main structures of the area. Here, the largest instrumentally measured earthquakes (Mw = 6.1) occurred in 2012 during the Emilia (N-Apennines) sequence (Govoni et al., 2014). Moving southward, crustal seismicity (M 4-6.5) is densely distributed and follows the Apennine chain axis. In this zone (Umbria-Marche), the largest instrumental earthquakes with extensional focal mechanisms occurred in the 1997 Colfiorito, Mw = 6.0 (Amato et al., 1998); 2016 Norcia, Mw = 6.5 (Chiaraluce et al., 2017); 2016 Amatrice, Mw = 6.0 (Chiaraluce et al., 2017); 2009 L'Aquila (Abruzzi), Mw = 6.3 (Chiarabba et al., 2009); and 1980 Irpinia (Campania), Mw = 6.9 (Nostro et al., 1997) earthquakes. A cluster of moderate (M 4.0-5.0) seismicity is recognized close to the Tyrrhenian coast in relation to active geothermal and volcanic districts (Gasparini et al., 1985). Larger earthquakes characterize the Apennines southern portion (Calabria), with historical seismic events that reached magnitudes up to ~~6.9-7.5 (Cello et al., 2003; Gasparini et al., 1985)~~≃7.1 (Rovida et al., 2016; Guidoboni et al., 2018).

The Calabrian Arc (Fig. 1) is mostly characterized by deep instrumental seismicity related to the NW dipping Benioff plane (Polonia et al., 2016; Selvaggi and Chiarabba, 1995). Both the Etna area and the northern on-shore portion of Sicily show clustered seismicity, where the latter is mainly characterized by extensional and oblique-extensional earthquakes (Azzaro and Barbano, 2000; Billi et al., 2006a). The strongest earthquakes (some of them with associated destructive tsunamis; Billi et al., 2010) from historical catalogues in the area occurred predominantly on extensional faults and are: the 1908 (Mw 7.2) earthquake of Messina and Reggio Calabria (Messina Straits, Sicily), the 1638 and 1905 (Mw 7.0) earthquakes of Nicastro (Calabria), and the 1693 (Mw 7.4) earthquake of eastern Sicily (Rovida et al., 2016).

The Southern Tyrrhenian (Fig. 1) is characterized by intense seismicity, with magnitudes up to 7.1, which occurred in 1938 at 290 km depth (Selvaggi and Chiarabba, 1995). The seismicity of shallow levels (< 30 km) below the southern Tyrrhenian

Sea indicates the presence of two adjacent domains characterized by different tectonic environments: (1) to the northwest of the Aeolian Islands, a N-S compressive tectonics is present, whereas (2) to the east and southeast of these same islands, a NW-SE extensional tectonics occurs (Fig. 2) (Goes et al., 2004; Pondrelli et al., 2004; Billi et al., 2006a; Cuffaro et al., 2010). Intermediate and deep seismicity concentrates along a roughly uninterrupted, narrow, and steep (70°) Benioff zone, which strikes SW-NE, dips toward NW, and reaches a depth of about 500 km; only one earthquake occurred inland at depth of 350 km (Pondrelli et al., 2004; Selvaggi and Chiarabba, 1995). Shallow compressive seismicity (< 30 km deep) is characterized by epicentres mainly aligned E-W (Pondrelli et al., 2004; Presti et al., 2013), off-shore northern Sicily, and it rotates roughly NNW-SSE moving eastward (Fig. 1). Sparse compressive events have also been recorded off-shore north-eastern and southern Sardinia.

3   Input data

3.1   Fault data

To build a comprehensive dataset of faults in Italy (Figs. 1-3; supplement; Petricca et al., 2018), the following databases were merged: (1) the entire fault collection of the Italian Geological Maps at the 1:100,000 scale (i.e., Carta Geologica d'Italia available online at www.isprambiente.it); (2) the fault compilation from the Structural Model of Italy at the 1:500,000 scale (Bigi et al., 1989); (3) all faults provided in the ITHACA-Italian Catalogue of Capable Faults (Michetti et al., 2000); and (4) the inventory of active faults from the GNDT (Gruppo Nazionale per la Difesa dai Terremoti; Galadini et al., 2000) database. The strength point of our approach is the assemblage of different fault datasets heterogeneously built for different purposes and based on different primary information and methods. In this approach, we consider all known faults (see above) to form a dataset as comprehensive as possible.

Faults from the 1:100,000 Italian Geological Maps and 1:500,000 Structural Model of Italy (black and black dashed lines, respectively, in Fig. 2) are essentially based on field surveys integrated with subsurface geophysical data and, therefore, were drawn and constrained by geological and geophysical observations.

The ITHACA-Italian Catalogue of Capable Faults (Michetti et al., 2000) is a database developed by the ISPRA (Istituto Superiore per la Protezione e la Ricerca Ambientale) containing cartographic and parametric information of active faults - i.e., faults with evidence of repeated reactivation during the last 40,000 years - capable of rupturing the ground surface in Italy. The database is available as a layer in a web GIS (http://www.isprambiente.gov.it/it/progetti/suolo-e-territorio-1/ithaca-catalogo-delle-faglie-capaci) and contains both the geographic location and a text description of each fault. The entire set of capable faults is included in this compilation (blue lines in Fig. 2).

The inventory of active faults of the GNDT database (Galadini et al., 2000) represents a collection of the Italian active faults. The activity of these faults is mainly deduced through surface geological evidence and (paleo)seismological data including historical information (red lines in Fig. 2).

To improve and implement these fault databases, we selected published complementary studies for some specific areas considered to not be exhaustively covered by the aforementioned collection of faults including Sardinia, SW Alps, Tuscany,

the Adriatic front, Puglia, and the Calabrian Arc. For these areas, we selected faults on the grounds of scientific contributions that documented faults presence based on field, seismic, and paleoseismological data (pink lines in Fig. 2). In particular, for the Campidano area (southern Sardinia), we used the fault pattern proposed by Casula et al. (2001), who reconstructed fault geometry with recent tectonic activity based on field and seismic reflection profiles. For the SW Alps, we followed the works of Augliera et al. (1994), Courboulex et al. (1998), Larroque et al. (2001), Christophe et al. (2012), Sue et al. (2007), Capponi et al. (2009), Turino et al. (2009) and Sanchez et al. (2010). For the Tuscany area, we consulted Brogi et al. (2003), Brogi et al. (2005), Brogi (2006), Brogi (2008), Brogi (2011) and Brogi and Fabbrini (2009). For the buried northern Apennines and Adriatic front, we used the fault datasets provided by Scrocca (2006), Cuffaro et al. (2010) and Fantoni and Franciosi (2010). For the Puglia region, we used data from Patacca and Scandone (2004) and Del Gaudio et al. (2007), whereas, for the Calabrian Arc, we used data from Polonia et al. (2016) and Polonia et al. (2017).

Furthermore, we are aware of the DISS compilation of seismogenic sources in Italy (Basili et al., 2008; DISS Working Group, 2018) as one of the most important integrated datasets of the Italian territory in this field. However, we did not use this dataset in this work since, as described in Basili et al. (2008), the dataset aims to identify the "seismogenic sources" rather than the actual faults. A composite seismogenic source (CSS in the DISS nomenclature) is a complex fault system showing homogeneous kinematic and geometric parameters and contains an unspecified number of aligned possible ruptures (i.e., faults) that cannot be isolated. Hence, a CSS, for its own nature, cannot be considered a real fault as declared in our scope.

The above-mentioned fault datasets form a comprehensive tectonic image of the Italian territory (Fig. 2). These fault data and the spatial grid are available for download as ASCII files in the supplement (see also Petricca et al., 2018). The major thrust faults occur along (1) the N-verging western and north-western external front of the northern Alps, (2) the S-verging frontal ramp of the southern Alps (Po Plain and Veneto-Friuli regions), (3) the E- to N-verging external front of the central-northern Apennines from the Po Plain down to the central Adriatic off-shore, (4) the SE-verging outer front of the Calabrian Arc, (5) the outer (southern) front of the Maghrebian-Apennines chain in Sicily, and (6) the E-W-trending contractional belt located in the southern Tyrrhenian Sea, close to the northern Sicily coast.

The major normal faults occur along the median zone of the Apennines fold-thrust belt (Fig. 2), namely: (1) in northern Tuscany, (2) in central Italy including the Tuscany, Umbria, Marche, and Abruzzi regions, (3) in the southern Apennines including the Molise, Campania, Basilicata, and Calabria regions, and (4) in eastern Sicily including the Messina Straits, part of the Ionian Sea areas, and the Hyblean foreland. In particular, SW-dipping, high-angle normal faults (NW-striking) host the strongest seismicity recorded along the northern-central Apennines belt (Figs. 1 and 3). This fault pattern rotates to a NE-trending direction toward the southern Calabria region consistently with the focal solutions of the area (Fig. 1). Moreover, extensional faults have also been mapped in the Sardinian region, specifically in the Campidano graben, mainly based on subsurface data (Casula et al., 2001).

Strike-slip faults are located in some areas of the Italian territory (e.g., Billi et al., 2003, 2007), in particular: (1) in the southern Alps (Veneto) with NNW-striking structures, (2) across the external front of the central-southern Apennines foreland-fold-thrust belt (e.g., south of the Montemurro area, Fig. 1), (3) along the central Adriatic-Gargano-Molise belt with E-W-striking structures, (4) across the Calabrian Arc with radial structures cutting through the accretionary wedge, (5) in eastern

7

Sicily from the Aeolian Islands (Tyrrhenian Sea) and southward into the Ionian Sea, and (6) in south-western Sicily and in the Sicily Channel with structures striking between N-S and NNE-SSW (Figs. 1 and 2).

3.2 Earthquake data

To obtain a complete earthquake dataset for the Italian territory (Figs. 1 and 3; supplement; Petricca et al., 2018), we integrated the existing most comprehensive catalogues of instrumental and historical seismicity: (1) the CSI1.1 instrumental database (csi.rm.ingv.it; Castello et al., 2006) for the 1981–2002 period; (2) the ISIDe instrumental database (iside.rm.ingv.it; Iside Working Group, 2016) for the 2003–2017 period; and (3) the CPTI15 historical-instrumental database (emidius.mi.ingv.it; Rovida et al., 2016) for the 1000-1981 period.

The CSI 1.1 database (Castello et al., 2006) is a catalogue of Italian relocated earthquakes for the 1997–2002 period. This collection derives from the work by Chiarabba et al. (2005), who relocated, using a homogeneous procedure, approximately 45,000 events provided by several seismological networks (both national, regional, and local) operating in the Italian territory. Most seismic events are lower than 4.0 in magnitude and are mostly located in the upper 12 km of the crust. A few earthquakes exceed magnitude 5.0, whereas the largest event is Mw 6.0. The time-span of this compilation is 1981–2002. From the CSI 1.1 database, we selected events with Mw > 4.0 (Fig. 3).

The ISIDe database (Iside Working Group, 2016) provides the parameters of earthquakes from real-time recordings and from the Italian Seismic Bulletin. The main aim of this database is to supply information on the seismicity as soon as it becomes available by integrating it with updated information on past seismicity. The time-span of this compilation begins in 1985 and lasts up to the present day. To avoid an overlap with the CSI database (1981–2002), from the ISIDe database, we considered events with Mw > 4.0 only from the 2003–2017 period (Fig. 3).

The CPTI15 historic database integrates the Italian macroseismic database version 2015 (DBMI15; Locati et al., 2016) and instrumental data from 26 different catalogues, databases, and regional studies (including the CSI and ISIDe databases) for the Italian territory, starting from 1000 A.D. until 2014. This catalogue provides moment magnitudes from macroseismic determination for more than 3200 earthquakes with values in the 4-7 range of Mw. To avoid any overlapping of data with the aforementioned instrumental datasets, we used data from the 1000-1981 period from the CPTI2015 catalogue.

We acknowledge that the earthquake magnitude used in this paper is the moment magnitude (Mw) and it should be noted that, for a few earthquakes from the aforementioned datasets, only the Ml (local magnitude) is available. However, according to Grünthal and Wahlström (2003), the difference between Mw an Ml can be ignored for magnitudes above 4, which represents the main focus of this study.

8

4 Method

4.1 ~~PEMM~~ FLEM computation

Starting from the entire dataset of faults in Italy, as a first step, we measured the length of each fault as the real fault trace length in map view, i.e., the length of the vertical projection of the fault trace as observed on the Earth's surface over a horizontal plane (Fig. 2; supplement; Petricca et al., 2018). Our complete dataset includes 12467 faults. Specifically, it includes 9169 A-class faults and 3298 B-class faults. Explanations for the classification into A- and B-class faults are given in the following sections. As most faults have a horizontal length that is less than 25 km regardless of the selected database (Fig. 4), we divided the Italian territory into a grid with square cells of 25x25 km (Fig. 5; i.e., see also the explanation below). The length of the longest fault crossing each cell determined the parameter "fault length" (Lf) of the considered cell. In the second step, we used these lengths (Lf) as input parameters to empirically derive the earthquake magnitude (i.e., ~~PEMM~~FLEM) of each cell containing at least one fault (Supplement; Petricca et al., 2018). Our only criterion to choose the fault from which the FLEM of the considered cell is computed is the greatest fault length in map view. In such a way, only one fault (the longest one) will provide the FLEM in a given cell. Therefore, faults cannot be and are not double-counted. Several studies investigated the scaling relationship between earthquake magnitudes and various geometric-kinematic parameters (i.e., fault dimensions and slip) of causative faults (e.g., Wells and Coppersmith, 1994; Leonard, 2010; Thingbaijam et al., 2017, and references therein), providing similar empirical equations. We used the equation proposed by Leonard (2010) (hereafter named as L10) that is expressed as:

$$\underline{PEMM}\underline{FLEM} = M = a + b * log(Lf) \tag{1}$$

where a and b are constants related to fault kinematics and are equal to 4.24 and 1.67, respectively (see table 6 in Leonard, 2010), and Lf is the fault length as explained above. From Eq. 1, in our study, ~~PEMM~~ FLEM values range from 4.74 to 7.40, where the two end members are obviously imposed by the minimum and maximum fault length of the dataset, i.e., $\simeq 2$ and $\simeq$ 75 km, respectively (Supplement; Petricca et al., 2018). Reasons for the choice of L10 are explained below.

4.2 Limits and assumptions

The method used in this study is based on some approximations and assumptions regarding the following points: (1) the arbitrary dimension of the cells (25x25 km); (2) the choice of the Leonard's equation and parameters (L10; Leonard, 2010) instead of others (e.g., Wells and Coppersmith, 1994); (3) the reliability of fault lengths; and (4) the assumption that all considered faults are active or can be potentially reactivated.

(1) Cell dimensions: as explained above, we choose a cell size of 25x25 km after considering the mean length (Figs. 4 and 5) of our fault dataset (Supplement; Petricca et al., 2018). Moreover, crustal earthquakes in Italy are mostly generated at a depth of 4-10 km. Within this depth range, the attitude of faults determines the distance between the fault trace and the epicentre over the Earth's surface. For instance, a hypocentral depth of 10 km along a causative fault dipping 45° implies a horizontal shift of about 10 km between the fault trace on the Earth's surface and the earthquake epicentre. Since the hypocentral depth is usually

less than 10 km, a cell dimension of 25 km favours the occurrence of causative faults and related earthquake epicentres in the same cell. Moreover, to test the suitability of the size (25 km) of our square cells, we tested the sensitivity of the FLEM and the difference between the FLEM and the catalogued earthquake magnitudes on the cell size. We performed this sensitivity test on central Italy that is one of the most seismic areas of Italy. In this area, we changed our grid (i.e., cell size 25x25 km) both into a finer grid characterized by a cell size of 12.5x12.5 km and into a coarser grid characterized by a cell size of 50x50 km (Figs. S1 and S2). Each 50 km side square cell includes four 25 km side square cells and sixteen 12.5 km side square cells. For all cells, we computed the FLEM (Fig. S1) and the difference between the FLEM and the catalogued earthquake magnitudes (Fig. S2). Then, cell by cell, we compared results (i.e., the FLEM) obtained for the largest and smallest grids (i.e., with square cell size of 12.5 and 50 km) against the FLEM obtained in the same geographical position using the intermediate grid (i.e., with square cell size of 25 km) (Fig. S3). This analysis shows that a change of grid size between 12.5 and 50 km does not provoke dramatic changes in the spatial distribution of both the FLEM (Fig. S1) and the difference between the FLEM and the catalogued earthquake magnitudes (Fig. S2). In particular, using the largest grid (cell size = 50 km), the FLEM tends to be smoothed toward an upper boundary between magnitude 6 and 7 (Fig. S3a). This is due to the fact that only the longest faults of the dataset are considered for the FLEM computation. On the contrary, using the smallest grid (cell size = 12.5 km), the FLEM tends to be rather scattered and depressed around a magnitude 6 (Fig. S3a). This is due to the fact that reducing the cell size, in many cases, minor (small) faults result as being the longest ones in small cells. These results are also synthetically expressed by the arithmetic averages of non-null FLEMs in the three different grids that are: $FLEM_{average}$ = 6.04, 6.19, and 6.62 for the grids with 12.5, 25, and 50 km sized cells, respectively. This sensitivity analysis shows that a microzonation (12.5 km sized cells) tends to locally overvalue small faults that are clearly poorly relevant when compared with adjacent (10-20 km distant) longer faults. On the contrary, a macrozonation (50 km sized cells) could overvalue long faults whose effect may be strongly reduced in a large area such as that included in a 50x50 km cell. Our choice (cell size = 25 km) appears therefore a good compromise between significant faults and their potential areal influence.

(2) Adopted equation parameters: The most popular scaling equations that directly relate fault length and earthquake magnitude are provided by Wells and Coppersmith (1994), Leonard (2010), and Thingbaijam et al. (2017), among others. In this work, we used the equation (L10) by Leonard (2010) for dip-slip faults (both extensional and compressional). This equation is particularly suitable for Italy, where most earthquakes are generated by dip-slip faults (e.g., Chiarabba et al., 2005). The main advantage of using Eq. 1 ~~with respect to the equations by Wells and Coppersmith (1994) and Thingbaijam et al. (2017)~~ is that L10 is valid for both buried and outcropping fault as well as for normal and reverse (dip-slip) faults. ~~Moreover, L10 is an advancement of the previous and successful equations provided by Wells and Coppersmith (1994) as the database used by Leonard (2010) is updated and larger than previous databases, even larger than the database used later by Thingbaijam et al. (2017).~~ To assess the difference (i.e., Fig. 6) between L10 and the equations provided by ~~Wells and Coppersmith (1994) and Thingbaijam et al. (2017)~~others, in Fig. 6a, we plotted the computed earthquake magnitude as a function of fault length for all scaling equations by Wells and Coppersmith (1994), Leonard (2010), and Thingbaijam et al. (2017). Fig. 6b shows the difference between L10 and all other equations. For large fault lengths (i.e., corresponding to large earthquake magnitudes), the difference is mostly less than 5~~%~~%. This difference increases to about 15~~%~~% for smaller faults (i.e., for fault length ≤ 2 km) corresponding to earthquake mag-

nitudes less than about 4.8 (Fig. 6a). These fault lengths ($\leq$ c. 2 km) and earthquake magnitudes ($\leq$ 4.8) represent the lower boundary of this study. For this reason, we assessed the difference of results from L10 with results from other scaling equations (Fig. 6) as acceptable for the aims of our study. In particular, also considering the version of L10 given for strike-slip faults, the difference with the version of L10 that we used (i.e., ~~dip slip~~ for dip-slip faults) is less than 3 ~~%~~ % (Fig. 6b). Note also that, due to the lower boundaries of the magnitude range for which the equations considered in Fig. 6 are valid (i.e., Mw $\geq$ 4.8-5.0 forWells and Coppersmith (1994) and Mw $\geq$ 5.8 for Thingbaijam et al. (2017)), Fig. 6 is relevant for Mw higher than these lower boundaries.

(3) Fault length reliability: ~~PEMM~~ FLEM is calculated through Eq. 1 from the longest fault falling in each cell (Fig. 5). For faults located on-shore and well exposed at the surface, detailed studies allow for a well-constrained and reliable characterization of fault length (class A faults). On the contrary, for some specific regions like the south-western Alps, the eastern front of the Po Plain, the eastern Alps, the off-shore Adriatic front and Calabrian Arc, where fault planes are not exposed at the surface (i.e., buried and/or off-shore faults), fault geometry has been mainly constrained from regional seismic reflection profiles or from earthquake sequences. Therefore, fault length and along strike continuity are not well constrained, hence, producing the longest faults of the whole dataset. We assess the dimension of these latter faults as poorly constrained and reliable (class B faults). Following this analysis on the accuracy on fault dimension, we decided to divide the dataset into two quality classes. Class A (high quality) includes exposed faults where subsurface and surface data allow for a detailed and reliable characterization of fault length (light purple cells in Fig. 5), whereas class B (low quality) contains buried and off-shore faults investigated mainly by seismic surveys, for which a precise characterization of fault length cannot be achieved (dark grey cells in Fig. 5). Moreover, we acknowledge that ~~PEMM (the potential expected maximum magnitudeof earthquakes~~ FLEM (fault length earthquake magnitude) is indeed the maximum magnitude expectable from the actual size of the causal faults based on Eq. 1. A co-seismic lengthening of the causal faults through, for instance, the rupture of a bridge separating two adjacent faults to form one may produce earthquakes with a magnitude greater than that expected from the length of each of the two faults as measured before the fault co-seismic junction.

(4) Fault orientation and activity: although it is well known that each earthquake is usually associated with a precise slip on a fault plane and that the potential of a fault to undergo (seismic) slip depends on its orientation within the stress field (Morris et al., 1996; Collettini and Trippetta, 2007), it is also true that the seismic history of the Earth is characterized by many examples of unexpected earthquakes occurring where plate boundaries are far away (i.e., intraplate earthquakes), and/or the stress field is apparently badly oriented to trigger earthquakes (Bouchon et al., 1998; Camelbeeck et al., 2007; Kafka, 2007; Stein and Mazzotti, 2007; Swafford et al., 2007; Braun et al., 2009; Boyd et al., 2013; Leonard et al., 2014; Talwani, 2014; Campbell et al., 2015; Walsh III and Zoback, 2016; Christophersen et al., 2017). Since our study aims to define the ~~Potential Expected Maximum Magnitude (PEMM~~ Fault-Length Earthquake Magnitude (FLEM) of each fault and cell, based on the aforementioned instances, we assumed that all faults are potentially reactivable. This notion becomes increasingly relevant when considering the prospective behaviour of faults over long terms. As mentioned above, indeed, for some societal challenges such as the safety of nuclear waste repositories, the recommendations are to consider the behaviour of faults in the future up to even 1 Ma

11

5 Results and discussion

Bearing in mind the limits mentioned above, we firstly calculated the ~~PEMM~~ FLEM for the Italian territory using the faults of

5   class A (Fig. 7; supplement; Petricca et al., 2018). Most of the Italian territory, including the entire Apennine belt, the north-eastern Alps, and the central part of the Po Plain, is characterized by $6.0 \leq$ ~~PEMM~~ FLEM ≤ 7.0. The largest ~~PEMMs~~ FLEMs have been obtained for the north-eastern Alps (~~PEMMs~~ FLEMs ≤ 7.4) and are mainly related to the E-W-striking thrusts of the area responsible for the 1976 Friuli earthquake (Mw = 6.4; Bressan et al., 1998; Cheloni et al., 2012). In this area, we recall also the Carinthian great earthquake of 1348 (Villach, Mw 7.0; Rohr, 2003). In the central Alps, long and continuous

10   thrust faults are reported in the ITHACA dataset (e.g., Maurer et al., 1997; Keller et al., 2006) and result in ~~PEMMs~~ FLEMs of about 6.5. These large thrust faults also characterize the western part of the Po Plain, producing ~~PEMMs~~ FLEMs of about 7.0. ~~PEMMs~~ FLEMs between 6.5 and 7.0 are also estimated toward the south along the Apennine chain and in the Tuscany region, where large normal faults are reported from the ITHACA dataset and confirmed by detailed studies (Brogi et al., 2003; Brogi and Fabbrini, 2009). The largest ~~PEMMs~~ FLEMs along the northern Apennines (Fig. 7) are due to the Alto Tiberina

15   low angle normal fault, a large regional structure that seems to accommodate part of the deformation by aseismic creep and microseismicity (Chiaraluce et al., 2007; Collettini, 2011; Anderlini et al., 2016).

Large ~~PEMMs~~ FLEMs occur also in the Vesuvius area (Campania region), where faults longer than 30 km have been reported in the ITHACA dataset (Fig. 5). Several studies (Finetti and Morelli, 1974; Scandone and Cortini, 1982; Vilardo et al., 1996; Brozzetti, 2011) confirm the presence of these long faults in the Vesuvius area. In the southern Apennines (Campania,

20   Basilicata, and Calabria regions), ~~PEMMs~~ FLEMs are in the range of 6.5-7.0, being related to the largest extensional faults of the area (Figs. 2 and 5). To the south, in the northern portion of Sicily, ~~PEMMs~~ FLEMs > 7.0 are related to long off-shore faults. Some of these ~~PEMMs~~ FLEMs are related to the transtensional-transpressional Tindari Fault System, located in NE Sicily. Other ~~PEMMs~~ FLEMs are connected to the extensional system of the Messina Straits (Ghisetti, 1979; Locardi and Nappi, 1979; Lanzafame and Bousquet, 1997; Billi et al., 2006b, 2007; Palano et al., 2012; Cultrera et al., 2017).

25   The map of ~~PEMMs~~ FLEMs derived using class B faults (Fig. 8) shows seismic events in the magnitude interval of 5.0-6.0 in the Tyrrhenian sector and in the southern portions of Puglia. Large ~~PEMMs~~ FLEMs (up to M $\simeq 7.85$) occur along the north-eastern Alps, the thrust fronts beneath the Po Delta, the north Adriatic front, the Ionian off-shore of the Calabria-Peloritani Arc, and some areas of Sardinia (Fig. 8). ~~PEMMs~~ FLEMs $\simeq 8.0$ derive from structures constrained only by subsurface data, for which the along-strike continuity cannot be properly assessed and, hence, the total length is likely to be largely overestimated.

30   The largest ~~PEMMs~~ FLEMs calculated for the Sardinian territory are related to structures inferred from large-scale (1:500,000) maps. These structures are longer (Fig. 5, red segments) than those derived, in the same areas, from detailed studies (Fig. 5, pink segments) and, therefore, the actual length is also likely to be overestimated in this case.

To compare the ~~PEMMs~~ FLEMs estimated on the grounds of geological fault length (Figs. 7 and 8) with the maximum magnitudes obtained from the historical and instrumental seismicity databases (i.e., catalogued earthquake magnitudes), we used the same grid presented above (Fig. 5). In particular, for each cell of Fig. 5, we selected the maximum earthquake magnitude recorded in historical or instrumental earthquake databases, applying a lower cut-off at magnitude 4.0 (Fig. 9).

5 Large earthquake magnitudes - i.e., M > 6.0 earthquakes - were recorded in the north-eastern Alps, in the Po Plain, and along the entire Apennine chain. The strongest events (M $\leq$ 7.4) were recorded in the north-eastern Alps and in the southern portion of the Apennines, including the Messina Straits and southern Sicily (Fig. 9). Earthquakes with magnitudes $\simeq$ 4.0-4.5 occurred almost everywhere in the Italian territory.

To spatially compare the earthquake magnitudes obtained through the ~~PEMM~~ FLEM computation (Figs. 7 and 8) and those

10 recorded in the historical-instrumental catalogues (Fig. 9), we realized a map of the earthquake magnitude differences to show for each cell the difference between ~~PEMMs~~ FLEMs obtained from the length of class A (Fig. 10) and class B (Fig. 11) faults and the magnitudes of historically/instrumentally-recorded earthquakes. In the case of class A faults, this comparison (Fig. 10) shows, in general, a difference of M $\leq$ 1.5. By fitting the differences distribution with a Gaussian curve, we obtained a mean of 0.86 with a 2σ (double standard deviation) of 1.47 on ~~PEMMs~~ FLEMs derived from class A faults (Fig. 12a). The 2σ value is

15 amplified to 1.85 (Fig. 12b) when also considering ~~PEMMs~~ FLEMs from poorly reliable fault lengths (i.e., difference for class A+B faults in Fig. 12b).

Finally we compared ~~PEMMs~~ FLEMs with only the strongest earthquakes (M $\geq$ 6.5) in the historical and instrumental catalogues since 1000 A.D. to 2017 (Fig. 13 and also Table 1). In this case, the difference with the spatially-corresponding ~~PEMMs~~ FLEMs (i.e., same cell) is less than 1.0 and, in most instances, less than 0.4 (Fig. 13a). In particular, the mean

20 difference is -0.09 with a 2σ value of 0.53 (Fig. 13c). Note also that, even when not equal to the spatially-corresponding catalogued earthquake magnitudes, yet many ~~PEMMs~~ FLEMs fall within the uncertainty interval (i.e., in Fig. 13b, see the red circles falling along the blue vertical bars) associated with these catalogued magnitudes.

In the histograms of Figs. 12 and 13(c), the values in the negative fields can be interpreted as ~~PEMM999~~ FLEM999s underestimation (i.e., where ~~PEMM~~ FLEM values do not reach the catalogued earthquake magnitudes, which are in turn affected

25 by uncertainty; e.g., Fig. 13b). In contrast, values in the positive fields of Figs. 12 and 13(c) could be interpreted either as ~~PEMM999~~ FLEM999s overestimation (i.e., where ~~PEMM~~ FLEM values unsuitably exceed the catalogued earthquake magnitudes) or as a sort of catalogue incompleteness (i.e., where the catalogued earthquake magnitudes do not properly represent larger seismic potentials of faults). Occurrences in the positive fields (green portions in Figs. 12 and 13c) are significantly more frequent than occurrences in the negative fields (red portions in Figs. 12 and 13c), particularly in Fig. 12. These positive and

30 negative occurrences are also mapped in Figs. 10 and 11 with green and red tones, respectively, whereas white cells are where ~~PEMM999~~ FLEM999s differences with respect to catalogued earthquake magnitudes are about null. Figs. 10 and 11 show that negative (red) occurrences are very limited.

It is also interesting to note that, in the period between our dataset of catalogued earthquakes (i.e., in times younger than December 2017) and the time of writing (September 2018), only one crustal M>5 earthquake occurred in Italy. Namely, the

35 Montecilfone Mw 5.1 earthquake occurred on August 16th, 2018, in the central Apennines at latitude 41.87N and Longitude

14.86E and depth of 20 km. In the same locality, our ~~PEMM~~ FLEM is 5.9, corroborating the observations and considerations made above on the difference between ~~PEMMs~~ FLEMs and catalogued earthquake magnitudes.

Summarizing, the difference between ~~PEMMs~~ FLEMs and catalogued earthquakes can be either real, indicating that some large earthquakes, possibly due to extremely long recurrence intervals, are not contained in the seismological records, or a bias induced mainly by the following factors: (1) impossibility to resolve fault continuity and segmentation with the adopted method and (2) deformation partially accommodated through aseismic creep.

The limited difference, as discussed above, between ~~PEMMs~~ FLEMs and the catalogued earthquake magnitudes (Figs. 12a and 13c) is due to the comprehensive knowledge of the exposed faults (particularly faults of class A, Fig. 12a). A large amount of data is indeed available from detailed field surveys and subsurface investigations realized over the years. However, some portions of the eastern Alps, northern Apennines, and southern Italy, including Sicily, show a difference in the magnitude of 2.0-2.5 (i.e., faults of class B, Fig. 12b). In these areas, more detailed studies should be developed in order to better characterize fault dimensions and properly assess seismic hazards. It is, however, very encouraging that when considering only the historical and instrumental earthquakes with M ≥ 6.5, the difference between ~~PEMM~~ FLEM values and the catalogued earthquake magnitudes significantly reduces (Fig. 13).

Regarding the ~~PEMMs~~ FLEMs evaluated using class B faults (Fig. 11), we observe a significant difference with catalogued earthquakes in several regions. Differences of up to 4.0 in magnitude (Fig. 12b) are estimated in correspondence of the north Adriatic thrust front, off-shore from the Calabria-Peloritani Arc, and the northeast part of the Alps (Fig. 11). Smaller, but still relevant, differences of M ≃ 2.0 are documented in correspondence of the Apennines front beneath the Po Plain. As mentioned above, class B fault lengths have been evaluated mostly using seismic reflection profiles. Due to the resolution of this technique and the quality of some datasets, fault segmentation cannot be properly evaluated. More evidence would be needed. In general, the significant differences between ~~PEMMs~~ FLEMs (class B faults) and the catalogued magnitudes require that extensive 3D geological and geophysical investigation of the structures of these areas should be performed in order to better characterize the geometry and continuity of faults.

6   ~~Comparison with similar studies in Italy and elsewhere~~

~~Several national and international seismic hazard projects have been recently carried out for New Zealand (Stirling et al., 2002), Europe (Giardini et al., 2013; Woessner et al., 2015), USA (Petersen et al., 2008, 2014), the Middle East (Danciu et al., 2016), California (Field et al., 2009, 2014), Central Asia (Ullah et al., 2015), Italy (Cinti et al., 2004; Basili et al., 2008; DISS Working Group, 20 as well as several other studies on other countries. We here briefly compare some of these projects with our study to understand the main differences and similarities as well as the advantages and disadvantages.~~

~~Stirling et al. (2002, 2012) provided a probabilistic seismic hazard analysis (PSHA) for New Zealand, using an improved version of the method proposed by Cornell (1968). The PSHA involved geologic data and~~ To this end, it is also noteworthy that studies on the ~~historical earthquake record to define the locations of earthquake sources and the likely magnitudes and~~

~~frequencies of earthquakes that may be produced by each source. Finally, estimates of the ground motions that the sources will produce at a grid of sites that covers the entire region were provided.~~

~~Petersen et al. (2008, 2014) produced time-independent seismic hazard maps of USA using a very large dataset of earthquake sources and ground motion models . Also in this case ,~~ 2016 Amatrice-Norcia (central Italy) earthquakes (Mw 6.0 and 6.5) revealed that the length of ~~the method used by Petersen et al. involved an extremely large set of data, datum types, and models to produce advanced and detailed hazard maps.~~

~~Danciu et al. (2016) produced maps with a seismic hazard assessment of the Middle East (from Pakistan to Turkey) using as much evidence as seismic sources, recorded seismicity, earthquake recurrences, active faults, and slip rates, as well as refined and advanced methods including data harmonization, assessment of catalogue completeness, and probabilistic seismic hazard analysis.~~ causative faults was only partially activated by the seismogenic slip (e.g., Chiaraluce et al., 2017); however, as this fault-slip behaviour seems rather frequent (Freymueller et al., 1994; Milliner et al., 2016; Chousianitis and Konca, 2018), it is most likely that this same behaviour is incorporated and implicitly expressed by the above-mentioned empirical scaling relationships between fault length and earthquake magnitude (e.g., Wells and Coppersmith, 1994; Leonard, 2010; Thingbaijam et al., 2017)

~~The method used by Danciu et al. (2016) for the Middle East derived from similar studies previously realized for Europe by Giardini et al. (2013), Woessner et al. (2015) (see also Giardini, 1999; Jiménez et al., 2001), aiming to assess the probabilistic seismic hazard of this continent on the basis of large tectonic and seismological datasets and advanced source models in a way similar to that previously explained for the study realized by Danciu et al. (2016).~~

6 Statistical Test of FLEM Values

~~Field et al. (2009, 2014) provided estimates of the magnitude, location, and time-averaged frequency of potentially damaging earthquakes in California, partly based on a time-dependent earthquake-probability model, and on recent earthquake rates and stress-renewal statistics conditioned on the date of~~ The reliability of estimated FLEM values may be quantitatively checked, in principle, using a formal statistical test on earthquake catalogues. Anyway, models of expected maximum magnitude (Mmax) are not readily testable. A statistical test helping to discriminate between competitive FLEM values is impossible in practice, even in the simplest case of discriminating between a double truncated Gutenberg-Richter (DTGR) law and an unbounded Gutenberg-Richter (UGR, Mmax=∞) law on excellent datasets (Holschneider et al., 2014). Suffice is to say that the DTGR's probability distribution differs from the UGR's one by a constant $c = 1 - 10^{-b(M_{max} - M_c)}$ (where M_c is the minimum magnitude). This value is very close to 1, if not when M_c is close to Mmax. This means that the upper cut-off of the Gutenberg-Richter distribution can be explored using only large, very rare earthquakes, with magnitudes close to the maximum possible value, on which statistical inference is necessarily limited (Holschneider et al., 2014). Therefore, it is essentially impossible to statistically infer, with sufficient confidence, the ~~last event. To do so, different new scaling relationships were developed also using supercomputers.~~

A probabilistic seismic hazard assessment (PSHA) was used also by Ullah et al. (2015) in central Asia, employing only shallow (depth < 50 km) seismicity through an updated earthquake catalogue for the region, arriving to calculate the seismic hazard maximum possible earthquake magnitude, in terms of alternative testing, from an earthquake catalogue alone (Holschneider et al., 20

In light of the limitations of purely statistical inference, geological and tectonic information provides, therefore, important and

5 exclusive constraints on the expected maximum magnitude. If we look at statistical testing in detail, we can check the FLEM values on a catalogue, while controlling the probability of wrongly rejecting them, but without reducing the probability of a wrong non-rejection (Holschneider et al., 2014). This makes it, indeed, impossible to discriminate between two likely values of FLEM. In other words, if we do not reject a FLEM value, we cannot say if it is true or if the data are inadequate in terms of macroseismic intensity (i.e., hazard maps in terms of 10% probability of exceedance in 50 years).

10 Cinti et al. (2004) elaborated a probability map for the next moderate to large earthquakes ($M \geq 5.5$) in Italy, applying a new nonparametric multivariate model to characterize the spatiotemporal distribution of earthquakes. The method accounted for many tectonic revealing its failure. Keeping all these considerations in mind, we test the estimated FLEM values on the CSI1.1 and ISIDe databases (available online at https:/ physic parameters that could potentially influence the spatiotemporal variability and tested their relative importance.

15 Basili et al. (2008) and DISS Working Group (2018) compiled the Database of Individual Seismogenic Sources (DISS) focusing on active structures in Italy and their seismogenic potential as derived from physical constraints including rates of crustal deformation, continuity of deformation belts, and spatial relationships between adjacent faults both at the surface and at depth. /csi.rm.ingv.it/ and http://iside.rm.ingv.it/, respectively). Since our analysis requests a database containing small magnitudes events, we consider ISIDe data of earthquakes occurred before April 16 2005, when the new INGV (Istituto Nazionale di

20 Geofisica e Vulcanologia) National Seismic Network, completely reorganized and equipped with a new acquisition system, became operational (Amato and Mele, 2008). Without this separation, the hypothesis of temporal homogeneity for magnitude data would not be appropriate. Moreover, most events in the ISIDe and CSI1.1 databases have a ML magnitude, while FLEM values are in moment magnitude scale. Therefore, we repeat the same testing procedure, described below, twice, without any difference in results: firstly, we consider original FLEM values and, secondly, we convert them in local magnitude scale through

25 the relations proposed by (Gasperini et al., 2013). We adopt the following test procedure.

For simplicity of data, assumptions, and modelling, the method that we used in this study for Italy is barely comparable with the methods used in some of the aforementioned studies (e.g., Giardini et al., 2013; Field et al., 2014; Petersen et al., 2014). We only used one type of data input (a) We select cells for which a test is helpful, i.e. , fault length) regardless of the age of faults and other parameters such as stress field and strain rate. We only classified faults into two reliability classes (A and B,

30 exposed and buried faults, respectively). For the computation of the expected earthquake magnitude (PEMM), we simply relied on Leonard's scaling law (i.e. , L10; Leonard, 2010). Moreover, our aim, consisting of computing PEMM from fault length, is different from and considerably simpler than the aims of most of the aforementioned studies that point toward the calculation of seismic hazard, i.e. , the probability that an earthquake will occur in a given geographic area, within a given window of time, and with ground motion intensity exceeding a given threshold. However, thanks to its simplicity and rapidity, the method that we

35 used in this study may have extremely effective results where historical and instrumental earthquake catalogues are limited and

~~information on the age of faults is poor. Bearing in mind the simplicity of our method, the observed correspondences (at least in many places) between PEMMs and the magnitudes from historically- and instrumentally-recorded earthquakes in Italy (Figs. 12a and 13c)are encouraging and suggests further validation for instance in New Zealand, USA, and other countries of Europe where the abundance of data and results (Petersen et al., 2008, 2014; Stirling et al., 2012; Giardini et al., 2013; Woessner et al., 2015) could allow a proper comparison and validation. In other words, our proposed method and results cannot replace existing estimates of time-dependent seismic hazard (e.g., Cinti et al., 2004; Basili et al., 2008; Petersen et al., 2008, 2014; Field et al., 2009, 2014; Stirling et al but rather can define the areas, i. e. those characterized by a large difference between PEMMs and catalogued earthquakes, where detailed studies are required. The main advantages of our method are the rapidity - once the faults are known~~having a FLEM value above the related historical/~~mapped, vectorized,~~ instrumental observed magnitude. In this way we exclude 41 of 1100 cells for which FLEM values are estimated. A further selection consists of keeping only cells for which the Gutenberg-Richter model, with a b-value equal to 1, is not rejected. In this way, we are sure that a possible rejection of FLEM values cannot be ascribed to the low reliability of a Gutenberg-Richter relation or to wrong b-values. To this end, we apply a goodness of fit test (GFT, Wiemer and Wyss, 2000), at a 95% confidence level, that also provides a completeness magnitude value, M_c, for each cell. The GFT is based on difference R of the observed (O_i) and expected (E_i) numbers of events in each magnitude bin. Values E_i are computed by assuming a UGR distribution, with a b-value equal to 1, above an ascending magnitude cutoff Mt. So that R is given by:

$$R(M_t) = 1 - \frac{\sum_i |E_i - O_i|}{\sum_i O_i} \tag{2}$$

where sums are done for magnitude bins above M_t. The completeness magnitude M_c is defined as the first value of M_t for which R(M_t)>0.95. The cells passing this test are 30 (Table S1) and 67 (Table S2) for the CSI1.1 and ISIDe databases, respectively. We stress that this first test does not require a Mmax value.

b) A first specific check of the DTGR distribution, having FLEM as maximum magnitude, is carried out by using a log-likelihood test. Specifically, for each cell passing the previous test, the log-likelihood value of the DTGR model is computed. By considering that a DTGR distribution has a probability density function given by:

$$f_{DTGR}(M) = \frac{\beta e^{\beta(M - M_c)}}{1 - e^{\beta(Mmax - M_c)}} \tag{3}$$

where $b = \beta ln(10)$; we compute for each cell the real log-likelihood LL_R on N events magnitudes $M_i, i = 1, ..., N$, by equation:

$$LL_R = \sum_{i=1}^{N} ln[f_{DTGR}(M_i)] \tag{4}$$

17

The DTGR model is rejected if LL_R is significantly lower than expected values. The probability of having smaller log-likelihood values than LL_R is estimated using 10^4 simulated datasets (having the same size of real datasets) by model DTGR. Specifically, for each cell, we compute this probability pLL as the proportion of simulated log-likelihoods smaller than LL_R. We select cells for which these probabilities are larger than 5%. In this way, the cells are reduced to 20 and 45 for the CSI1.1 and ISIDe databases, respectively (Figure 14 and Tables S1 and ~~georeferenced - and the independence from time and (paleo)seismological information. The novelty is not~~ S2). We stress that we select the same cells by assuming a UGR model, suggesting that the problem of excluded cells lies in the whole Gutenberg-Richter relation and not in the FLEM values.

c) Finally, FLEM values are tested by applying the procedure proposed by (Holschneider et al., 2014), involving a comparison of the ~~method itself that has long been known, but its applicability at the national scale also for faults considered inactive or undetermined~~ maximum observed magnitude with a suitable threshold magnitude, computed by the DTGR model. Specifically, we reject the FLEM values, if the observed magnitude (oMmax) is larger than a threshold value M_t, given by:

$$M_t = M_c - \frac{1}{\beta} ln\{1 - (1-\alpha)^{\frac{1}{n}}(1 - e^{-\beta(FLEM-M_c)})\} \tag{5}$$

where $\alpha = 0.05$ (see Holschneider et al., 2014, for details). The computed threshold values (M_t1) are listed in Tables S1 and S2, together with oMmax values. All previously selected cells pass this test, for both the CSI1.1 and ISIDe databases, suggesting that related FLEM values cannot be rejected (Figure 14 and Tables S1 and S2).

d) The last two steps are repeated by reducing the magnitude range covered by data. Specifically, we increase, where possible, the minimum magnitude to FLEM-2.0. The relative threshold values M_t2 are listed in Tables S1 and S2 for the CSIv1.1 and ISIDe databases, respectively. Also in this case, we cannot reject the FLEM values. As stated above, this analysis does not exclude alternative values of FLEM; as matter of fact, it is also the case that a UGR model cannot be rejected in all the selected cells.

7   Conclusions

In this study, (1) we first provided an updated compilation of all mapped faults in Italy, (2) then, using known scaling laws, calculated the related ~~potential expected maximum magnitude of earthquakes (PEMM~~ Fault-Length Earthquake Magnitude (FLEM), and, (3) finally, compared ~~PEMM~~ FLEM values with historically/instrumentally-catalogued earthquake magnitudes. Where faults are geologically well constrained (class A faults), either good agreements or some differences are observed between ~~PEMMs~~ FLEMs and historically/instrumentally-catalogued earthquake magnitudes~~. The~~: the agreement is increased for $M \geq 6.5$ earthquakes~~, whereas large differences are observed for poorly constrained faults~~. In areas where fault geometries are poorly constrained (class B faults ~~), particularly the on-shore and off-shore buried ones that are inferred solely through~~ inferred solely by subsurface 2D investigations~~. These~~), large differences are observed: these areas have to be further characterized to better estimate fault dimensions and hence properly assess the FLEM. Our results are partly encouraging and suggest the testing and validation of this experiment elsewhere. ~~In case it is successfully validated elsewhere, this method would be~~

~~extremely useful as well as fast where historical and instrumental earthquake catalogues are limited, the returning time of~~ ~~(strong) earthquakes is possibly very long, and information on the age of faults is poor.~~ This method cannot, however, be a substitute for time-dependent (paleo)seismological methods for seismic hazard assessments. Rather, it can ~~rapidly~~ provide an approximate perspective time-independent seismic potential of faults and highlight areas where further detailed studies are

5   required.

References

Amato, A.: Crustal and deep seismicity in Italy: a Review, Special volume of the Italian Geological Society for the IGC, 32, 201–208, 2004.

Amato, A. and Mele, F.: Performance of the INGV National Seismic Network from 1997 to 2007, Annals of Geophysics, 51, 417–431, https://doi.org/10.4401/ag-4454, 2008.

5 Amato, A., Azzara, R., Basili, A., Chiarabba, C., Ciaccio, M., Cimini, G., Di Bona, M., Frepoli, A., Hunstad, I., Lucente, F., et al.: Geodynamic evolution of the Northern Apennines from recent seismological studies, Mem. Soc. Geol. It, 52, 337–343, 1998.

Anderlini, L., Serpelloni, E., and Belardinelli, M. E.: Creep and locking of a low-angle normal fault: Insights from the Altotiberina fault in the Northern Apennines (Italy), Geophysical Research Letters, 43, 4321–4329, https://doi.org/10.1002/2016GL068604, 2016.

Augliera, P., Béthoux, N., Déverchère, J., and Eva, C.: The Ligurian Sea: new seismotectonic evidence, Bollettino di Geofisica Teorica ed
10 Applicata, 36, 363–380, 1994.

Azzaro, R. and Barbano, M. S.: Analysis of the seismicity of Southeastern Sicily: a proposed tectonic interpretation, Annals of Geophysics, 43, 171–188, https://doi.org/10.4401/ag-3628, 2000.

Barchi, M., Minelli, G., and Pialli, G.: The CROP 03 profile: a synthesis of results on deep structures of the Northern Apennines, Mem. Soc. Geol. Ital, 52, 383–400, 1998.

15 Basili, R. and Meghraoui, M.: Coseismic and postseismic displacements related with the 1997 Earthquake Sequence in Umbria-Marche (Central Italy), Geophysical research letters, 28, 2695–2698, https://doi.org/10.1029/2000GL012102, 2001.

Basili, R., Valensise, G., Vannoli, P., Burrato, P., Fracassi, U., Mariano, S., Tiberti, M. M., and Boschi, E.: The Database of Individual Seismogenic Sources (DISS), version 3: summarizing 20 years of research on Italy's earthquake geology, Tectonophysics, 453, 20–43, https://doi.org//10.1016/j.tecto.2007.04.014, 2008.

20 Bazzurro, P. and Cornell, A.: Disaggregation of seismic hazard, Bulletin of the Seismological Society of America, 89, 501–520, 1999.

Bigi, G., Bonardi, G., Catalano, R., Cosentino, D., Lentini, F., Parotto, M., Sartori, R., Scandone, P., Turco, E., and (Eds.): Structural Model of Italy 1:500,000, C.N.R., Progetto Finalizzato Geodinamica, 1989.

Bilham, R., Gaur, V. K., and Molnar, P.: Himalayan seismic hazard, Science, 293, 1442–1444, 2001.

Billi, A., Salvini, F., and Storti, F.: The damage zone-fault core transition in carbonate rocks: implications for fault growth, structure and
25 permeability, Journal of Structural geology, 25, 1779–1794, https://doi.org/10.1016/S0191-8141(03)00037-3, 2003.

Billi, A., Barberi, G., Faccenna, C., Neri, G., Pepe, F., and Sulli, A.: Tectonics and seismicity of the Tindari Fault System, southern Italy: Crustal deformations at the transition between ongoing contractional and extensional domains located above the edge of a subducting slab, Tectonics, 25, https://doi.org/10.1029/2004TC001763, 2006a.

Billi, A., Barberi, G., Faccenna, C., Neri, G., Pepe, F., and Sulli, A.: Tectonics and seismicity of the Tindari Fault System, southern Italy:
30 Crustal deformations at the transition between ongoing contractional and extensional domains located above the edge of a subducting slab, Tectonics, 25, https://doi.org/10.1029/2004TC001763, 2006b.

Billi, A., Presti, D., Faccenna, C., Neri, G., and Orecchio, B.: Seismotectonics of the Nubia plate compressive margin in the south Tyrrhenian region, Italy: Clues for subduction inception, Journal of Geophysical Research: Solid Earth, 112, https://doi.org/10.1029/2006JB004837, 2007.

35 Billi, A., Minelli, L., Orecchio, B., and Presti, D.: Constraints to the cause of three historical tsunamis (1908, 1783, and 1693) in the Messina Straits region, Sicily, southern Italy, Seismological Research Letters, 81, 907–915, https://doi.org/10.1785/gssrl.81.6.907, 2010.

Billi, A., Faccenna, C., Bellier, O., Minelli, L., Neri, G., Piromallo, C., Presti, D., Scrocca, D., and Serpelloni, E.: Recent tectonic reorgani-
zation of the Nubia-Eurasia convergent boundary heading for the closure of the western Mediterranean, Bulletin de la Société Géologique
de France, 182, 279–303, https://doi.org/10.2113/gssgfbull.182.4.279, 2011.

Bohnhoff, M., Martínez-Garzón, P., Bulut, F., Stierle, E., and Ben-Zion, Y.: Maximum earthquake magnitudes along different sections of the
5   North Anatolian fault zone, Tectonophysics, 674, 147–165, https://doi.org/10.1016/j.tecto.2016.02.028, 2016.

Bommer, J. J., Scherbaum, F., Bungum, H., Cotton, F., Sabetta, F., and Abrahamson, N. A.: On the use of logic trees for
ground-motion prediction equations in seismic-hazard analysis, Bulletin of the Seismological Society of America, 95, 377–389,
https://doi.org/10.1785/0120040073, 2005.

Bouchon, M., Campillo, M., and Cotton, F.: Stress field associated with the rupture of the 1992 Landers, California, earthquake and its
10   implications concerning the fault strength at the onset of the earthquake, Journal of Geophysical Research: Solid Earth, 103, 21 091–
21 097, https://doi.org/10.1029/98JB01982, 1998.

Boyd, O., Calais, E., Langbein, J., Magistrale, H., Stein, S., and Zoback, M.: Workshop on New Madrid geodesy and the challenges of
understanding intraplate earthquakes, Tech. rep., US Geological Survey, 2013.

Braun, J., Burbidge, D., Gesto, F., Sandiford, M., Gleadow, A. J. W., Kohn, B., and Cummins, P.: Constraints on the current rate of deforma-
15   tion and surface uplift of the Australian continent from a new seismic database and low-T thermochronological data, Australian Journal
of Earth Sciences, 56, 99–110, https://doi.org/10.1080/08120090802546977, 2009.

Bressan, G., Snidarcig, A., and Venturini, C.: Present state of tectonic stress of the Friuli area (eastern Southern Alps), Tectonophysics, 292,
211–227, https://doi.org/10.1016/S0040-1951(98)00065-1, 1998.

Brogi, A.: Neogene extension in the Northern Apennines (Italy): insights from the southern part of the Mt. Amiata geothermal area, Geodi-
20   namica Acta, 19, 33–50, https://doi.org/10.3166/ga.19.33-50, 2006.

Brogi, A.: Fault zone architecture and permeability features in siliceous sedimentary rocks: insights from the Rapolano geothermal area
(Northern Apennines, Italy), Journal of Structural Geology, 30, 237–256, https://doi.org/10.1016/j.jsg.2007.10.004, 2008.

Brogi, A.: Bowl-shaped basin related to low-angle detachment during continental extension: the case of the controversial Neogene Siena
Basin (central Italy, Northern Apennines), Tectonophysics, 499, 54–76, https://doi.org/10.1016/j.tecto.2010.12.005, 2011.

25 Brogi, A. and Fabbrini, L.: Extensional and strike-slip tectonics across the Monte Amiata–Monte Cetona transect (Northern Apennines, Italy)
and seismotectonic implications, Tectonophysics, 476, 195–209, https://doi.org/10.1016/j.tecto.2009.02.020, 2009.

Brogi, A., Lazzarotto, A., Liotta, D., and Ranalli, G.: Extensional shear zones as imaged by reflection seismic lines: the Larderello geothermal
field (central Italy), Tectonophysics, 363, 127–139, https://doi.org/10.1016/S0040-1951(02)00668-6, 2003.

Brogi, A., Lazzarotto, A., and Liotta, D.: Structural features of southern Tuscany and geological interpretation of the CROP 18 Seismic
30   Reflection Survey (Italy), Bollettino della Società Geologica Italiana. Volume speciale, pp. 213–236, 2005.

Brozzetti, F.: The Campania-Lucania Extensional Fault System, southern Italy: A suggestion for a uniform model of active extension in the
Italian Apennines, Tectonics, 30, https://doi.org/10.1029/2010TC002794, 2011.

Calais, E., Camelbeeck, T., Stein, S., Liu, M., and Craig, T.: A new paradigm for large earthquakes in stable continental plate interiors,
Geophysical Research Letters, 43, 10–621, https://doi.org/10.1002/2016GL070815, 2016.

35 Camelbeeck, T., Vanneste, K., Alexandre, P., Verbeeck, K., Petermans, T., Rosset, P., Everaerts, M., Warnant, R., Van Camp, M., Stein, S.,
et al.: Relevance of active faulting and seismicity studies to assessments of long-term earthquake activity and maximum magnitude in
intraplate northwest Europe, between the Lower Rhine Embayment and the North Sea, SPECIAL PAPERS-GEOLOGICAL SOCIETY
OF AMERICA, 425, 193, https://doi.org/10.1130/2007.2425(14), 2007.

Campbell, G., Walker, R., Abdrakhmatov, K., Jackson, J., Elliott, J., Mackenzie, D., Middleton, T., and Schwenninger, J.-L.: Great earth-quakes in low strain rate continental interiors: an example from SE Kazakhstan, Journal of Geophysical Research: Solid Earth, 120, 5507–5534, https://doi.org/10.1002/2015JB011925, 2015.

Capponi, G., Crispini, L., Federico, L., Piazza, M., and Fabbri, B.: Late Alpine tectonics in the Ligurian Alps: constraints from the Tertiary Piedmont Basin conglomerates, Geological Journal, 44, 211–224, https://doi.org/10.1002/gj.1140, 2009.

Carminati, E. and Doglioni, C.: Alps vs. Apennines: the paradigm of a tectonically asymmetric Earth, Earth-Science Reviews, 112, 67–96, https://doi.org/10.1016/j.earscirev.2012.02.004, 2012.

Carminati, E., Lustrino, M., Cuffaro, M., and Doglioni, C.: Tectonics, magmatism and geodynamics of Italy: what we know and what we imagine, Journal of the Virtual Explorer, 36, 8, https://doi.org/10.3809/jvirtex.2009.00226, 2010.

Castello, B., Selvaggi, G., Chiarabba, C., and Amato, A.: CSI Catalogo della sismicità italiana 1981-2002, versione 1.1., INGV-CNT, Roma, https://doi.org/http://csi.rm.ingv.it/., 2006.

Casula, G., Cherchi, A., Montadert, L., Murru, M., and Sarria, E.: The Cenozoic graben system of Sardinia (Italy): geodynamic evolution from new seismic and field data, Marine and Petroleum Geology, 18, 863–888, https://doi.org/10.1016/S0264-8172(01)00023-X, 2001.

Cello, G., Tondi, E., Micarelli, L., and Mattioni, L.: Active tectonics and earthquake sources in the epicentral area of the 1857 Basilicata earthquake (southern Italy), Journal of Geodynamics, 36, 37–50, https://doi.org/10.1016/S0264-3707(03)00037-1, 2003.

Cheloni, D., D'Agostino, N., D'Anastasio, E., and Selvaggi, G.: Reassessment of the source of the 1976 Friuli, NE Italy, earthquake sequence from the joint inversion of high-precision levelling and triangulation data, Geophysical Journal International, 190, 1279–1294, https://doi.org/10.1111/j.1365-246X.2012.05561.x, 2012.

Chiarabba, C., Jovane, L., and DiStefano, R.: A new view of Italian seismicity using 20 years of instrumental recordings, Tectonophysics, 395, 251–268, https://doi.org/10.1016/j.tecto.2004.09.013, 2005.

Chiarabba, C., De Gori, P., and Boschi, E.: Pore-pressure migration along a normal-fault system resolved by time-repeated seismic tomography, Geology, 37, 67–70, https://doi.org/10.1130/G25220A.1, 2009.

Chiarabba, C., De Gori, P., and Mele, F. M.: Recent seismicity of Italy: Active tectonics of the central Mediterranean region and seismicity rate changes after the Mw 6.3 L'Aquila earthquake, Tectonophysics, 638, 82–93, https://doi.org/10.1016/j.tecto.2014.10.016, 2015.

Chiaraluce, L., Chiarabba, C., Collettini, C., Piccinini, D., and Cocco, M.: Architecture and mechanics of an active low-angle normal fault: Alto Tiberina fault, northern Apennines, Italy, Journal of Geophysical Research: Solid Earth, 112, https://doi.org/10.1029/2007JB005015, 2007.

Chiaraluce, L., Di Stefano, R., Tinti, E., Scognamiglio, L., Michele, M., Casarotti, E., Cattaneo, M., De Gori, P., Chiarabba, C., Monachesi, G., et al.: The 2016 central Italy seismic sequence: A first look at the mainshocks, aftershocks, and source models, Seismological Research Letters, 88, 757–771, https://doi.org/10.1785/0220160221, 2017.

Chousianitis, K. and Konca, A. O.: Coseismic slip distribution of the 12 June 2017 Mw= 6.3 Lesvos earthquake and imparted static stress changes to the neighboring crust, Journal of Geophysical Research: Solid Earth, 123, 8926–8936, https://doi.org/10.1029/2018JB015950, 2018.

Christophe, L., Scotti, O., and Ioualalen, M.: Reappraisal of the 1887 Ligurian earthquake (western Mediterranean) from macroseismicity, active tectonics and tsunami modelling, Geophysical Journal International, 190, 87–104, https://doi.org/10.1111/j.1365-246X.2012.05498.x, 2012.

Christophersen, A., Rhoades, D. A., and Colella, H. V.: Precursory seismicity in regions of low strain rate: insights from a physics-based earthquake simulator, Geophysical Journal International, 209, 1513–1525, https://doi.org/10.1093/gji/ggx104, 2017.

Cinti, F., Faenza, L., Marzocchi, W., and Montone, P.: Probability map of the next M> 5.5 earthquakes in Italy, Geochemistry, Geophysics, Geosystems, 5, https://doi.org/10.1029/2004GC000724, 2004.

Collettini, C.: The mechanical paradox of low-angle normal faults: Current understanding and open questions, Tectonophysics, 510, 253–268, https://doi.org/10.1016/j.tecto.2011.07.015, 2011.

5 Collettini, C. and Trippetta, F.: A slip tendency analysis to test mechanical and structural control on aftershock rupture planes, Earth and Planetary Science Letters, 255, 402–413, https://doi.org/10.1016/j.epsl.2007.01.001, 2007.

Collettini, C., Niemeijer, A., Viti, C., and Marone, C.: Fault zone fabric and fault weakness, Nature, 462, 907, https://doi.org/10.1038/nature08585, 2009.

Cornell, C. A.: Engineering seismic risk analysis, Bulletin of the seismological society of America, 58, 1583–1606, 1968.

10 Courboulex, F., Deschamps, A., Cattaneo, M., Costi, F., Deverchere, J., Virieux, J., Augliera, P., Lanza, V., and Spallarossa, D.: Source study and tectonic implications of the 1995 Ventimiglia (border of Italy and France) earthquake (M L= 4.7), Tectonophysics, 290, 245–257, https://doi.org/10.1016/S0040-1951(98)00024-9, 1998.

Cowie, P., Phillips, R., Roberts, G. P., McCaffrey, K., Zijerveld, L., Gregory, L., Walker, J. F., Wedmore, L., Dunai, T., Binnie, S., et al.: Orogen-scale uplift in the central Italian Apennines drives episodic behaviour of earthquake faults, Scientific Reports, 7, 44 858, 15 https://doi.org/10.1038/srep44858, 2017.

Cuffaro, M., Riguzzi, F., Scrocca, D., Antonioli, F., Carminati, E., Livani, M., and Doglioni, C.: On the geodynamics of the northern Adriatic plate, Rendiconti Lincei, 21, 253–279, https://doi.org/10.1007/s12210-010-0098-9, 2010.

Cultrera, F., Barreca, G., Burrato, P., Ferranti, L., Monaco, C., Passaro, S., Pepe, F., and Scarfì, L.: Active faulting and continental slope instability in the Gulf of Patti (Tyrrhenian side of NE Sicily, Italy): a field, marine and seismological joint analysis, Natural Hazards, 86, 20 253–272, https://doi.org/10.1007/s11069-016-2547-y, 2017.

Danciu, L., Şeşetyan, K., Demircioglu, M., Gülen, L., Zare, M., Basili, R., Elias, A., Adamia, S., Tsereteli, N., Yalçın, H., et al.: The 2014 earthquake model of the Middle East: seismogenic sources, Bulletin of Earthquake Engineering, pp. 1–32, https://doi.org/10.1007/s10518-017-0096-8, 2016.

Dawson, J., Cummins, P., Tregoning, P., and Leonard, M.: Shallow intraplate earthquakes in Western Australia observed by interferometric 25 synthetic aperture radar, Journal of Geophysical Research: Solid Earth, 113, https://doi.org/10.1029/2008JB005807, 2008.

Del Gaudio, C., Aquino, I., Ricco, C., and Serio, C.: Movimenti verticali del suolo ai Campi Flegrei: risultati della livellazione geometrica di precisione eseguita nel periodo Dicembre 2006-Gennaio 2007, Open File Report, 2007.

DeMets, C., Gordon, R. G., Argus, D., and Stein, S.: Current plate motions, Geophysical journal international, 101, 425–478, https://doi.org/10.1111/j.1365-246X.1990.tb06579.x, 1990.

30 Dewey, J., Helman, M., Knott, S., Turco, E., and Hutton, D.: Kinematics of the western Mediterranean, Geological Society, London, Special Publications, 45, 265–283, https://doi.org/10.1144/GSL.SP.1989.045.01.15, 1989.

DISS Working Group: Database of Individual Seismogenic Sources (DISS), Version 3.2.1: A compilation of potential sources for earthquakes larger than M 5.5 in Italy and surrounding areas., Istituto Nazionale di Geofisica e Vulcanologia, p. http://diss.rm.ingv.it/diss/, https://doi.org/10.6092/INGV.IT-DISS3.2.1, 2018.

35 Dixon, T. H., Norabuena, E., and Hotaling, L.: Paleoseismology and Global Positioning System: Earthquake-cycle effects and geodetic versus geologic fault slip rates in the Eastern California shear zone, Geology, 31, 55–58, https://doi.org/10.1130/0091-7613(2003)031<0055:PAGPSE>2.0.CO;2, 2003.

Doglioni, C.: A proposal for the kinematic modelling of W-dipping subductions-possible applications to the Tyrrhenian-Apennines system, Terra Nova, 3, 423–434, https://doi.org/10.1111/j.1365-3121.1991.tb00172.x, 1991.

Doglioni, C., Gueguen, E., Harabaglia, P., and Mongelli, F.: On the origin of west-directed subduction zones and applications to the western Mediterranean, Geological Society, London, Special Publications, 156, 541–561, https://doi.org/10.1144/GSL.SP.1999.156.01.24, 1999.

5 Faccenna, C., Piromallo, C., Crespo-Blanc, A., Jolivet, L., and Rossetti, F.: Lateral slab deformation and the origin of the western Mediterranean arcs, Tectonics, 23, https://doi.org/10.1029/2002TC001488, 2004.

Fantoni, R. and Franciosi, R.: Tectono-sedimentary setting of the Po Plain and Adriatic foreland, Rendiconti Lincei, 21, 197–209, https://doi.org/10.1007/s12210-010-0102-4, 2010.

Ferranti, L., Palano, M., Cannavò, F., Mazzella, M. E., Oldow, J. S., Gueguen, E., Mattia, M., and Monaco, C.: Rates of geodetic deformation
10 across active faults in southern Italy, Tectonophysics, 621, 101–122, https://doi.org/10.1016/j.tecto.2014.02.007, 2014.

Field, E. H., Dawson, T. E., Felzer, K. R., Frankel, A. D., Gupta, V., Jordan, T. H., Parsons, T., Petersen, M. D., Stein, R. S., Weldon, R., et al.: Uniform California earthquake rupture forecast, version 2 (UCERF 2), Bulletin of the Seismological Society of America, 99, 2053–2107, https://doi.org/10.1785/0120080049, 2009.

Field, E. H., Arrowsmith, R. J., Biasi, G. P., Bird, P., Dawson, T. E., Felzer, K. R., Jackson, D. D., Johnson, K. M., Jordan, T. H., Madden, C.,
15 et al.: Uniform California earthquake rupture forecast, version 3 (UCERF3)-The time-independent model, Bulletin of the Seismological Society of America, 104, 1122–1180, https://doi.org/10.1785/0120130164, 2014.

Field, E. H., Biasi, G. P., Bird, P., Dawson, T. E., Felzer, K. R., Jackson, D. D., Johnson, K. M., Jordan, T. H., Madden, C., Michael, A. J., et al.: Long-term time-dependent probabilities for the third Uniform California Earthquake Rupture Forecast (UCERF3), Bulletin of the Seismological Society of America, 105, 511–543, https://doi.org/10.1785/0120140093, 2015.

20 Finetti, I. and Morelli, C.: Esplorazione sismica a riflessione dei Golfi di Napoli e Pozzuoli, Boll. Geofis. Teor. Appl, 16, 175–222, 1974.

Freymueller, J., King, N., and Segall, P.: The co-seismic slip distribution of the Landers earthquake, Bulletin of the Seismological Society of America, 84, 646–659, 1994.

Galadini, F., Meletti, C., and Vittori, E.: Stato delle conoscenze sulle faglie attive in Italia: elementi geologici di superficie, Le ricerche del GNDT nel campo della pericolosità sismica (1996–1999), pp. 107–136, 2000.

25 Galli, P.: New empirical relationships between magnitude and distance for liquefaction, Tectonophysics, 324, 169–187, https://doi.org/10.1016/S0040-1951(00)00118-9, 2000.

Galli, P., Galadini, F., and Pantosti, D.: Twenty years of paleoseismology in Italy, Earth-Science Reviews, 88, 89–117, https://doi.org/10.1016/j.earscirev.2008.01.001, 2008.

Gasparini, C., Iannaccone, G., and Scarpa, R.: Fault-plane solutions and seismicity of the Italian peninsula, Tectonophysics, 117, 59–78,
30 https://doi.org/10.1016/0040-1951(85)90236-7, 1985.

Gasperini, P., Lolli, B., and Vannucci, G.: Empirical calibration of local magnitude data sets versus moment magnitude in Italy, Bulletin of the Seismological Society of America, 103, 2227–2246, https://doi.org/10.1785/0120120356, 2013.

Ghisetti, F.: Evoluzione neotettonica dei principali sistemi di faglie della Calabria centrale, Bollettino della Società Geologica Italiana, 98, 387–430, 1979.

35 Giardini, D.: The global seismic hazard assessment program (GSHAP)-1992/1999, Annals of Geophysics, 42, 1999.

Giardini, D., Woessner, J., Danciu, L., Crowley, H., Cotton, F., Grünthal, G., Pinho, R., Valensise, G., Akkar, S., Arvidsson, R., et al.: Seismic Hazard Harmonization in Europe (SHARE): Online Data Resource, Swiss Seism. Serv ETH Zurich Zurich Switz. Doi, 10, 2013.

Goes, S., Giardini, D., Jenny, S., Hollenstein, C., Kahle, H.-G., and Geiger, A.: A recent tectonic reorganization in the south-central Mediterranean, Earth and Planetary Science Letters, 226, 335–345, https://doi.org/10.1016/j.epsl.2004.07.038, 2004.

Govoni, A., Marchetti, A., De Gori, P., Di Bona, M., Lucente, F. P., Improta, L., Chiarabba, C., Nardi, A., Margheriti, L., Agostinetti, N. P., et al.: The 2012 Emilia seismic sequence (Northern Italy): Imaging the thrust fault system by accurate aftershock location, Tectonophysics, 622, 44–55, https://doi.org/10.1016/j.tecto.2014.02.013, 2014.

Grasso, M. and Reuther, C.: The western margin of the Hyblean Plateau: a neotectonic transform system on the SE Sicilian foreland, Annales Tectonicae, 2, 107–120, 1988.

Grünthal, G. and Wahlström, R.: An Mw based earthquake Catalogue for central, northern and northwestern Europe using a hierarchy of magnitude conversions, Journal of Seismology, 7, 507–531, https://doi.org/10.1023/B:JOSE.0000005715.87363.13, 2003.

Guidoboni, E., Ferrari, G., Mariotti, D., Comastri, A., Tarabusi, G., Sgattoni, G., and Valensise, G.: CFTI5Med, Catalogo dei Forti Terremoti in Italia (461 aC-1997) e nell'area Mediterranea (760 aC-1500), https://doi.org/10.6092/ingv.it-cfti5, 2018.

Henry, C. and Das, S.: Aftershock zones of large shallow earthquakes: fault dimensions, aftershock area expansion and scaling relations, Geophysical Journal International, 147, 272–293, https://doi.org/10.1046/j.1365-246X.2001.00522.x, 2001.

Holschneider, M., Zöller, G., Clements, R., and Schorlemmer, D.: Can we test for the maximum possible earthquake magnitude?, Journal of Geophysical Research: Solid Earth, 119, 2019–2028, https://doi.org/10.1002/2013JB010319, 2014.

IAEA: Environmental Change in Post-closure Safety Assessment of Solid Radioactive Waste Repositories. International Atomic Energy Agency, Report IAEA-TECDOC-1799, Vienna, pp.147, 2016.

Iside Working Group: Italian Seismological Instrumental and parametric Data–basE version 1.0, https://doi.org/10.13127/ISIDe, http://iside.rm.ingv.it, 2016.

Jiménez, M., Giardini, D., Grünthal, G., Group, S. W., et al.: Unified seismic hazard modelling throughout the Mediterranean region, Applicata, 42, 3–18, 2001.

Kafka, A. L.: Does seismicity delineate zones where future large earthquakes are likely to occur in intraplate environments?, Special Papers Geological Society of America, 425, 35, https://doi.org/10.1130/2007.2425(03), 2007.

Keller, L. M., Fügenschuh, B., Hess, M., Schneider, B., and Schmid, S. M.: Simplon fault zone in the western and central Alps: Mechanism of Neogene faulting and folding revisited, Geology, 34, 317–320, https://doi.org/10.1130/G22256.1, 2006.

Lanzafame, G. and Bousquet, J.: The Maltese escarpment and its extension from Mt. Etna to Aeolian Islands (Sicily): importance and evolution of a lithosphere discontinuity, Acta Vulcanologica, 9, 113–120, 1997.

Larroque, C., Béthoux, N., Calais, E., Courboulex, F., Deschamps, A., Déverchère, J., Stéphan, J., Ritz, J., and Gilli, E.: Active and recent deformation at the Southern Alps-Ligurian basin junction, Geologie en Mijnbouw, 80, 255–272, 2001.

Leonard, M.: Earthquake Fault Scaling: Self-Consistent Relating of Rupture Length, Width, Average Displacement, and Moment ReleaseEarthquake Fault Scaling: Self-Consistent Relating of Rupture Length, Width, Average Displacement, Bulletin of the Seismological Society of America, 100, 1971, https://doi.org/10.1785/0120090189, 2010.

Leonard, M., Burbidge, D., Allen, T., Robinson, D., McPherson, A., Clark, D., and Collins, C.: The challenges of probabilistic seismic-hazard assessment in stable continental interiors: An Australian example, Bulletin of the Seismological Society of America, 104, 3008–3028, https://doi.org/10.1785/0120130248, 2014.

Liu-Zeng, J., Heaton, T., and DiCaprio, C.: The effect of slip variability on earthquake slip-length scaling, Geophysical Journal International, 162, 841–849, https://doi.org/10.1111/j.1365-246X.2005.02679.x, 2005.

Locardi, E. and Nappi, G.: Tettonica e vulcanismo recente nell9isola di Lipari, Bollettino della Societa Geologica Italiana, 98, 447–456, 1979.

Locati, M., CCamassi, R. D., Rovida, A. N., Ercolani, E., Bernardini, F. M. A., Castelli, V., Caracciolo, C. H., Tertulliani, A., Rossi, A., Azzaro, R., et al.: DBMI15, the 2015 version of the Italian Macroseismic Database. Istituto Nazionale di Geofisica e Vulcanologia, 2016.

Mai, P. M. and Beroza, G. C.: Source scaling properties from finite-fault-rupture models, Bulletin of the Seismological Society of America, 90, 604–615, https://doi.org/10.1785/0119990126, 2000.

Main, I.: Statistical physics, seismogenesis, and seismic hazard, Reviews of Geophysics, 34, 433–462, https://doi.org/10.1029/96RG02808, 1996.

Malinverno, A. and Ryan, W. B.: Extension in the Tyrrhenian Sea and shortening in the Apennines as result of arc migration driven by sinking of the lithosphere, Tectonics, 5, 227–245, https://doi.org/10.1029/TC005i002p00227, 1986.

Mariotti, G. and Doglioni, C.: The dip of the foreland monocline in the Alps and Apennines, Earth and Planetary Science Letters, 181, 191–202, https://doi.org/10.1016/S0012-821X(00)00192-8, 2000.

Maurer, H., Burkhard, M., Deichmann, N., and Green, A.: Active tectonism in the central Alps: contrasting stress regimes north and south of the Rhone Valley, Terra Nova, 9, 91–94, https://doi.org/10.1111/j.1365-3121.1997.tb00010.x, 1997.

McCalpin, J. P.: Paleoseismology, vol. 95, Academic press, 2009.

McGuire, R. K.: Probabilistic seismic hazard analysis and design earthquakes: closing the loop, Bulletin of the Seismological Society of America, 85, 1275–1284, 1995.

Michetti, A., Giardina, F., Livio, F., Mueller, K., Serva, L., Sileo, G., Vittori, E., Devoti, R., Riguzzi, F., Carcano, C., et al.: Active compressional tectonics, Quaternary capable faults, and the seismic landscape of the Po Plain (N Italy), Annals of geophysics, https://doi.org/10.4401/ag-5462, 2012.

Michetti, A. M., Serva, L., and Vittori, E.: ITHACA Italy Hazard from Capable Faults: a database of active faults of the Italian onshore territory, CD-Rom Explan. notes, pp. 1–150, 2000.

Michetti, A. M., Marco, S., et al.: Future trends in paleoseismology: Integrated study of the seismic landscape as a vital tool in seismic hazard analyses, Tectonophysics, 408, 3–21, https://doi.org/10.1016/j.tecto.2005.05.035, 2005.

Milliner, C., Sammis, C., Allam, A., Dolan, J., Hollingsworth, J., Leprince, S., and Ayoub, F.: Resolving fine-scale heterogeneity of co-seismic slip and the relation to fault structure, Scientific reports, 6, 27 201, https://doi.org/10.1038/srep27201, 2016.

Montone, P. and Mariucci, M. T.: The new release of the Italian contemporary stress map, Geophysical Journal International, 205, 1525–1531, https://doi.org/10.1093/gji/ggw100, 2016.

Morris, A., Ferrill, D. A., and Henderson, D. B.: Slip-tendency analysis and fault reactivation, Geology, 24, 275–278, https://doi.org/10.1130/0091-7613(1996)024<0275:STAAFR>2.3.CO;2, 1996.

Murchison, R. I.: On the Geological Structure of the Alps, Apennines and Carpathians, more especially to prove a transition from Secondary to Tertiary rocks, and the development of Eocene deposits in Southern Europe, Quarterly Journal of the Geological Society, 5, 157–312, https://doi.org/10.1144/GSL.JGS.1849.005.01-02.27, 1849.

NEA: Post-Closure Safety Case For Geological Repositories. Nuclear Energy Agency, Organisation for Economic Co-operation and Development, Report No. 3679, Paris, pp. 56, 2004.

Neri, G., Barberi, G., Orecchio, B., and Aloisi, M.: Seismotomography of the crust in the transition zone between the southern Tyrrhenian and Sicilian tectonic domains, Geophysical Research Letters, 29, https://doi.org/10.1029/2002GL015562, 2002.

Neri, G., Barberi, G., Oliva, G., and Orecchio, B.: Spatial variations of seismogenic stress orientations in Sicily, south Italy, Physics of the Earth and Planetary Interiors, 148, 175–191, https://doi.org/10.1016/j.pepi.2004.08.009, 2005.

Nicolas, A., Hirn, A., Nicolich, R., and Polino, R.: Lithospheric wedging in the western Alps inferred from the ECORS-CROP traverse, Geology, 18, 587–590, https://doi.org/10.1130/0091-7613(1990)018<0587:LWITWA>2.3.CO;2, 1990.

5 Nostro, C., Cocco, M., and Belardinelli, M. E.: Static stress changes in extensional regimes: an application to southern Apennines (Italy), Bulletin of the Seismological Society of America, 87, 234–248, 1997.

Nuriel, P., Weinberger, R., Rosenbaum, G., Golding, S. D., Zhao, J.-x., Uysal, I. T., Bar-Matthews, M., and Gross, M. R.: Timing and mechanism of late-Pleistocene calcite vein formation across the Dead Sea Fault Zone, northern Israel, Journal of Structural Geology, 36, 43–54, https://doi.org/10.1016/j.jsg.2011.12.010, 2012.

10 Orecchio, B., Aloisi, M., Cannavo, F., Palano, M., Presti, D., Pulvirenti, F., Totaro, C., Siligato, G., and Neri, G.: Present-day kinematics and deformation processes in the southern Tyrrhenian region: new insights on the northern Sicily extensional belt, Italian Journal of Geosciences, 136, 418–433, https://doi.org/10.3301/IJG.2017.01, 2017.

Pagani, U.: Linea di Faglia e terremoti del pesarese, Bolletino Della Soc. Geologica Italiana, 26, 175–188, 1907.

Palano, M., Ferranti, L., Monaco, C., Mattia, M., Aloisi, M., Bruno, V., Cannavò, F., and Siligato, G.: GPS velocity and strain fields in
15   Sicily and southern Calabria, Italy: updated geodetic constraints on tectonic block interaction in the central Mediterranean, Journal of Geophysical Research: Solid Earth, 117, https://doi.org/10.1029/2012JB009254, 2012.

Palumbo, L., Benedetti, L., Bourles, D., Cinque, A., and Finkel, R.: Slip history of the Magnola fault (Apennines, Central Italy) from 36 Cl surface exposure dating: evidence for strong earthquakes over the Holocene, Earth and Planetary Science Letters, 225, 163–176, https://doi.org/10.1016/j.epsl.2004.06.012, 2004.

20 Parsons, T., Toda, S., Stein, R. S., Barka, A., and Dieterich, J. H.: Heightened odds of large earthquakes near Istanbul: an interaction-based probability calculation, Science, 288, 661–665, https://doi.org/10.1126/science.288.5466.661, 2000.

Patacca, E. and Scandone, P.: The 1627 Gargano earthquake (Southern Italy): identification and characterization of the causative fault, Journal of Seismology, 8, 259–273, https://doi.org/10.1023/B:JOSE.0000021393.77543.1e, 2004.

Patacca, E., Scandone, P., Di Luzio, E., Cavinato, G. P., and Parotto, M.: Structural architecture of the central Apennines: Interpretation of the
25   CROP 11 seismic profile from the Adriatic coast to the orographic divide, Tectonics, 27, https://doi.org/10.1029/2005TC001917, 2008.

Pegler, G. and Das, S.: Analysis of the relationship between seismic moment and fault length for large crustal strike-slip earthquakes between 1977–92, Geophysical Research Letters, 23, 905–908, https://doi.org/10.1029/96GL00963, 1996.

Petersen, M., Moschetti, M., Powers, P., Mueller, C., Haller, K., Frankel, A., Zeng, Y., Rezaeian, S., Harmsen, S., Boyd, O., et al.: Documentation for the 2014 update of the United States national seismic hazard maps: U.S. Geological Survey Open-File Report 2014-1091, Tech.
30   rep., Geological Survey (US), https://doi.org/10.3 33/ofr20141091, 2014.

Petersen, M. D., Frankel, A. D., Harmsen, S. C., Mueller, C. S., Haller, K. M., Wheeler, R. L., Wesson, R. L., Zeng, Y., Boyd, O. S., Perkins, D. M., et al.: Documentation for the 2008 update of the United States national seismic hazard maps, Tech. rep., Geological Survey (US), 2008.

Petricca, P., Trippetta, F., Billi, A., Collettini, C., Cuffaro, M., Scrocca, D., Doglioni, C., Ventura, G., Morgante, A., and Chiaravalli,
35   F.: Revised dataset of known faults in Italy., GFZ Data Services, https://doi.org/10.5880/fidgeo.2018.003, http://pmd.gfz-potsdam.de/panmetaworks/, 2018.

Polonia, A., Torelli, L., Artoni, A., Carlini, M., Faccenna, C., Ferranti, L., Gasperini, L., Govers, R., Klaeschen, D., Monaco, C., et al.: The Ionian and Alfeo–Etna fault zones: New segments of an evolving plate boundary in the central Mediterranean Sea?, Tectonophysics, 675, 69–90, https://doi.org/10.1016/j.tecto.2016.03.016, 2016.

Polonia, A., Torelli, L., Gasperini, L., Cocchi, L., Muccini, F., Bonatti, E., Hensen, C., Schmidt, M., Romano, S., Artoni, A., et al.: Lower plate serpentinite diapirism in the Calabrian Arc subduction complex, Nature communications, 8, 2172, https://doi.org/10.1038/s41467-017-02273-x, 2017.

Pondrelli, S., Piromallo, C., and Serpelloni, E.: Convergence vs. retreat in Southern Tyrrhenian Sea: insights from kinematics, Geophysical Research Letters, 31, https://doi.org/10.1029/2003GL019223, 2004.

Pondrelli, S., Salimbeni, S., Ekström, G., Morelli, A., Gasperini, P., and Vannucci, G.: The Italian CMT dataset from 1977 to the present, Physics of the Earth and Planetary Interiors, 159, 286–303, https://doi.org/10.1016/j.pepi.2006.07.008, 2006.

Presti, D., Billi, A., Orecchio, B., Totaro, C., Faccenna, C., and Neri, G.: Earthquake focal mechanisms, seismogenic stress, and seismotectonics of the Calabrian Arc, Italy, Tectonophysics, 602, 153–175, https://doi.org/10.1016/j.tecto.2013.01.030, 2013.

Reicherter, K., Michetti, A. M., and Barroso, P. S.: Palaeoseismology: historical and prehistoric records of earthquake ground effects for seismic hazard assessment, Geological Society, London, Special Publications, 316, 1–10, https://doi.org/10.1144/SP316.1, 2009.

Roberts, G. P. and Michetti, A. M.: Spatial and temporal variations in growth rates along active normal fault systems: an example from The Lazio–Abruzzo Apennines, central Italy, Journal of Structural Geology, 26, 339–376, https://doi.org/10.1016/S0191-8141(03)00103-2, 2004.

Rockwell, T., Lindvall, S., Herzberg, M., Murbach, D., Dawson, T., and Berger, G.: Paleoseismology of the Johnson Valley, Kickapoo, and Homestead Valley faults: Clustering of earthquakes in the eastern California shear zone, Bulletin of the Seismological Society of America, 90, 1200–1236, https://doi.org/10.1785/0119990023, 2000.

Rohr, C.: Man and natural disaster in the Late Middle Ages: The earthquake in Carinthia and northern Italy on 25 January 1348 and its perception, Environment and History, 9, 127–149, https://doi.org/10.3197/096734003129342791, 2003.

Rosenbaum, G. and Lister, G. S.: Neogene and Quaternary rollback evolution of the Tyrrhenian Sea, the Apennines, and the Sicilian Maghrebides, Tectonics, 23, https://doi.org/10.1029/2003TC001518, 2004.

Rovida, A. N., Locati, M., CAMASSI, R. D., Lolli, B., and Gasperini, P.: CPTI15, the 2015 version of the Parametric Catalogue of Italian Earthquakes. Istituto Nazionale di Geofisica e Vulcanologia, 2016.

Sanchez, G., Rolland, Y., Schreiber, D., Giannerini, G., Corsini, M., and Lardeaux, J.-M.: The active fault system of SW Alps, Journal of Geodynamics, 49, 296–302, https://doi.org/10.1016/j.jog.2009.11.009, 2010.

Scandone, R. and Cortini, M.: Il Vesuvio: un vulcano ad alto rischio, Le Scienze, 163, 92–105, 1982.

Schmid, S. M., Pfiffner, O.-A., Froitzheim, N., Schönborn, G., and Kissling, E.: Geophysical-geological transect and tectonic evolution of the Swiss-Italian Alps, Tectonics, 15, 1036–1064, https://doi.org/10.1029/96TC00433, 1996.

Scrocca, D.: Thrust front segmentation induced by differential slab retreat in the Apennines (Italy), Terra Nova, 18, 154–161, https://doi.org/10.1111/j.1365-3121.2006.00675.x, 2006.

Scrocca, D., Carminati, E., and Doglioni, C.: Deep structure of the southern Apennines, Italy: Thin-skinned or thick-skinned?, Tectonics, 24, https://doi.org/10.1029/2004TC001634, 2005.

Selvaggi, G. and Chiarabba, C.: Seismicity and P-wave velocity image of the Southern Tyrrhenian subduction zone, Geophysical Journal International, 121, 818–826, https://doi.org/10.1111/j.1365-246X.1995.tb06441.x, 1995.

Serpelloni, E., Anzidei, M., Baldi, P., Casula, G., and Galvani, A.: Crustal velocity and strain-rate fields in Italy and surrounding regions: new results from the analysis of permanent and non-permanent GPS networks, Geophysical Journal International, 161, 861–880, https://doi.org/10.1111/j.1365-246X.2005.02618.x, 2005.

Sherlock, S. C., Strachan, R. A., and Jones, K. A.: High spatial resolution 40Ar/39Ar dating of pseudotachylites: geochronological evidence for multiple phases of faulting within basement gneisses of the Outer Hebrides (UK), Journal of the Geological Society, 166, 1049–1059, https://doi.org/10.1144/0016-76492008-125, 2009.

Sibson, R. H.: A note on fault reactivation, Journal of Structural Geology, 7, 751–754, https://doi.org/10.1016/0191-8141(85)90150-6, 1985.

Stein, R.: Progressive failure on the northern Anatolian fault since 1939 by earthquake triggering, Geophys. J. Int., 128, 694–704, 1997.

Stein, S. and Mazzotti, S.: Continental intraplate earthquakes: science, hazard, and policy issues, vol. 425, Geological Society of America, 2007.

Stirling, M., McVerry, G., Gerstenberger, M., Litchfield, N., Van Dissen, R., Berryman, K., Barnes, P., Wallace, L., Villamor, P., Langridge, R., et al.: National seismic hazard model for New Zealand: 2010 update, Bulletin of the Seismological Society of America, 102, 1514–1542, https://doi.org/10.1785/0120110170, 2012.

Stirling, M. W., Verry, G. H. M., and Berryman, K. R.: A new seismic hazard model for New Zealand, Bulletin of the Seismological Society of America, 92, 1878–1903, https://doi.org/10.1785/0120010156, 2002.

Sue, C. and Tricart, P.: Widespread post-nappe normal faulting in the Internal Western Alps: a new constraint on arc dynamics, Journal of the Geological Society, 159, 61–70, https://doi.org/10.1144/0016-764901-026, 2002.

Sue, C., Thouvenot, F., Fréchet, J., and Tricart, P.: Widespread extension in the core of the western Alps revealed by earthquake analysis, Journal of Geophysical Research: Solid Earth, 104, 25 611–25 622, https://doi.org/10.1029/1999JB900249, 1999.

Sue, C., Delacou, B., Champagnac, J.-D., Allanic, C., Tricart, P., and Burkhard, M.: Extensional neotectonics around the bend of the Western/Central Alps: an overview, International Journal of Earth Sciences, 96, 1101–1129, https://doi.org/10.1007/s00531-007-0181-3, 2007.

Swafford, L., Stein, S., and Mazzotti, S.: Limitations of the short earthquake record for seismicity and seismic hazard studies, Special Papers Geological Society of America, 425, 49, https://doi.org/10.1130/2007.2425(04), 2007.

Talwani, P.: Unified model for intraplate earthquakes, Intraplate Earthquakes. Cambridge University Press, Cambridge, pp. 275–327, 2014.

Thingbaijam, K. K. S., Martin Mai, P., and Goda, K.: New Empirical Earthquake Source-Scaling Laws, Bulletin of the Seismological Society of America, 107, 2225–2246, https://doi.org/10.1785/0120170017, 2017.

Turino, C., Scafidi, D., Eva, E., and Solarino, S.: Inferences on active faults at the Southern Alps–Liguria basin junction from accurate analysis of low energy seismicity, Tectonophysics, 475, 470–479, https://doi.org/10.1016/j.tecto.2009.06.007, 2009.

Ullah, S., Bindi, D., Pilz, M., Danciu, L., Weatherill, G., Zuccolo, E., Ischuk, A., Mikhailova, N., Abdrakhmatov, K., and Parolai, S.: Probabilistic seismic hazard assessment for Central Asia, Annals of Geophysics, 58, https://doi.org/10.4401/ag-6687, 2015.

Vai, G. B.: Structure and stratigraphy: an overview, in: Anatomy of an orogen: the Apennines and adjacent Mediterranean basins, pp. 15–31, Springer, 2001.

Viete, D. R., Hacker, B. R., Allen, M. B., Seward, G. G., Tobin, M. J., Kelley, C. S., Cinque, G., and Duckworth, A. R.: Metamorphic records of multiple seismic cycles during subduction, Science advances, 4, eaaq0234, https://doi.org/10.1126/sciadv.aaq0234, 2018.

Viganò, A., Scafidi, D., Ranalli, G., Martin, S., Della Vedova, B., and Spallarossa, D.: Earthquake relocations, crustal rheology, and active deformation in the central–eastern Alps (N Italy), Tectonophysics, 661, 81–98, https://doi.org/10.1016/j.tecto.2015.08.017, 2015.

Vilardo, G., De Natale, G., Milano, G., and Coppa, U.: The seismicity of Mt. Vesuvius, Tectonophysics, 261, 127–138, https://doi.org/10.1016/0040-1951(96)00061-3, 1996.

Viola, C.: Appunti geologici ed idrologici sui dintorni di Teramo, Boll. del R. Com. Geol. d'Italia, 1, 221–228, 1893.

von Zittel, K. A.: Geologische Beobachtungen aus den Central-Apenninen, vol. 2, Oldenbourg, 1869.

Walsh III, F. R. and Zoback, M. D.: Probabilistic assessment of potential fault slip related to injection-induced earthquakes: Application to north-central Oklahoma, USA, Geology, 44, 991–994, https://doi.org/10.1130/G38275.1, 2016.

Wang, S., Xu, W., Xu, C., Yin, Z., Bürgmann, R., Liu, L., and Jiang, G.: Changes in groundwater level possibly encourage shallow earthquakes in central Australia: The 2016 Petermann Ranges earthquake, Geophysical Research Letters, https://doi.org/10.1029/2018GL080510, 2019.

Wells, D. L. and Coppersmith, K. J.: New empirical relationships among magnitude, rupture length, rupture width, rupture area, and surface displacement, Bulletin of the seismological Society of America, 84, 974–1002, 1994.

Wiemer, S. and Wyss, M.: Minimum magnitude of complete reporting in earthquake catalogs: examples from Alaska, the Western United States, and Japan, Bulletin of the Seismological Society of America, 90, 859–869, https://doi.org/10.1785/0119990114, 2000.

Woessner, J., Laurentiu, D., Giardini, D., Crowley, H., Cotton, F., Grünthal, G., Valensise, G., Arvidsson, R., Basili, R., Demircioglu, M. B., et al.: The 2013 European seismic hazard model: key components and results, Bulletin of Earthquake Engineering, 13, 3553–3596, https://doi.org/10.1007/s10518-015-9795-1, 2015.

Zoback, M. D., Zoback, M. L., Mount, V. S., Suppe, J., Eaton, J. P., Healy, J. H., Oppenheimer, D., Reasenberg, P., Jones, L., Raleigh, C. B., Wong, I. G., Scotti, O., and Wentworth, C.: New Evidence on the State of Stress of the San Andreas Fault System, Science, 238, 1105–1111, https://doi.org/10.1126/science.238.4830.1105, 1987.

Figure 1. Tectonic map of Italy with instrumentally-recorded earthquakes (epicentres of M ≥ 2.0) in the 1981-2017 interval (ISIDe and CSI1.1 databases). Focal mechanisms are for M ≥ 4.0 events (Pondrelli et al., 2006), showing extensional tectonics along the Apennine chain and compressional tectonics in the NE portion of the Alps and in the N-NE portion of the Apennines.
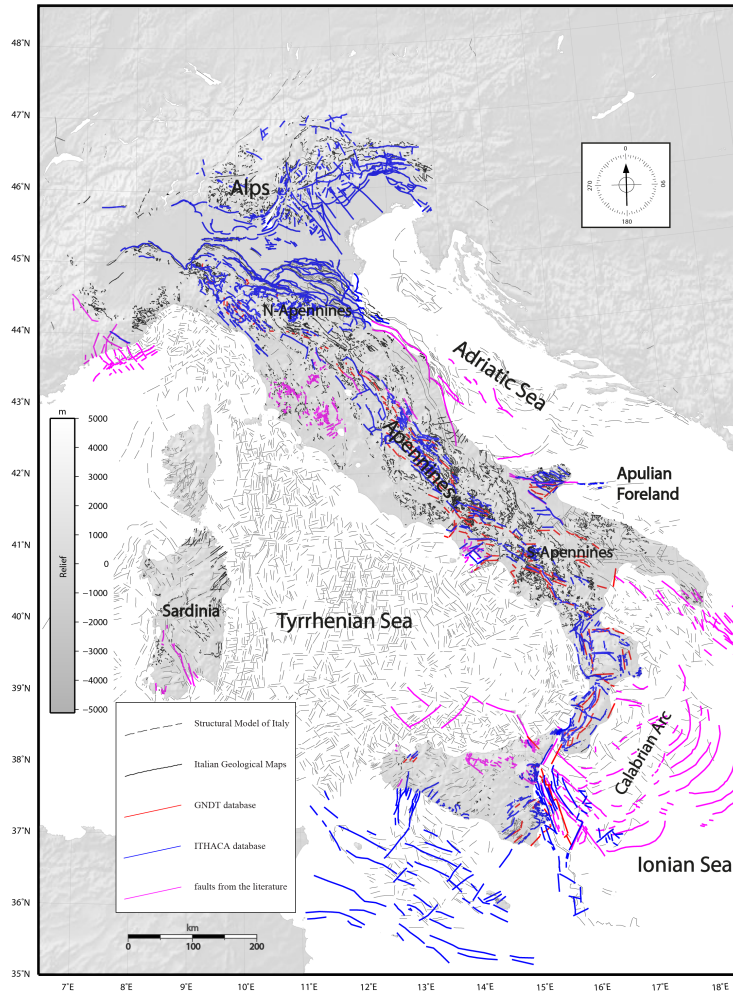
Figure 2. Map of faults from the five datasets used in this work: the Structural Model of Italy at the 1:500,000 scale (dashed black; Bigi et al., 1989); the Italian Geological Maps at the 1:100,000 scale (black; available online at www.isprambiente.it); the GNDT database of active faults (red; Galadini et al., 2000); the ITHACA database (blue; Michetti et al., 2000); and selected active faults from complementary studies published by different authors (pink; see text for explanations).

Figure 3. Instrumental seismicity (epicenters of M ≥ 4.0 earthquakes) distribution in Italy from ISIDe (stars) and CSI (diamonds) datasets. The CSI1.1 database (http://csi.rm.ingv.it; Castello et al., 2006) reports events in the 1981-2002 time interval, whereas the ISIDe database (http://iside.rm.ingv.it/iside/standard/index.jsp; Iside Working Group, 2016) reports events in the time interval 2003-2017. Events are differentiated by depth (change in color every 10 km).

Figure 4. Histogram of fault lengths (Lf) derived from all analyzed datasets. Inset shows the same histogram for fault lengths ≥ 45 km.

Figure 5. Map of the Italian territory divided into a grid with 25x25 km square cells. The map shows also the longest faults (from the analyzed datasets) falling into each cell. Light purple cells are for class A faults whereas dark grey cells are for class B faults.

Figure 6. Earthquake magnitude vs. fault length, obtained using empirical scaling laws from: L10 = Leonard (2010); WC94 = Wells and Coppersmith (1994); and TMG17 = Thingbaijam et al. (2017). Keys: DS = dip slip faults; NS = normal slip faults; RS = reverse slip faults; SS = strike-slip faults; SCR = stable continental region faults; AF = all faults; SRL = surface rupture length; and RLD = sub-surface rupture length. (b) Difference vs. fault length. The difference is between earthquake magnitudes obtained from L10 vs. each of all other scaling laws (namely, WC94 and TMG17).
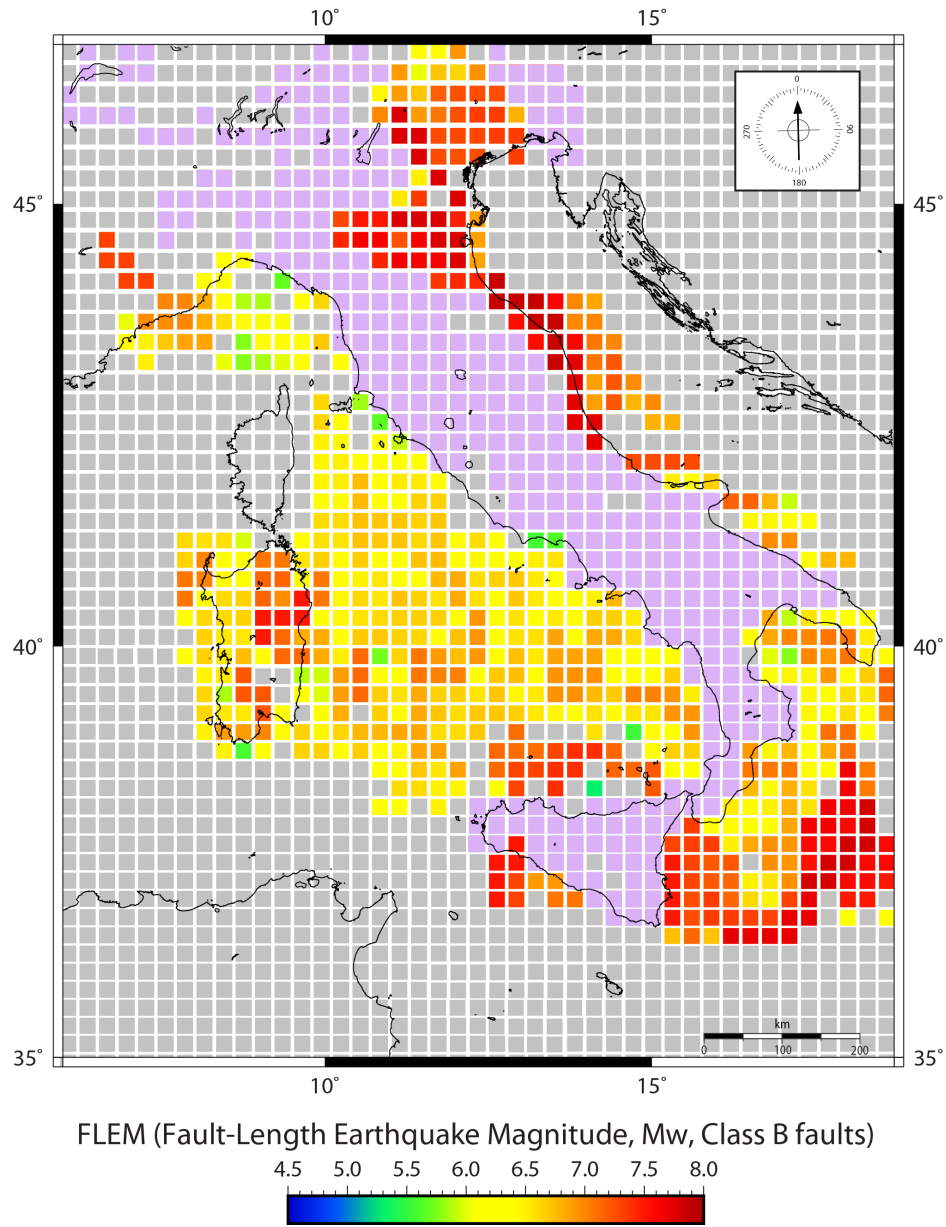
Figure 7. Map of the ~~Potential Expected Maximum~~ Fault-Length Earthquake Magnitude (~~PEMM~~FLEM) calculated, for each cell, from the length of class A faults. ~~PEMM~~ FLEM values are obtained using L10. Light grey is for cells with no data whereas dark grey is for cells where the longest faults belong to the class B set. Note that these results should be considered more in a theoretical and methodological perspective for comparison with future similar studies rather than in an applicative perspective for the case of Italy. In particular, our assessed earthquake magnitudes for the Italian territory are here proposed for scientific reasons and not for their use for civil protection and prevention purposes.
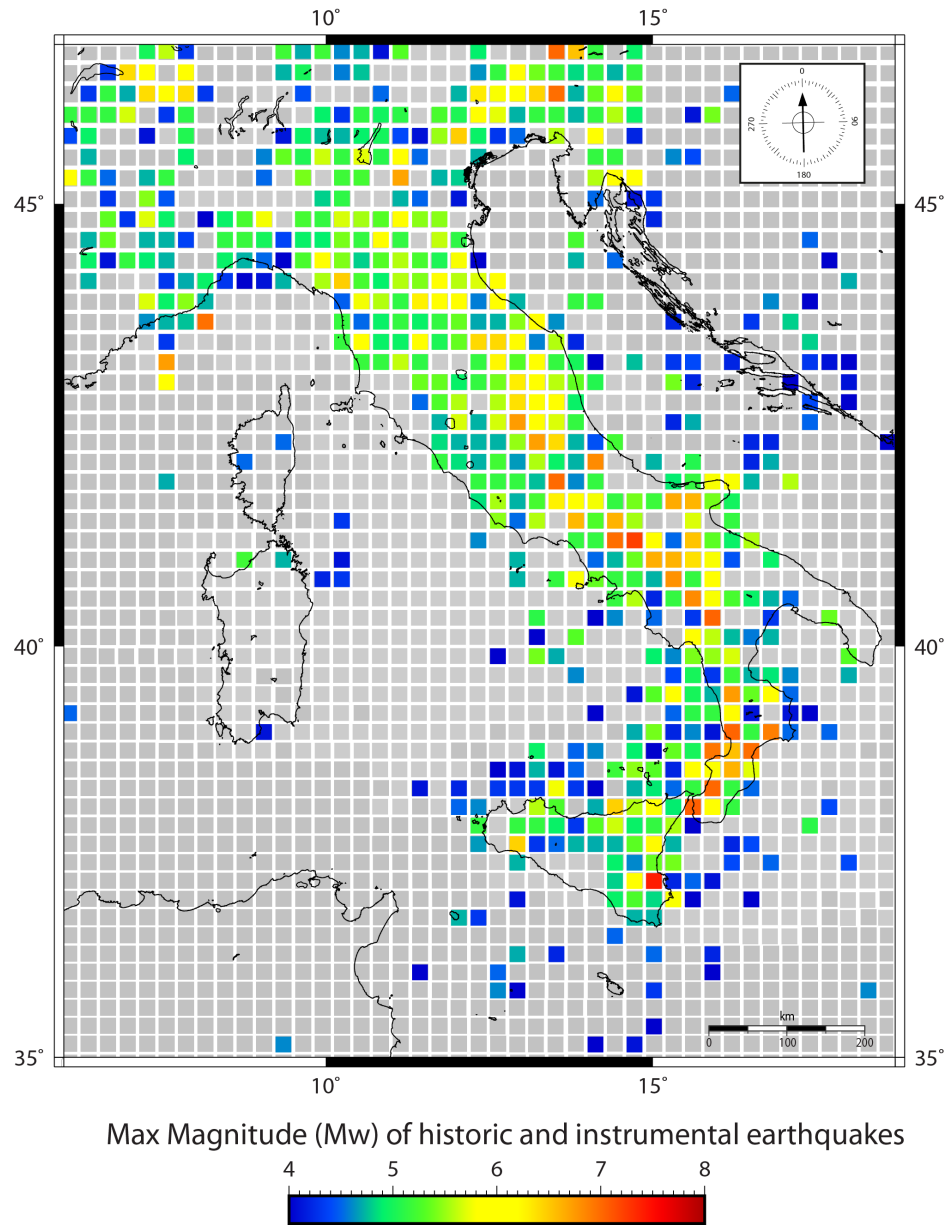
Figure 8. Map of the ~~Potential Expected Maximum~~ Fault-Length Earthquake Magnitude (~~PEMM~~FLEM) calculated, for each cell, from the length of class B faults. ~~PEMM~~ FLEM values are obtained using L10. Light grey is for cells with no data whereas light purple is for cells where the longest faults belong to the class A set. Note that these results should be considered more in a theoretical and methodological perspective for comparison with future similar studies rather than in an applicative perspective for the case of Italy. In particular, our assessed earthquake magnitudes for the Italian territory are here proposed for scientific reasons and not for their use for civil protection and prevention purposes.

Figure 9. Map of maximum magnitude (for each cell) from historic or instrumental earthquakes as recorded in the CSI 1.1, ISIDe, and CPTI15 databases within the 1000-2017 period. Grey is for cells with no data.
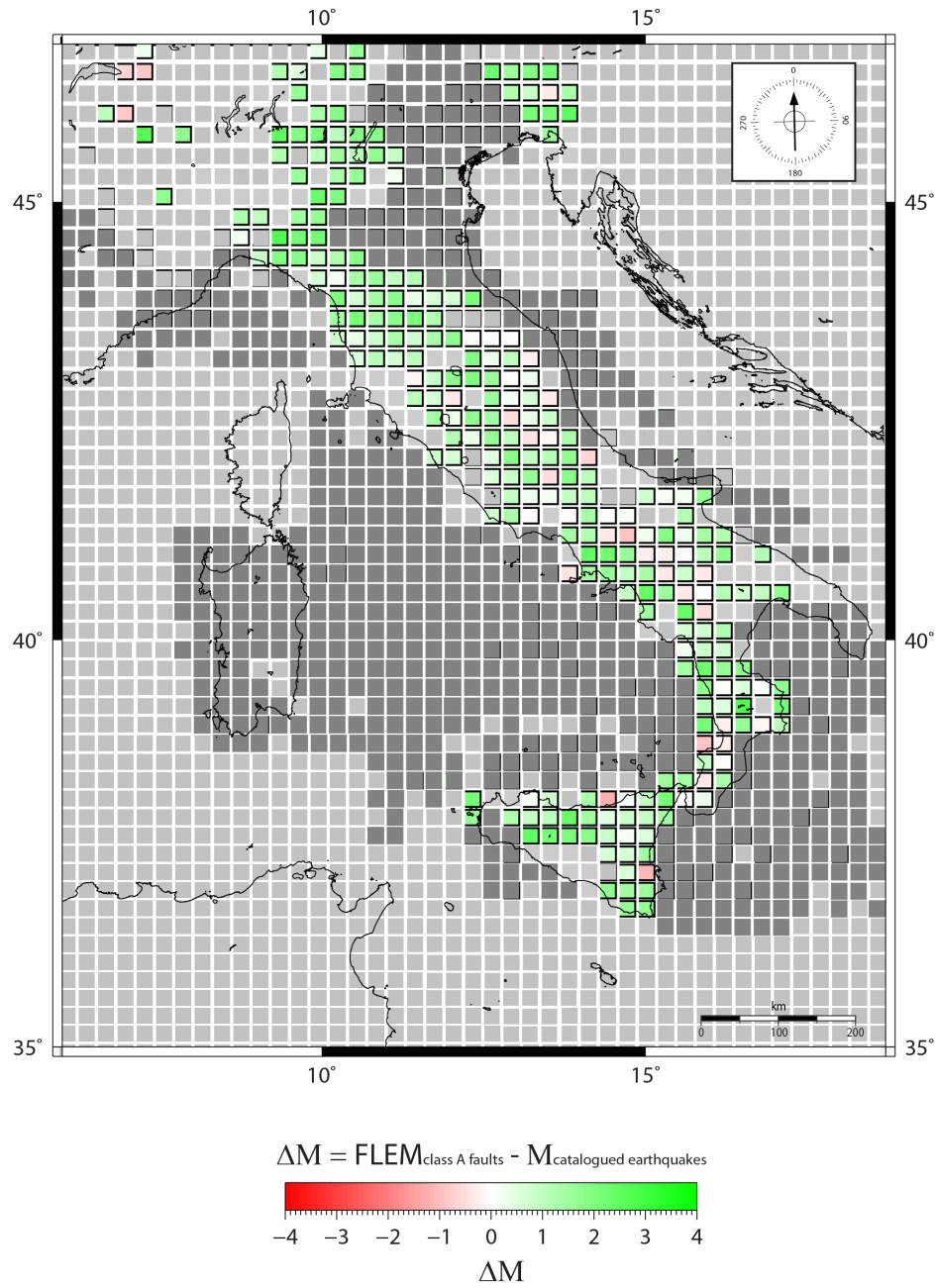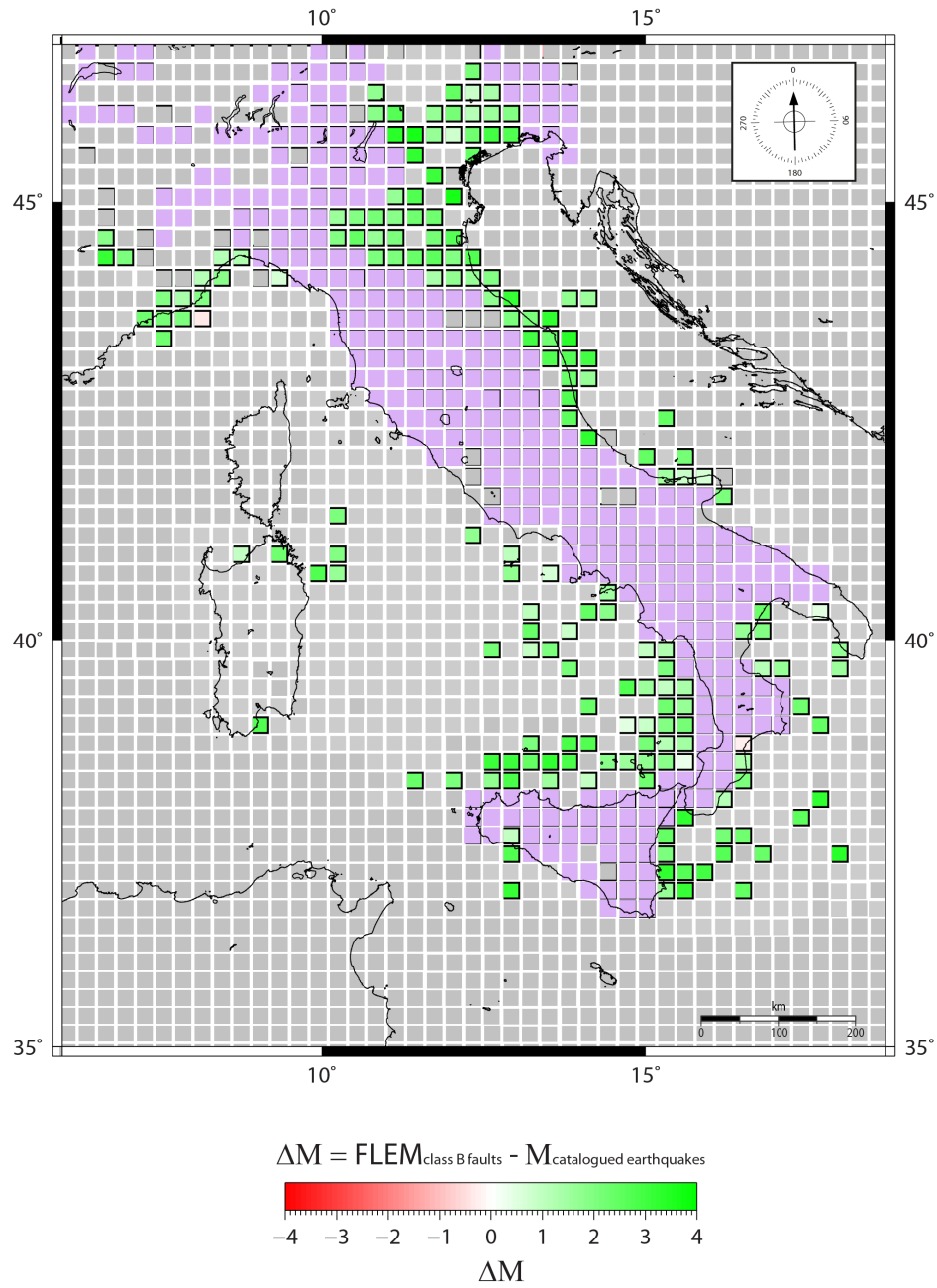
Figure 10. Map of the difference between ~~PEMM~~ FLEM values (only from class A faults; Fig. 7) and maximum magnitudes from historic or instrumental earthquakes (Fig. 9). Light grey is for cells with no data whereas dark grey is for cells where the longest faults belong to the class B set. See Fig. 12 for the interpretation of red vs. green cells.

Figure 11. Map of the difference between ~~PEMM~~ FLEM values (only from class B faults; Fig. 8) and maximum magnitudes from historic or instrumental earthquakes (Fig. 9). Light grey is for cells with no data whereas light purple is for cells where the longest faults belong to the class A set. See Fig. 12 for the interpretation of red vs. green cells.
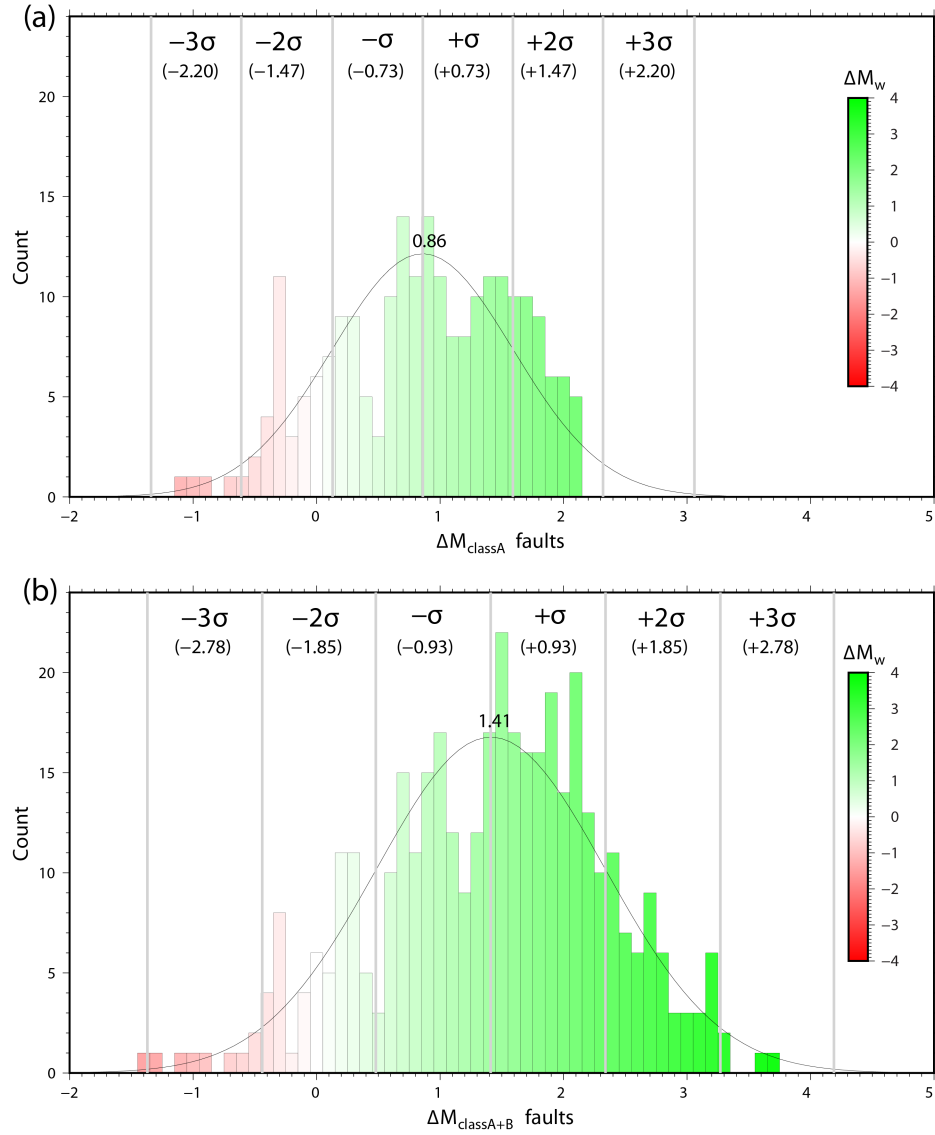
Figure 12. (a) Histogram of the difference between ~~PEMMs~~ FLEMs (from class A faults) and spatially-coincident (same cell) historical/instrumental- catalogued magnitudes of earthquakes. Mean = 0.86; deviation standard σ = 0.73. (b) Histogram of the difference between ~~PEMMs~~ FLEMs (from class A and B faults) and spatially-coincident (same cell) historical/instrumental-catalogued magnitudes of earthquakes. Mean = 1.41; deviation standard σ = 0.93. In both histograms, values in the negative fields can be interpreted as ~~PEMM999~~ FLEM999s underestimation with respect to catalogued earthquake magnitudes whereas values in the positive fields could be interpreted either as ~~PEMM999~~ FLEM999s overestimation with respect to catalogued magnitudes or as a sort of catalogue incompleteness. Occurrences in the positive fields (green portions) are significantly more frequent than occurrences in the negative fields (red portions). Green and red colors in Figs. 10, 11, and 13(c) have the same meaning as in this figure. See text for further information.
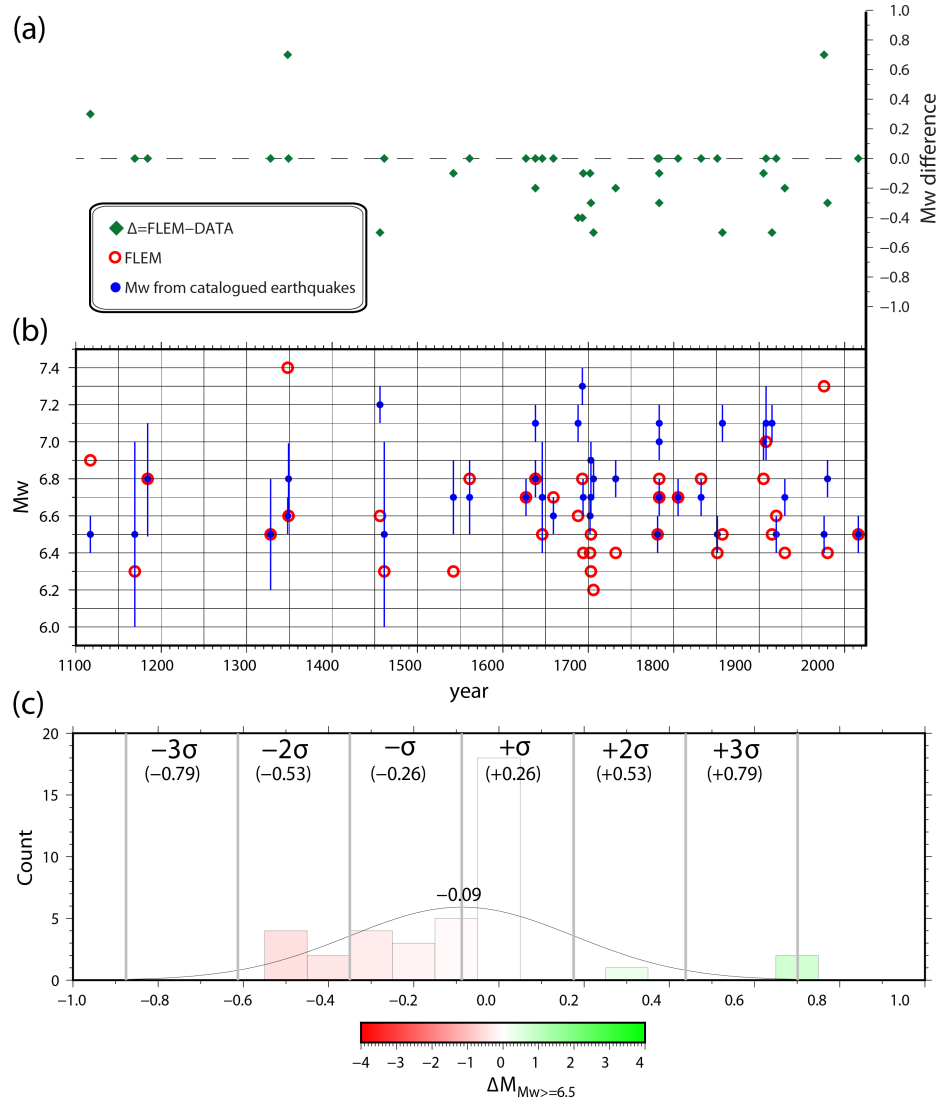
Figure 13. (a) Temporal series (since 1000 A.D.) of the difference between ~~PEMMs~~ FLEMs (from class A faults) and spatially-coincident (same cell) historical/instrumental-catalogued magnitudes of earthquakes (only M ≥ 6.5). (b) In blue, temporal series of magnitudes from catalogued historical or instrumental earthquakes (M ≥ 6.5, 1000-2017 period). Blue vertical bars are for magnitude uncertainty. In red, ~~PEMM~~ FLEM values from the same cells hosting the catalogued historical or instrumental earthquakes drawn in blue. (c) Histogram of the difference between ~~PEMMs~~ FLEMs (from class A faults) and spatially-coincident (same cell) historical/instrumental-catalogued magnitudes of earthquakes (M ≥ 6.5, 1000-2017 period). Mean = -0.09; standard deviation σ = 0.26. See Fig. 12 for the interpretation of red vs. green portions of the histogram.
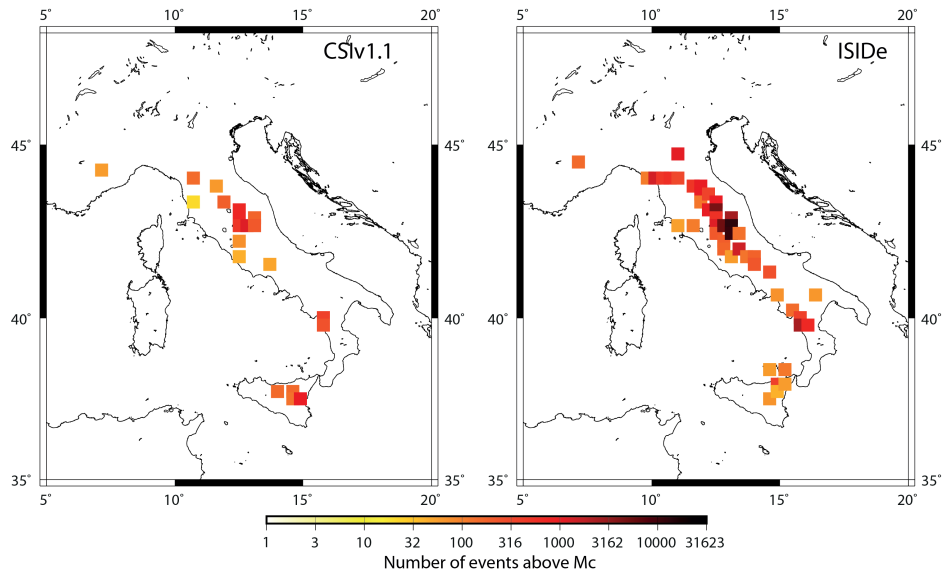
Figure 14. Maps of cells for which FLEM values are tested, on the CSIv1.1 (left panel, 20 cells) and ISIDe (right panel, 45 cells) databases (Tables S1 and S2). Colours are scaled with the number of events above the estimated completeness magnitude, M_c. In these cells the magnitude of events is distributed accordingly using a DTGR law, with a b-value equal to 1.

Table 1. Catalogued historical and instrumental earthquakes (M ≥ 6.5, 1000-2017 period) plotted in Fig. 13 with spatially-coincident (same 25x25 km cell) ~~PEMM~~FLEM. Catalogued data are from Castello et al. (2006), Iside Working Group (2016), and Rovida et al. (2016).

Region	Year	Lat	Lon	Mw Data	Err Mw Data	~~PEMM~~FLEM	Min DIFF
Apennine (S)	1456	41.30	14.71	7.2	0.1	6.6	-0.5
Sicily (SE)	1693	37.14	15.01	7.3	0.1	6.8	-0.4
Calabria	1783	38.79	16.46	7.0	0.1	6.8	-0.1
Calabria	1783	38.30	15.97	7.1	0.1	6.7	-0.3
Apennine (S)	1857	40.35	15.84	7.1	0.1	6.5	-0.5
Calabria	1905	38.81	16.00	7.0	0.1	6.8	-0.1
Messina Straits	1908	38.15	15.69	7.1	0.2	7.0	0
Abruzzi	1915	42.01	13.53	7.1	0.1	6.5	-0.5
Apennine (S)	1688	41.28	14.56	7.1	0.1	6.6	-0.4
Calabria	1638	39.05	16.29	7.1	0.1	6.8	-0.2
Apennine (N)	1920	44.19	10.28	6.5	0.1	6.6	0
Apennine (S)	1930	41.07	15.32	6.7	0.1	6.4	-0.2
Alps (E)	1976	46.24	13.12	6.5	0.1	7.3	0.7
Irpinia	1980	40.84	15.28	6.8	0.1	6.4	-0.3
Umbria	2016	42.83	13.11	6.5	0.1	6.5	0
Po Plain	1117	45.27	11.02	6.5	0.1	6.9	0.3
Sicily	1169	37.22	14.95	6.5	0.5	6.3	0
Calabria	1184	39.40	16.19	6.8	0.3	6.8	0
Umbria	1328	42.86	13.02	6.5	0.3	6.5	0
Alps (E)	1348	46.50	13.58	6.6	0.1	7.4	0.7
Latium-Molise	1349	41.55	13.94	6.8	0.2	6.6	0
Abruzzi	1461	42.31	13.54	6.5	0.5	6.3	0
Sicily	1542	37.22	14.94	6.7	0.2	6.3	-0.1
Apennine (S)	1561	40.56	15.51	6.7	0.2	6.8	0
Gargano	1627	41.74	15.34	6.7	0.1	6.7	0
Calabria	1638	39.28	16.81	6.8	0.1	6.8	0
Gargano	1646	41.91	15.99	6.7	0.3	6.5	0
Calabria	1659	38.69	16.25	6.6	0.1	6.7	0
Irpinia	1694	40.86	15.41	6.7	0.1	6.4	-0.1
Irpinia	1702	41.12	14.99	6.6	0.1	6.4	-0.1
Abruzzi	1703	42.43	13.29	6.7	0.1	6.3	-0.3
Umbria	1703	42.71	13.07	6.9	0.1	6.5	-0.3
Abruzzi	1706	42.08	14.08	6.8	0.1	6.2	-0.5
Irpinia	1732	41.06	15.06	6.8	0.1	6.4	-0.2
Marche	1781	43.60	12.51	6.5	0.1	6.5	0
Calabria	1783	38.58	16.20	6.7	0.1	6.7	0
Molise	1805	41.50	14.47	6.7	0.1	6.7	0
Calabria	1832	39.08	16.92	6.7	0.1	6.8	0
Apennine (S)	1851	40.96	15.67	6.5	0.1	6.4	0